NUREG/IA-0054

International Agreement Report

Assessment of RELAP5/MOD2, Cycle 36.02, Using NEPTUN Reflooding Experimental Data

Prepared by
M. Richner, G. Th. Analytis, S. N. Aksan

Paul Scherrer Institute (PSI)
Wurenlingen and Villigen
CH-5232 Villigen PSI
Switzerland

Office of Nuclear Regulatory Research
U.S. Nuclear Regulatory Commission
Washington, DC 20555

August 1992

Prepared as part of
The Agreement on Research Participation and Technical Exchange
under the International Thermal-Hydraulic Code Assessment
and Application Program (ICAP)

Published by
U.S. Nuclear Regulatory Commission

NOTICE

Available from

Superintendent of Documents
U.S. Government Printing Office
P.O. Box 37082
Washington, D.C. 20013-7082

and

National Technical Information Service
Springfield, VA 22161

NUREG/IA-0054

International Agreement Report

Assessment of RELAP5/MOD2, Cycle 36.02, Using NEPTUN Reflooding Experimental Data

Prepared by
M. Richner, G. Th. Analytis, S. N. Aksan

Paul Scherrer Institute (PSI)
Wurenlingen und Villigen
CH-5232 Villigen PSI
Switzerland

Office of Nuclear Regulatory Research
U.S. Nuclear Regulatory Commission
Washington, DC 20555

August 1992

Prepared as part of
The Agreement on Research Participation and Technical Exchange
under the International Thermal-Hydraulic Code Assessment
and Application Program (ICAP)

Published by
U.S. Nuclear Regulatory Commission

NOTICE

Abstract

Seven NEPTUN reflooding experiments with varying parameters flooding rate, single rod power, pressure and initial rod temperatures were simulated with the code RELAP5/MOD2, version 36.02, to assess the code, especially its reflood model. These calculations were performed with the specific objectives of evaluating the general prediction capability as well as specific problem areas of the RELAP5/Mod2 code in modelling boil-off and reflood behavior.

First a study of the effect of the hydraulic and conduction nodalization to the results of the code was performed using a high and a low flooding rate experiment. After the choice of a proper nodalization, base case calculations were done for all seven NEPTUN reflooding tests. The differences between code predictions and experiments are described and analysed. Implementing new correlations into the code and modifying or correcting existing correlations, for example for wall heat transfer or interphase friction, some of the weak points of the code during reflooding could be identified.

These modifications were checked with all seven NEPTUN experiments. Additionally, two FLECHT-SEASET tests were simulated with the frozen version and also with the modifications mentioned above.

Contents

1 Introduction

The best estimate thermalhydraulic transient computer code RELAP5/MOD2 was used at Paul Scherrer Institute (PSI, formerly EIR) for assessment calculations of NEPTUN boil-off and reflooding experiments.

NEPTUN is a half length, electrically heated 37 rod bundle facility (33 heater rods and 4 guide tubes) for core boil-off and forced bottom reflooding experiments. In this facility 40 reflooding experiments were performed during 1981-1983. Seven of them were chosen for assessment calculations with RELAP5/MOD2.

This report summarizes the work which was done at PSI using RELAP5/MOD2 code with respect to NEPTUN reflooding experiments. These assessment calculations are part of the contributions of the PSI to the "International Code Assessment and Application Program" (ICAP), of the US. Nuclear Regulatory Commission (NRC).

This assessment work was performed in the following order. First, hydraulic and conduction nodalization studies were done with a high and a low flooding rate experiment. After the nodalization was chosen, all seven experiments were calculated with the frozen version of the code. The differences between calculations and experiments were analyzed and described. It was tried to find the reasons for these differences and if possible, to eliminate them by modifying correlations in the code or by implementing better correlations. In this way, a modified version of RELAP5/MOD2, especially tested for reflooding, was created. With this modified version, all seven NEPTUN reflooding experiments were calculated again. As a final test, two FLECHT-SEASET experiments were simulated with the frozen and the modified version of RELAP5/MOD2.

The contents of the report follows the same order as described above. In chapter two, a description of the NEPTUN test facility and of the seven NEPTUN reflooding tests used for this work are given. In chapter three, the used code version is described and the evaluation of a proper nodalization for the NEPTUN test section is reported. In chapter four the base case results of all seven NEPTUN reflood experiments are given. Chapter five describes model improvements to the code which were found as a real improvement in the NEPTUN reflooding experiments. Chapter six gives the comparison of the frozen version and the modified version of RELAP5/MOD2 calculations for two FLECHT-SEASET experiments. Chapter seven contains a discussion of the results of the calculations with the frozen and the modified version of the code for the seven NEPTUN and the two FLECHT-SEASET tests. Run statistics of the two NEPTUN experiments with highest and lowest flooding rate are given in chapter eight. Finally, in chapter nine, the main conclusions of this work are summarized and recommendations are made. In the appendices, one finds a sample input deck of one NEPTUN experiment, the updates to create the modified version of RELAP5/MOD2

and the mathematical formulation of the implementation of the new bubbly/sl
interphase friction correlation into RELAP5/MOD2.

2 Facility and Tests Description

2.1 NEPTUN test facility

The NEPTUN test facility (Figure 1) was originally built to study reflooding in bundle geometries. The NEPTUN heater rod bundle consists of 33 electrically heated rods and four guide-tubes. A cross section of the NEPTUN bundle can be seen in Figure 2 and the dimensions of a NEPTUN heater rod is shown in Figure 3. The outer dimensions of the rods are similar to those of a PWR fuel rods except being half length in size (1.68 m heated length, heated rods with diameter 10.7 mm, p/d = 1.33). The whole bundle is placed in a insulated octagonal housing. The axial power profile of a NEPTUN heater rod is of the form of a cosine with a peaking factor of 1.58 (Figure 4). There are five fuel assembly spacer grids, axially located at equal distances.

At eight measurement levels, rod cladding temperatures, fluid temperatures and differential pressures are measured as shown in Figure 5. Each heater rod is instrumented with four to eight thermocouples, placed inside of the cladding at the eight different measurement levels. The five centrally located heater rods are additionally supplied with external thermocouples. There are further measurements of flooding water, fresh steam and exhaust steam mass flow rates, water carry over, absolute pressures and heating power. From the absolute pressure measurement and the pressure difference measurements the void fractions between all measurement levels and the collapsed liquid level of the whole test section can be obtained. The pressure in the upper plenum of the test section is held constant during the experiments by a pressure control system.

Further details about the NEPTUN test facility are given in reference 1.

2.2 The NEPTUN reflood experiments used for assessment calculations

40 reflood tests were performed in the NEPTUN test facility from 1981 until 1983. Seven of them were chosen for the assessment of the RELAP5/MOD2 code, as representative cases. Their test parameters are shown in table 1.

The experimental procedure of such a reflood experiment is given in ref. 1 and will be summarized here. Before the start of the test, the flooding water in its circuit is brought to the desired conditions. The test section is kept at a defined experimental pressure and is filled with saturated steam. Then the power at the heater rods is switched on and the heater rod temperatures start increasing. A short time before the cladding temperatures reach the desired value, the valve for th- flooding water is opened and the water enters into the test section. The power at the bundle is held constant until the end of the experiment.

2.3 Measurement uncertainty

There exists no detailed quantification of the measurement accuracy in the NEPTUN test facility. Hence, the errors of the test parameters and the data of the NEPTUN reflooding tests have to be estimated. For example, the collapsed liquid level in the test section can be determined by the sum of all Δp-measurements along the test section and, also, by one Δp measured between bottom and top of the bundle. From the difference of these two values the accuracy of the measurement of the collapsed liquid level can be determined.

The scattering of the rod cladding temperatures in the bundle was estimated from plots of these temperatures for different rods at measurement levels 4 and 5. The rod temperature data used in this work for comparison with code calculation were taken from the so called representative rod [11,12] and gives average values for cladding temperatures and quench times between all the rods. This was rod E3 (Figure 2), and at the measurement levels, where this rod is not instrumented, it was rod E1.

Six of the seven used NEPTUN experiments were repeated [3]; in these repetition experiments the five centrally located rods where instrumented without external thermocouples. The idea of these repetition tests was to determine the influence of the external thermocouples to the bundle during reflooding, especially to the representative rod. This effect was negligible, except to around 35°C lower quench temperatures (and therefore a little later quench times in the tests without external thermocouples) and the amount of water expelled from the test section. The water entrainment was higher without external thermocouples in the tests with low flooding rates (see table 3).

These repeat experiments gave also an indication of how good a NEPTUN reflood test can be reproduced. Except for some special cases, the reproducibility was very good. The largest differences between original and repeat experiments can be seen in table 3.

The uncertainty of the test parameters or measured data in the seven used NEPTUN tests can be seen in table 2.

Table 1: Test parameters of the seven used NEPTUN reflooding experiments

Exp.Nr.	Pressure (bar)	Flooding water Velocity (cm/s)	Subcooling (°C)	Single rod power (kW)	Maximum initial cladd. temp. (°C)
5036	4.1	1.5	11	2.45	757
5052	"	2.5	78	"	867
5051	"	4.5	"	"	"
5025	"	10.	"	"	757
5050	"	15.	"	"	867
5049	1.0	2.5	"	"	"
5056	4.1	2.5	"	4.19	"

Table 2: Measurement errors and scattering of the data during NEPTUN refiooding tests.

Quantity	Probable error	Largest scattering min. to max. of the data
Flooding water mass flow	± 5.3 %	
Flooding water temperature	± 0.5 °C	
Test section pressure	± 0.03 bar	0.42 bar during exp. 5050
Rod power	± 1.8 %	
Collapsed water level	± 4 cm	
Void fractions	± 0.04	
Rod cladding temperatures between all rods without external thermocouples	± 5°C	48°C during exp. 5050 90°C during exp. 5036
Quench times between all rods without external thermocouples at measurement levels 4 and 5	± 1.2s	2.5s during exp. 5050 14.2s during exp. 5036

Table 3: Differences of the data between NEPTUN reflooding tests and repetition experiments

Quantity	Largest scattering between original and repetition test
Rod cladding temperature at representative rod	20°C between exp. 5050 and repetition experiment 90°C between exp. 5036 and repetition experiment
Quench time of representative rod at measurement levels 4 and 5	4.2s between exp. 5050 and repetition experiment 9.2s between exp. 5036 and repetition experiment
Water entrainment	Identical during experiments with 4.5 - 15 cm/s flooding velocity 5 % higher in repetition experiment during experiments with 2.5 cm/s flooding velocity 33 % higher in repetition experiment during experiment with 1.5 cm/s flooding velocity

3 Code and Model Description

3.1 Code description

The code used for this work was RELAP5/MOD2, Cycle 36.02 (Frozen version), with no further updates. This code was used for the nodalization study and the base case calculations. During the course of this work, modifications were made to the code which will be explained in due course. The details of the models can be seen in the code manual [2].

3.2 Model description and study of the effect of the nodalization

The model used to describe the NEPTUN test section was very simple (Figure 6). A pipe component representing the test section fluid volumes is connected to a time dependent volume at the bottom by a time dependent junction. The upper plenum is a time dependent volume with constant pressure, connected to the upper end of the pipe by a single junction. Guide tubes and housing were neglected in the calculation, but their effect on the flooding behaviour of the NEPTUN bundle is very small. Comparison of an experiment with heated guide tubes and heated housing to an experiment without heating of these components leads to this conclusion as indicated in reference [3].

Before choosing a final model, the effect of different nodalizations to the results of RELAP5/MOD2 was investigated for two experiments, 5050 with the highest and 5036 with the lowest flooding rate. Of interest was the influence of the number of hydraulic volumes chosen and the effect of the number of fine me.h conduction nodes selected in the heat conduction elements.

The different nodalization were selected and tested using 10, 18 and 32 volumes for the bundle (Figure 6) by fixing the number of fine mesh nodes in the heat conduction elements. In the high flooding rate experiment the effect of the nodalization on the cladding temperatures is small (Figure 7). Higher number of volumes results in higher wall heat transfer and earlier quenching.

In the low flooding rate experiment as it can be seen from Figure 8, the effect of the nodalization to the results of RELAP5/MOD2 is not systematic. At axial level 4, nodalizations with 18 and 32 volumes give similar results and nodalization with 10 volumes gives the worst wall heat transfer and later quenching. At axial level 5,32 volumes gives the worst heat transfer, highest cladding temperatures and latest quench. The main reason for this deviation could not be identified. Though, in this calculation, there are large differences between measurements and code predictions; hence, unsystematic effects have to be expected. The same nodalization study was performed with a modified version EIR-update 75 of RELAP5/MOD2, which gives better results for this experiment (EIR-update 75 is very similar to EIR-update which will be documented in section 5). With this modified version, the results are much more systematic (Figure 9). The code calculates lowest cladding temperatures at least before quenching and earliest quench with 32 volumes than with 10 volumes.

All the calculations to be presented latter in this report were performed by selecting the nodalization with 18 volumes as the basis.

Calculations by fixing the nodalization and varying the number of fine mesh nodes in the heat conduction elements were also performed. In Figure 10 the result for experiment 5050 at measurement level 4 can be seen with 16 and 64 fine mesh nodes per heat slab. The number of fine mesh nodes does not have an influence on precursory cooling wall heat transfer, but it has an effect on the quench temperature and thus on the quench time.

Based on the nodalization studies described above, it was decided to use 16 fine mesh points per heat slab for further calculations.

4 Base Case Results

Using the nodalization scheme mentioned above, base case calculations were performed for all seven NEPTUN reflooding experiments. The results can be seen in Figures 11a-26a. They will be summarized for the different flooding rate groups:

a) At high flooding rates the code overpredicts the wall heat transfer coefficient during film boiling (Figures 11a, 12a). Therefore, the rod cladding temperatures decrease too fast before the quench. The quench temperatures are predicted 130-170 K lower than in the experiment and thus quenching occurs latter than in the measurements.

b) At medium flooding rates, the same behaviour can be observed as in the high flooding rate cases: the overprediction of the wall heat transfer during film boiling (Figure 13a) and the quench temperatures are 90-150K lower than in the measurements.

c) In the low flooding rate experiments the first phase of steam cooling is well predicted by the code; calculated and measured surface temperatures agree well until the measured turnaround temperature point (fig. 14a-17a). Though, during dispersed film boiling and film boiling, the calculated wall heat transfer is much lower than in the experiment and hence, the turnaround points are calculated at higher temperatures and turnaround-times occur later. Calculated and experimental temperatures differ by as much as 300 K before the quench. The quench-times deviate within a factor of 2 from the measured ones.

At the same time, the code grossly overpredicts the amount of water expelled and consequently, underpredicts the collapsed liquid level (figs. 21a - 24a, especially Figure 24a). This behaviour is typical for all low flooding rate experiments. The calculated void fractions are over-predicted (Figures 25, 26, middle figures) and show unphysical instabilities. The collapsed liquid levels also exhibit instabilities and stepwise decreases, while the water entrainment increases by steps at the same time (fig. 24a).

5 Model Improvements

The discrepancies between experiments and calculations reported in the last chapter could partly be eliminated by implementing better correlations into the code.

The over-prediction of the wall heat transfer coefficient during film boiling in the high and medium flooding rate experiments could be eliminated by bringing back the Modified Bromley correlation for the film boiling heat transfer coefficient to its original form as it stands in the code manual [2]. Missing coefficients had to be added and an empirical factor had to be removed (fig. 27). As a result of this modification, the rod cladding temperature histories calculated by RELAP5/MOD2 during film boiling become parallel to the experimental ones (Figures 28, 29); the problem of the low quench temperatures predicted by the code and consequently, the late quenching, will be discussed later.

The analysis of 6 NEPTUN boiloff tests using TRAC-BD1 version 12 [7,8] and TRAC-BD1/MOD1 [5,9] has shown, that TRAC overpredicts the amount of water expelled and underpredicts the collapsed liquid level for these experiments. The same behaviour was found with RELAP5/MOD2 for one NEPTUN boiloff experiment [9]. The amount of water expelled in a boiloff experiment is mainly determined by the interphase friction in the bubbly and slug flow regimes. It was found that both codes overestimate the interphase friction in these flow regimes for rod bundle geometries.

Actually, the correlations used in these codes for the interphase friction were developped for tubes and not for rod bundles. For the boiloff experiments this problem could be solved by implementing a new correlation [4] from the CATHARE code for the interphase friction in bubbly and slug flow, which is applicable for rod bundles [5,7,8,9].

This new correlation was also implemented in RELAP5/MOD2. The mathematical formulations of the implementation into RELAP5/MOD2 can be found in Appendix C. Figure 30 shows the formula as it was implemented in RELAP5/MOD2. With this new correlation, the severity of the problem of too low collapsed liquid levels in the low flooding rate experiments could be reduced (Figures 31, 32). Also, the amount of water expelled from the bundle was reduced, which was before over-predicted (Figures 31, 32). This modification also improved the predicted void fractions (Fig. 33), and the cladding temperatures became a little closer to the experimental ones (Fig. 34).

One could observe in the calculation of the low flooding rate experiment 5036 that the collapsed liquid level always decreased by step changes (Figure 31) at the times the entrained water increased by a step. This occured just at the times when the steam velocities in the test section exhibited numerical spikes.

These numerical oscillations are probably due to the interpolation of the reflood wall heat transfer coefficient between two set points for void fractions $0.91 < \alpha < 0.99$. At the higher end, the Modified Bromley correlation is used with an $(1 - \alpha)$ factor, at the lower end the Modified Bromley correlation is taken without any additional factors (Figure 35). This short transition between Modified Bromley correlation and $(1 - \alpha)$ times Modified Bromley correlation probably caused the numerical oscillations mentioned above. By implementing the Forslund-Rohsenow correlation [6] into the code and using it for void fractions $\alpha > 0.8$, using the Modified Bromley correlation for $\alpha < 0.6$ and making interpolation in between (Figure 35), improved results were achieved.

Actually, with this new wall heat transfer logic, the instabilities disappeared. The predicted collapsed liquid level is smoother and in good agreement with the measured one for the low flooding rate experiment 5036 (Figure 36). The entrained water prediction has become better (Figure 37). The cladding temperatures of the rods are also smoother (Figure 38) and the turnaround time and turnaround temperatures are now in better agreement with the experimental ones. As an important by-product, the calculation has become more stable. The oscillations in the steam velocities are much smaller and the big spikes have disappeared (Figure 39). This is an example, where the choice of a suitable heat transfer correlation and logic has reduced thermalhydraulic instabilities and has given better results in cladding temperatures, collapsed water level and water entrainment.

One of the remaining problems in the low flooding rate experiment 5036 is the underprediction of the wall heat transfer after the turnaround points (Figure 38b). The reason for this deviation between experiment and calculation are the too high void fractions calculated by the code for low flooding rate experiments. Reducing the interphase friction in the rod bundle geometry in the inverted-slug flow regime by a factor of 2.5 and in the (dispersed) flow by a factor of 2 (Figure 48), better agreement could be achieved between calculated and experimental void fractions (Figure 40). As a result, the cladding temperature histories agreed better with the experimental ones (Figure 41). The collapsed liquid level increased a little and the water entrainment was very well predicted.

Two addidonal problems remained: One was unphysical void fraction discontinuities which occured in the low flooding rate experiments around the quench time in the lower part of the test section (Figure 43, middle). The other was the too low quench temperatures and therefore much too late quench times calculated by the code especially in the high flooding rate experiments (Figure 28b).

The reason of the void fraction discontinuities in the low flooding rate experiments is probably due to the criterion for selecting the pre-dry out interphase friction correlations near the quench front. If a node had quenched, the code continued selecting the post-dry out interphase friction correlations. The criterion for choosing the pre-dry out interphase friction formulas in the code is given in Figure 42 as well as the modification which was performed to eliminate the void fraction discontinuities. As one can see from Figure 43, the oscillation is smaller with the modification, but it has not disappeared. One can choose $T_g - T_s - 40$ instead of $T_g - T_s - 40(1 - \alpha)$ in this correction. Then, this oscillation completely disappears in the lower part of the test section, but the code calculates too high void fractions and therefore too high cladding temperatures in the upper parts of the test section. One obtains worse results compared with the experiment. The choice of $T_g - T_s - 40(1 - \alpha)$ is a compromise, which although does not solve completely the problem of the void fraction oscillations in the lower part of the test section, it also does not influence too much the void fraction in the upper part. In Figure 47, one can see that by introduction of the last modification, this void fraction oscillations have almost completely disappeared.

We saw in the analysis of all NEPTUN reflooding experiments that RELAP5/MOD2 calculates too low quench temperatures which results in later quench times; in the high flooding rate experiments, this delay of quench time can be large (Figure 28b). The effective quenching point in RELAP5/MOD2 is the crossing point between the film boiling heat transfer coefficient and the Weismann transition film boiling heat transfer coefficient. There exists a second criterion [2], which calculates a rewetting temperature. But in all our cases, this crossing point between film boiling and transition boiling heat transfer coefficient was higher than the rewetting temperature, so this crossing point is automatically taken as the effective quenching point. The crossing point could be changed to higher temperatures by changing an exponent in the Weismann transition boiling correlation (Figure 44).

A second modification was performed to the code at the same time: To account for the effect of the subcooling of the fluid on the wall heat transfer during film boiling, the Modified Bromley heat transfer correlation was multiplied by a correction factor (Figure 44). This factor has only a small effect in the lower part of the test section.

The effects of these modifications to the rod cladding temperatures can be seen in Figures 45 and 46. Good agreement was obtained between the experimental data and calculational results. Figure 47 shows that the void fraction oscillations mentioned above have almost disappeared with this last change.

The summary of all the updates performed in RELAP5/MOD2 at PSI is given in figure 48. With the version EIR-update 83 the seven NEPTUN reflood experiments were re-calculated. The results of the rod cladding temperatures, collapsed liquid levels, liquid carry over and some void fractions can be seen in Figures 11b-26b, compared with the calculation with the frozen version (Figures 11a-26a).

The modified version of RELAP5/MOD2 gives significantly better results for all seven NEPTUN reflooding experiments. In particular, the low flooding rate experiments were much better predicted by the modified version.

6 Calculations of two FLECHT-SEASET reflooding experiments using the frozen and the modified versions of RELAP5/MOD2

6.1 The two FLECHT-SEASET tests used for calculations and the used nodalization

Results of code calculations can be dependent on geometries and facilities. As a test, in order to assess if the modifications introduced in the last chapter were also resulting in improved predictions for experiments in other facilities, two FLECHT-SEASET tests [10] were calculated with the frozen and the modified version of RELAP5/MOD2. The test parameters of these two tests are given in Table 4. Test no. 34006 is a low flooding rate experiment, while test no. 31701 is a high flooding rate test.

The input deck for test 31701 was recieved from EG&G, Idaho. The FLECHT test section is simulated by a pipe of 20 volumes of the same length. Upper and lower plenum are simulated by a time dependent volume, similar to the NEPTUN nodalization (Figure 6).

6.2 Results with frozen and modified versions of RELAP5/MOD2

The two FLECHT reflooding experiments were calculated with the frozen and the modified versions of RELAP5/MOD2. The results can be seen in Figures 49-55.

In the high flooding rate experiment, the results of the frozen and the modified versions are both very good (Figure 49). No large differences can be seen between the two versions with respect to rod cladding temperatures. The deviations of the calculations from the experiment are very small. The water in the bundle and the water entrainment are almost identical with both versions; the mass in the bundle is underpredicted, while the water entrainment is overpredicted by the code (Figure 50).

In the low flooding rate experiment, with the frozen version, only the first phase of steam cooling is well predicted by the code (Figure 51a). During dispersed film boiling the code calculates a too high wall heat transfer. This results in 100-150K lower turnaround temperatures than in the experiment. During this phase of the calculation the steam temperatures in the test section oscillate by 450K (Figure 52a). The mass in the bundle is a little underpredicted (Figure 53a) but the water entrainment is grossly overpredicted (Figure 54a). The steam velocities in the test section oscillate and have large spikes (Figure 55a). The void fractions (Figure 56a) exhibit large oscillations and are too high, similar to the NEPTUN low flooding rate experiments.

With the modified version of RELAP5/MOD2, the underprediction of the turnaround temperature is as large as with the frozen version (Figure 51). Quench times are predicted earlier than with the frozen version (similar to NEPTUN) and the amplitude of the steam temperature oscillations is somehow reduced (Figure 52). With the modified version, the mass in the bundle is calculated very well and without the numerical oscillations of the frozen version, similar to the NEPTUN calculations (Figure 53), and the water entrainment is smaller than with the frozen version (Figure 54), but is still overpredicted. The steam velocities in the test section oscillate with the modified version less than with the frozen version (Figure 55), and the large velocity spikes have disappeared. This is the same behaviour as in the NEPTUN calculations(Figure 39).

The void fractions are calculated much better with the modified version of RELAP5/MOD2 (Figure 56). The large oscillations have disappeared and the measured collapsed water level is well predicted. Finally, the void fractions predicted by the modified version of RELAP5/MOD2 are closer to the measured ones than the ones predicted by the frozen version.

7 Discussion

This assessment work has shown, that the frozen version of the RELAP5/MOD2 code gives relatively good results for the NEPTUN high and medium flooding rate experiments. Large deviations between predictions and measurements occur in the low flooding rate tests.

Two areas in the code were found, which are mainly responsible for the differences between predictions and measurements in the NEPTUN facility: Interphase friction and wall heat transfer. In the low flooding rate experiments one always faces the same problems: Overprediction of the amount of water expelled from the bundle and, at the same time, underprediction of the collapsed water level.

This behaviour was found to be due to the interphase friction correlations in the code, especially in the bubbly and slug flow regimes. Actually, all the correlations in the code are developped from tube geometry experiments. Though, in a rod bundle, the interphase friction is smaller than in a tube, as experiments have shown [4]. Therefore, the code overpredicts the amount of water expelled in the NEPTUN bundle. By implementing a correlation used in the CATHARE code for the interphase friction in bubbly and slug flow, which is suitable for rod bundles, the problem of the overprediction of the water entrainment could be solved. In the other flow regimes, the interphase friction was reduced by multiplying factors in this work. This was done because there were no existing correlations for the interphase friction in the rod bundle geometry for these flow regimes.

The reduction of the interphase friction in the rod bundle geometry is most important in the bubbly and slug flow regimes. These flow regimes determine mainly the amount of water which is expelled from the bundle in low flooding rate cases; though, whether in the other flow regimes a reduction of the interphase friction in the rod bundle geometry is necessary, has to be tested by further assessment calculations of other experimental facilities.

The new correlation for the interphase friction in bubbly and slug flow gave also perfect agreement for the prediction of the collapsed liquid level in the FLECHT-SEASET low flooding rate experiment. But in this full length facility, the underprediction of the liquid level by the frozen version was not as large as in the NEPTUN low flooding rate experiments.

The changes in the interphase friction also greatly improved the predicted void fractions of the low flooding rate experiments, both in NEPTUN and FLECHT. One sees that the interphase friction is one of the important parameters in the low flooding rate experiments during the reflood phase and both void fractions and heat transfer coefficients are strongly dependent on it.

It seems to be of importance that the interphase friction in RELAP5/MOD2 has to be reduced in the core region and consequently, that the code should use different correlations for the core and the other components. The distinction between core and other components was made in this work by a check on the hydraulic diameter. The core is the component with the smallest hydraulic diameter.

One of the weak points of the reflood model in RELAP5/MOD2 is the reflood wall heat transfer correlation for high void-fractions. The interpolation between the Bromley correlation and $(1 - \alpha)$ times Bromley at high void fractions results in numerical instabilities, which disappeared after implementing the Forslund-Rohsenow correlation into the code and modifying somewhat the selection logic. In any case, using the

Bromley heat transfer coefficient up to void fractions of 0.91, as in the frozen version of RELAP5/MOD2 is questionable. The prefactor of 0.2 in the Forslund-Rohsenow correlation, which was set to 0.4 in this work, could be increased even more. It was tried with 0.75 for example by using only the Forslund-Rohsenow correlation to very low void fractions (which is also questionable), instead of using the Modified Bromley correlation, with good results for the NEPTUN experiments. An important fact is, that with the Forslund-Rohsenow correlation and the modification in the selection logic one obtains quite a smooth and well predicted transition from steam cooling to dispersed film boiling and film boiling, because this formula contains a void fraction dependence, which goes to zero when the void fraction goes to 1.0. Additionally, the turnaround temperatures and times were very well predicted in the NEPTUN low flooding rate experiment 5036.

It is very interesting that the spikes in the steam ocities in the test section calculated by the code disappeared, and the oscillation these velocities were suppressed after implementing the Forslund-Rohsenow correlation into the code and modifying the interpolation between Bromley and Forslund- Rosenow for high void fractions. This effect was very significant both in the calculations of NEPTUN and of FLECHT.

For the high flooding rate NEPTUN tests, the "modified" Bromley correlation is selected for the Post-Dry out heat transfer; though, this correlation is somewhat modified and differs from its original form, and is multiplied by an unjustified void-depended factor, which results in over-prediction of the film boiling heat transfer. In the FLECHT high flooding rate experiment, the frozen version calculated quite well the rod cladding temperatures. The empirical factor, with which the modified Bromley correlation was multiplied, fitted well this experiment, but not the NEPTUN tests. By bringing back the Modified Bromley correlation to its original form, taking into account the subcooling by another more physical factor and by changing an exponent in the Weismann transition film boiling correlation, the rod surface temperature histories were well predicted by the code for the high flooding rate experiments in both facilities, FLECHT and NEPTUN. Without this change in the Weismann correlation, the film boiling wall heat transfer would be a little underpredicted in the high flooding rate FLECHT experiment.

The correction of the criterion for selecting the pre-dry out interphase friction correlations near the quench front eliminated the void fraction oscillations in calculating both facilities, FLECHT and NEPTUN. The good prediction of void fractions in the NEPTUN and FLECHT low flooding rate experiments with the modified version EIR-update 83 is mainly due to the new bubbly-slug interphase friction correlation and the suppression of oscillations is also due to the modifications mentioned above.

In the NEPTUN facility the quench temperatures calculated by RELAP5/MOD2 were too low for all experiments. The change of an exponent in the Weismann transition film boiling correlation resulting in an increased transition boiling heat transfer increased the predicted quench temperatures in RELAP5/MOD2. To what extent this modification is reasonable, can only be said after analyzing tests in other facilities. In FLECHT for example, the experimental quench temperatures were lower than in NEPTUN. For determining a reasonable value for this exponent in the Weismann correlation extensive data from quenching of nuclear rods should be analyzed, for example from LOFT, since the quench behaviour of nuclear rods could be different from the one of electrically heated rods [13,14].

An effect not understood is the different behaviour of RELAP5/MOD2 at low flooding rates in calculating the two facilities NEPTUN and FLECHT. For NEPTUN, the code calculates lower wall heat transfer during dispersed film boiling and therefore higher turnaround temperatures and later turnaround times, while in FLECHT the opposite phenomenon is observed: lower turnaround temperatures. In FLECHT, this overprediction of the wall heat transfer until the turnaround point is caused by water droplets, which evaporate. This momentarily decreases the steam temperatures and causes large oscillations in the steam temperatures and hence, to the wall-to-vapour heat flux. The driving force of this behaviour is the interphase heat transfer (or area), which is probably too high.

An unresolved problem is also the water entrainment in the FLECHT low flooding rate experiment, which is overpredicted by the code by a factor of [illegible] with the frozen version and by a factor of 6 with the modified version.

The effect of the nodalization chosen is smaller than the deviation of the code from the experiment. In the calculated high and low flooding rate NEPTUN tests, the difference of the cladding temperatures and of the quench times for the three tested nodalizations with 10, 18 and 32 volumes was only 50 percent of the deviation of the frozen version of the code from the experiment. For a core, not more than 20 volumes should be used, because there will not be big differences in the results and the computer costs will increase by using more number of volumes. 10 volumes for a core should be the minimum.

As shown in tables 2 and 3 some uncertainties exist in the NEPTUN tests, for example, in the flooding water mass flow rate or in the measured entrainment in low flooding rate experiment 5036. It can be stated that the main conclusions drawn from this work are independent of these uncertainties. The differences of the results of RELAP5/MOD2 by changing the flooding water mass flow rate by 5.3 percent are small. Hence, one can safely say that for the separate effect tests analyzed in this work, the differences between measurements and predictions resulting from model deficiencies in the code are dominant over any experimental uncertainties.

Concluding this section, we feel that some final remarks are necessary for clarifying a few points related to the actual physical modeling of the reflooding process and the way it is treated in RELAP5/MOD2, but also in other thermal-hydraulic transient analysis codes. In this work, we have tried to explain the differences between measurements and code predictions and, if possible, try to eliminate them by appropriately modifying the code. With the exception of the modification of the bubbly/slug interfacial shear in rod bundles which is by now well-established and tested, all the other modifications reported in this work, are based on modifying in the code correlations which are in many situations used out of content; we shall demonstrate this by two examples.

a) High flooding rate and subcooling reflooding: The code uses the modified Bromley correlation for the wall heat transfer to the liquid. Though, this correlation was derived by assuming certain interphacial shear and heat transfer relations which may not be compatible with the ones used in the (two-fluid) codes; additionally, for this situation, the codes assume a heat transfer coefficient **both** to the liquid (Bromley) and to the vapour while strictly speaking, the Bromley represents an **over-all** heat transfer to the mixture and as such, would be suitable for 4 equation codes.

b) Low flooding rate, saturated liquid at the quench front: Downstream, the codes also use the modified Bromley for the wall heat transfer to the liquid. This gives an almost constant heat transfer coefficient, contrary to the experimental findings that there is a rather strong exponential increase of the heat transfer coefficient as we approach the quench front from the dry region. In this respect, even for this situation, the Bromley correlation is used totally out of content and a more appropriate approach would have been to use a wall heat transfer coefficient to the liquid which, among other parameters, is a function of the distance from the quench front. Though, we do appreciate the fact that in a general purpose code, such an approach would probably create more problems than it would solve, since it is not clear how (if at all) such an approach could handle multiple quench fronts. Hence, one can conclude that in general, the very nature of the wide variety of cases which these codes are supposed to model as well as the relatively large nodes required for having a cost-effective calculation, makes the introduction of sophisticated and physically sound models in these codes an extremely difficult task without any guarantee that the outcome of such an approach would result in better agreement between measurements and predictions.

8 Run statistics

The model used for the NEPTUN facility consisted of 20 volumes (18 in the test section, an upper and a lower plenum), 2 junctions and 16 heat structures.

For run statistics, two experiments are shown, 5036 with the lowest flooding rate and 5050 with the highest flooding rate. The CPU time of this two experiments can be seen in figures 57 and 58. In figures 59 and 60 the time step chosen by the code and the user specified maximum time step of these two experiments are shown.

The number

$$\frac{CPU \cdot 10^3}{C \cdot DT}$$

where	CPU	= used computer time
	C	= number of volumes
	DT	= number of time steps

was 33.4 for the 400 seconds of transient time of the experiment 5036 and 27.8 for the 70 seconds of transient time of the experiment 5050.

The code was running on a CDC cyber 170-730. Later on, for all calculations with modifications of the code, a cyber 180-855 was used, which is 5-6 times faster than the cyber 170-730.

9 Conclusions

As shown in the previous section, in this work some deficiencies of RELAP5/MOD2 during reflooding could be identified, and in some cases, they could be eliminated. On the basis of these findings, the following conclusions can be drawn and recommendations given:

i. High and medium flooding rate experiments were predicted relatively well with RELAP5/MOD2. This is an important fact, because in full scale best estimate power plant calculations, relatively high flooding rates are to be expected during the reflood phase of a LOCA [14].

ii. Calculations for low flooding rates show large differences between measurement and predictions of RELAP5/MOD2. Changes in interfacial friction and wall heat transfer brought some improvements to RELAP5/MOD2 predictions.

iii. The interphase friction correlations of the code which are obtained from tube experiments may not always be applicable for the rod bundle geometry of a reactor core. The interphase friction is smaller in rod bundle geometries than in tubes, and it is this parameter which determines mainly the amount and the distribution of the water in the bundle during reflooding.

iv. The implementation of a new bubbly/slug flow interphase friction correlation for rod bundles from CATHARE into the RELAP5/MOD2 code gives very good prediction of the amount of water in the test section during reflooding at low flooding rates.

v. The use of different correlations for the interphase friction in rod bundles and in tubes makes necessary to have different correlations for core and for the other system components. It is suggested that other correlations are used in the core than the ones used for pipes.

vi. The modifications of the wall to liquid heat transfer during reflooding resulted in better agreement between measurements and predictions and eliminated some numerical oscillations which were resulting in "numerical" liquid carry-over.

vii. The interphase friction is one of the dominant parameters during reflooding, mainly for low flooding rates. Void fractions and therefore heat transfer coefficients are strongly dependent on the interphase friction.

viii. Attention should be paid to the quench temperatures predicted by RELAP5/MOD2: the code calculates too low quench temperatures. Within the framework of existing logic in the code, we have shown that this problem can be solved by modifying the Weismann transition boiling correlation.

ix. Nodalization effects are not very important during precursory cooling but acquire some importance in calculating the quench temperature. For a reactor core, 15–20 volumes are recommended, but we believe that one should not use less than 10 core volumes for large break LOCA calculations.

Exp.Nr.	Pressure (bar)	Flooding water Velocity (cents)	Subcooling (°C)	Single Rod Power (kW)	Maximum Initial Cladding Temperature (°C)
34006	2.7	1.5	79	Max 2.90 Min 1.51	882
31701	2.8	15	78	Max 5.00 Min 3.64	872

Table 4: Test parameters of the two FLECHT-SEASET reflooding experiments calculated with RELAP5/MOD2.

References

[1] H. Grütter, F. Stierli, S.N. Aksan, G. Varadi (1981)
NEPTUN bundle reflooding experiments: Test facility description.
EIR-report Nr. 386

[2] Victor H. Ransom et al (1985)
RELAP5/MOD2 Code Manual, Vol. 1+2.
NUREG/CR-4312

[3] M. Richner (1987)
Vergleich der Flutversuche NEPTUN 1 und NEPTUN 2.
EIR internal report TM-32-87-06.

[4] D. Bestion (1985)
Interfacial friction determination for the 1D-6 equations two fluid model used in the CATHARE code.
European Two-Phase Flow Group Meeting, Southhampton, England.

[5] G.Th. Analytis (1986)
Assessment of a new interfacial friction correlation in TRAC-BD1/MOD1.
Trans.Amer.Nucl.Soc., 52, 481.

[6] R.P. Forslund, W.M. Rohsenow (1968)
Dispersed Flow Film Boiling
Journal of Heat Transfer, 90, 399-407

[7] Analytis, G.Th. and Aksan, S.N. (1984)
"TRAC-BD1 assessment using boil-off experiments in a rod bundle"
Trans.Amer.Nucl.Soc., 47, 493.

[8] Analytis, G.Th. and Aksan, S.N. (1984)
"Trac-BD1 Assessment under Severe Accident Boil-Off Conditions",
5th Intern. Meeting on Thermal Nuclear Reactor Safety, Karlsruhe, Sept. 9-13, 1984. KfK 3880, Vol.3, pp. 1821-1830.

[9] Analytis, G.Th., Richner, M., Andreani, M. and Aksan, S.N. (1986),
"Assessment and Uncertainty Identification for RELAP5/MOD2 and TRAC-BD1/MOD1 Codes under Core Uncovery and Reflooding Conditions".
Presented at the 14th Water Reactor Safety Information Meeting, October 27-31, Gaithersburg, Maryland, USA.

[10] Loftus M.J. et al. (1980)
PWR FLECHT-SEASET Unblocked Bundle, forced and Gravity Reflood Task Data Report
NUREG/CR-1532, Vol.2.

[11] G. Yadigaroglu, S.N. Aksan (1985)
The NEPTUN Working Databank
First Meeting, International Thermal Hydraulics Code Assessment and Applications Program, Silver Springs, Md. April 23-26, 1985.

[12] Peter Taube, unpublished work at EIR (1984)

[13] S.N.Aksan, E.L. Tolman, R.A. Nelson (1983)
Application of Analytical Capability to Predict Rapid Cladding Cooling and Quench during the Blowdown Phase of a Large Break Loss-of-Coolant Accident
Proceedings of the Second International Topical Meeting on Nuclear Reactor Thermal-Hydraulics Vol. 1, Santa Barbara, CA, USA, January 1983

[14] S.M. Modro, S.N. Aksan, V... Berta, A.B. Wahba (1988)
Review of LOFT Large Break Experiments
OECD/LOFT-T-3900, August 1988

APPENDIX A

Listing of Input Deck of NEPTUN test 5036

```
***************************************************************************************
* RELAP5/MOD2/36.02 - SIMULATION OF NEPTUN-REFLOOD-EXPERIMENT 5036
***************************************************************************************
*
* MISCELLANEOUS CONTROL CARDS
*
00000100 NEW      TRANSNT
00000101 RUN
00000105 1.       2.
*
* TIME STEP CONTROL CARDS
*
00000201 400.    1.0E-6  0.02     3         50       2000     4000
*
* MINOR EDIT REQUESTS
*
00000301 TEMPG    002030000
00000302 TEMPF    002030000
00000303 VOIDG    002030000
00000304 HTRNR    001100301
00000305 HTHTC    001100301
00000306 HTTEMP   001100310
00000307 TEMPG    002070000
00000308 TEMPF    002070000
00000309 VOIDG    002070000
00000310 HTRNR    001100701
00000311 HTHTC    001100701
00000312 HTTEMP   001100710
00000313 HTTEMP   001100910
00000314 TEMPG    002110000
00000315 TEMPF    002110000
00000316 VOIDG    002110000
00000317 HTRNR    001101101
00000318 HTHTC    001101101
00000319 HTTEMP   001101110
00000320 CNTRLVAR 1
00000321 CNTRLVAR 2
00000322 CNTRLVAR 3
00000323 CNTRLVAR 6
*
* TRIP FOR WATER INLET
*
00000401 TIME    0        GE       NULL     0        0.       L
*
* HYDRODYNAMIC COMPONENTS
*
* WATER TANK
0010000 TANK      TMDPVOL
0010101 1.0E+6  1.       0.       0.       90.      1.       0.       0.       10
0010200 101
0010201 0.        407.15  0.
*
* TEST SECTION
0020000 CORE      PIPE
0020001 18
0020101 1.0026E-4 16
0020102 2.4002E-4 18
0020301 0.10      1
0020302 0.124     2
0020303 0.116    13
0020304 0.09     15
0020305 0.06     16
0020306 0.042    18
0020601 90.      18
0020801 0.        8.6161E-3 16
0020802 0.        8.6375E-2 18
0021001 00       18
0021101 30000    15
0021102 30100    16
0021103 30000    17
```

```
0021201 103      4.12400E+5  615.94 0.  0.       0.      1
0021202 103      4.12400E+5  707.43 0.  0.       0.      2
0021203 103      4.12400E+5  797.73 0.  0.       0.      3
0021204 103      4.12400E+5  866.4. 0.  0.       0.      4
0021205 103      4.12400E+5  916.01 0.  0.       0.      5
0021206 103      4.12400E+5  949.58 0.  0.       0.      6
0021207 103      4.12400E+5  959.47 0.  0.       0.      7
0021208 103      4.12400E+5  927.44 0.  0.       0.      8
0021209 103      4.12400E+5  873.93 0.  0.       0.      9
0021210 103      4.12400E+5  815.95 0.  0.       0.      10
0021211 103      4.12400E+5  735.12 0.  0.       0.      11
0021212 103      4.12400E+5  623.43 0.  0.       0.      12
0021213 103      4.12400E+5  525.79 0.  0.       0.      13
0021214 103      4.12400E+5  513.10 0.  0.       0.      14
0021215 103      4.12400E+5  512.25 0.  0.       0.      15
0021216 103      4.12400E+5  429.69 0.  0.       0.      16
0021217 103      4.12400E+5  428.09 0.  0.       0.      17
0021218 103      4.12400E+5  426.02 0.  0.       0.      18
0021300 1
0021301 0.       0.       0.       17
*
* UPPER PLENUM
0030000 UPPERPL  TMDPVOL
0030101 1.0E+6   1.       0.       0.       90.      1.       0.       0.       10
0030200 102
0030201 0.       4.124E+5 1.
*
* LOWER JUNCTION
0040000 LOWJUNCT TMDPJUN
0040101 001000000  002000000  1.3026E-4
0040200 1        401
0040201 0.       0.       0.       0.
0040202 0.       1.422E-3  0.      0.
*
* UPPER JUNCTION
0050000 UPJUNCT SNGLJUN
0050101 002010000  003000000  2.4002E-4 0.       0.       30100
0050201 1        0.       0.       0.
*
* HEAT STRUCTURES
*
* HEATER RODS
10011000 16      10       2        0        0.       401      1        16
10011100 0       1
10011101 1       1.42E-3
10011102 1       2.8E-3
10011103 1       3.1E-3
10011104 1       3.9E-3
10011105 1       4.2E-3
10011106 1       4.5E-3
10011107 1       4.743E-3
10011108 1       5.0E-3
10011109 1       5.36-3
10011201 5       1
10011202 4       2
10011203 1       3
10011204 3       4
10011205 1       5
10011206 2       6
10011207 1       9
10011301 1.      1
10011302 0.      9
10011400 -1
10011401  629.35  626.11  619.54  618.98  618.92  618.65  618.13
+         618.32  617.95  617.91
10011402  726.27  721.88  712.00  711.26  711.17  710.83  709.90
+         709.75  709.65  709.60
10011403  821.63  816.27  803.09  802.19  802.08  801.67  800.25
+         800.07  799.95  799.89
10011404  894.36  888.32  872.42  871.43  871.30  870.83  868.98
+         868.78  868.64  868.58
10011405  946.59  940.13  922.30  921.26  921.09  920.63  918.41
+         918.20  918.05  917.98
10011406  981.23  974.64  955.83  954.76  954.61  954.10  951.71
+         951.49  951.34  951.27
10011407  990.57  984.07  965.41  964.35  964.20  963.71  961.31
+         961.09  960.95  960.88
```

```
10011408  956.39   950.17   932.82   931.80   931.66   931.19   929.03
*         928.83   928.69   928.62
10011409  899.32   843.54   878.45   877.51   877.38   876.95   875.16
*         874.98   874.85   874.79
10011410  836.51   831.57   819.25   818.43   818.32   817.94   816.60
*         816.43   816.32   816.27
10011411  749.75   745.83   736.74   736.13   736.06   735.75   734.87
*         734.74   734.65   734.62
10011412  631.16   628.47   622.99   622.53   622.48   622.26   621.82
*         621.73   621.67   621.64
10011413  527.71   526.25   523.62   523.36   523.33   523.21   523.03
*         522.98   522.95   522.93
10011414  517.87   516.54   514.17   513.93   513.91   513.80   513.64
*         513.59   513.56   513.54
10011415  517.79   516.46   514.09   513.85   513.83   513.72   513.56
*         513.51   513.48   513.46
10011416  418.99   418.99   418.99   418.99   418.99   418.99   419.00
*         419.00   419.00   419.00
10011501 0         0        0        0        0.       16
10011601 002010000 0        1        1        0.10     1
10011602 002020000 0        1        1        0.124    2
10011603 002030000 10000 1           1        0.116    13
10011604 002140000 10000 1           1        0.09     15
10011605 002160000 0        1        1        0.06     16
10011701 100      3.7239E-2 0.      0.       1
10011702 100      6.6530E-2 0.      0.       2
10'11703 100      8.0456E-2 0.      0.       3
10011704 100      9.4522E-2 0.      0.       4
10011705 100      0.104033  0.      0.       5
10011706 100      0.106275  0.      0.       6
10011707 100      0.107084  0.      0.       7
10011708 100      0.100801  0.      0.       8
10011709 100      8.4825E-2 0.      0.       9
10011710 100      7.4768E-2 0.      0.       10
10011711 100      [illegible]68E-2 0.      0.       11
10011712 100      [illegible]45E-2 0.      0.       12
10011713 100      1[illegible]06E-2 0.      0.       13
10011714 100      1.2874E-2 0.      0.       15
10011715 0        0.        0.      0.       16
10011901 0        1.3568E-2 0.      0.       16
*
* THERMAL PROPERTY DATA
*
20100100 TBL/FCTN 1       -1       *INCONEL 600
20100200 TBL/FCTN 1       -1       *AL203
20100300 TBL/FCTN 1       -1       *COPPER
20100400 TBL/FCTN 1       -1       *BORON NITRID
20100500 TBL/FCTN 1       -1       *KANTHAL
*
* THERMAL CONDUCTIVITIES (W/M-K)
* INCONEL 600
20100101 293.15   14.49     373.15  15.64     473.15   17.53
20100102 573.15   19.21     673.15  20.90     773.15   22.59
20100103 823.15   23.43     873.15  24.28     973.15   25.97
20100104 1023.15  26.61     1073.15 27.65     1173.15  29.34
20100105 1273.15  31.03     1373.1  32.72     1473.15  34.41
20100106 1573.15  36.10
*
* AL203
20100201  293.15  16.31      373.15 13.13      473.15  10.23
20100202  573.15   8.03      673.15  6.36      773.15   5.21
20100203  873.15   4.45      973.15  3.89     1073.15   3.48
20100204 1173.15   3.19     1273.15  2.99     1373.15   2.55
20100205 1473.15   2.75     1573.15  2.70
*
* COPPER
20100301  323.15  395.7      373.15 391.5      473.15  383.2
20100302  573.15  374.8      673.15 366.4      773.15  358.0
20100303  873.15  350.9      973.15 344.2     1073.15  337.5
20100304 1173.15  330.8     1273.15 324.1     1373.15  317.4
*
* BORON NITRID
20100401  293.15  15.67      323.15 15.57      373.15  15.075
20100402  473.15  14.07      573.15 13.065     673.15  12.33
20100403  773.15  11.88      873.15 11.43      973.15  10.995
20100404 1073.15  10.74     1173.15 10.59     1273.15  10.44
20100405 1373.15  10.29     1473.15 10.14     1573.15   9.99
```

```
*
* KANTHAL
20100501  323.15  17.1        373.15  17.7        473.15  19.1
20100502  573.15  20.4        673.15  21.7        773.15  23.1
20100503  873.15  24.4        973.15  25.8       1073.15  27.1
20100504 1173.15  28.4       1273.15  29.8       1373.15  31.1
20100505 1473.15  32.4
*
* VOLUMETRIC HEAT CAPACITIES (J/M3-K)
* INCONEL 600
20100151  3.6491E+6   3.9073E+6   4.1096E+6   4.2757E+6   4.4258E+6
20100152  4.5800E+6   4.6618E+6   4.7630E+6   5.0470E+6   5.1297E+6
20100153  5.1760E+6   5.2392E+6   5.2696E+6   5.3404E+6   5.3910E+6
20100154  5.4416E+6
*
* AL2O3
20100251  3.1190E+6   3.5442E+6   3.9064E+6   4.1572E+6   4.3358E+6
20100252  4.4612E+6   4.5524E+6   4.6284E+6   4.6930E+6   4.7500E+6
20100253  4.7456E+6   4.8246E+6   4.8564E+6   4.8830E+6
*
* COPPER
20100351  3.4381E+6   3.5095E+6   3.6470E+6   3.7685E+6   3.8488E+6
20100352  3.9560E+6   4.0721E+6   4.1792E+6   4.2596E+6   4.3668E+6
20100353  4.4382E+6   4.5007E+6
*
* BORON NITRID
20100451  1.4254E+6   1.6175E+6   1.8711E+6   2.3052E+6   2.6529E+6
20100452  2.9180E+6   3.0467E+6   3.2426E+6   3.3771E+6   3.4962E+6
20100453  3.5461E+6   3.6787E+6   3.7421E+6   3.7901E+6   3.8205E+6
*
* KANTHAL
20100551  3.0956E+6   3.2163E+6   3.4435E+6   3.6778E+6   3.9121E+6
20100552  4.1464E+6   4.3736E+6   4.6079E+6   4.8422E+6   5.0765E+6
20100553  5.3037E+6   5.5380E+6   5.7723E+6
*
* POWER TABLE
*
20210000 POWER
20210001 0.       2448.5
20210002 1000.    2448.5
*
* CONTROL VARIABLES
*
* COLLAPSED LIQUID LEVEL
20500100 COLIQLEV SUM     1.      0.      0
20500101 0.       0.1     VOIDF   002010000
20500102 0.124    VOIDF   002020000
20500103 0.116    VOIDF   002030000
20500104 0.116    VOIDF   002040000
20500105 0.116    VOIDF   002050000
20500106 0.116    VOIDF   002060000
20500107 0.116    VOIDF   002070000
20500108 0.116    VOIDF   002080000
20500109 0.116    VOIDF   002090000
20500110 0.116    VOIDF   002100000
20500111 0.116    VOIDF   002110000
20500112 0.116    VOIDF   002120000
20500113 0.116    VOIDF   002130000
20500114 0.09     VOIDF   002140000
20500115 0.09     VOIDF   002150000
20500116 0.06     VOIDF   002160000
20500117 0.092    VOIDF   002170000
20500118 0.092    VOIDF   002180000
*
* ENTRAINMENT MASSFLOW
20500200 ENTRMFLO MULT    2.4002E-4 0.    0
20500201 RHOFJ    005000000
20500202 VELFJ    005000000
20500203 VOIDFJ   005000000
```

```
*
* ENTRAINMENT TANK CONTENT
20500300 ENTRAINM INTEGRAL 1.     0.       0
20500301 CNTRLVAR 2
*
* TIME STEP
20500400 OLDTIME  SUM      1.       0.       0
20500401 0.       1.       CNTRLVAR 5
*
20500500 NEWTIME  SUM      1.       0.       0
20500501 0.       1.       TIME     0
*
20500600 TSTEP    SUM      1.       0.       0
20500601 0.       -1.      CNTRLVAR 4
20500602 1.       CNTRLVAR 5
*
. . . . . RELAP5/MOD2 TERMINATOR CARD
```

APPENDIX B

Updates to create version EIR-update 83 of RELAP5/MOD2

```
*IDENT MARTIN
*I PHAINT.9
      COMMON/IFLG2/IFLAG2(1000)
      DIMENSION IFLAG1(1000)
*I PHAINT.15:
      IIFL1=(I-IV+IVSKP)/IVSKP
      IFLAG1(IIFL1)=0
*I PHAINT.294
      TGSAT = TGSAT - 40.*VOIDF(I)
*I PHAINT.370
      IF(FRUP.GT.0.0.OR.FSLUG.GT.0.0.AND.DIAMV(I).LT.0.018)
     1 IFLAG1(IIFL1)=1
*I PHAINT.390
      IF(DIAMV(I).LT.0.018) THEN
      FIC=65.0*VOIDG(I)*VOIDF(I)**3.0*RHOG(I)/DIAMV(I)
      ENDIF
*I PHAINT.421
      IF(DIAMV(I).LT.0.018) THEN
      FIC1=65.0*VOIDG(I)*VOIDF(I)**3.0*RHOG(I)/DIAMV(I)
      ENDIF
*I PHAINT.424
      IF(DIAMV(I).GE.0.018) THEN
*I PHAINT.425
      ENDIF
*I PHAINT.495
      IF(DIAMV(I).LT.0.018) FIC1=FIC1*0.5
*I PHAINT.633
      IF(DIAMV(I).LT.0.018) THEN
      FIC1 = VOID*(FIC1*0.5+1.225*0.4*RHOG(I)*SLSLG*VJID**2.)
      ELSE
*I PHAINT.634
      ENDIF
*I PHAINT.656
      IF(DIAMV(I).LT.0.018) FIC=FIC*0.5
*I PHAINT.462
      IF(DIAMV(I).LT.0.018) FIC=FIC*0.5
*I PHAINT.855
      IIFL2=(I-IJ+IJSKP)/IJSKP
      IFLAG2(IIFL2)=0
*I PHAINT.919
      INDK=(K-IV+IVSKP)/IVSKP
      INDL=(L-IV+IVSKP)/IVSKP
      IF(IFLAG1(INDK).EQ.1.OR.IFLAG1(INDL).EQ.1) IFLAG2(IIFL2)=1
*D QFHTRC.156
      HTV2(INDZ)=HCCHFA*EXP(-0.0175*TERM)+GTERM*EXP(-0.012*TERM)
*D QFHTRC.178
      FACBR = (1.+0.025*AMAX1(0.,SATT(IDX)-TEMPF(IDX)))
      HCBR=AMAX1(HTV2(INDZ),(CONVAP*TERM1*TERM2*((SATHG(IDX)-SATHF(IDX))
*D QFHTRC.179
     1/AMAX1(TMPBDY-SATT(IDX),0.01)+0.68*CSUBPG(IDX))*9.81/(2.*3.14159)
*D QFHTRC.180
     2     *SQRT(9.81*TERM1/SIGMA(IDX)/VISCG(IDX))**0.25*0.62*FACBR)
      VELD=AMAX1(VELG(IDX)-VELF(IDX),0.001)
      DDROP=3.*SIGMA(IDX)/(RHOG(IDX)*VELD**2)
      IF(DDROP.LT.1.5E-4) DDROP=1.5E-4
      IF(DDROP.GT.3.0E-3) DDROP=3.0E-3
      TERM5=1./(1.+0.35*CSUBPG(IDX)*AMAX1(TMPBDY-SATT(IDX),0.0001)
     1     /AMAX1(SATHG(IDX)-SATHF(IDX),0.01))**3.
      HCFD=0.4*3.14159/4.*(6.*(1.-VOIDG(IDX))/3.14159)**0.6666667
     1     *(9.81*RHOF(IDX)*RHOG(IDX)*AMAX1(SATHG(IDX)-SATHF(IDX),0.01)
     2     *TERM5*CONVAP/(AMAX1(TMPBDY-TEMPF(IDX),0.0001)*VISCG(IDX)
     3     *(3.14159/6.)**0.3333333*DDROP))**0.25
```

```
          IF(VOIDG(IDX).LT.0.6) THEN
            HCFB=HCBR
          ELSE
            IF(VOI^G(I[X).GE.0.8) THEN
              HCFB= .FD
            ELSE
              HCFB=(VOIDG(IDX)-0.6)/0.2*HCFD+(0.8-VOIDG(IDX))/0.2
     1            *HCBR
            ENDIF
          ENDIF
*  QFHTRC.187,188
          TERM=TERM2+HCFB
*D QFHTRC.209
     1      *AMAX1(0.023*(REYN2)**0.4/DIAMV(IDX),TERM4)
*D QFHTRC.221,223
          VELD=AMAX1(VELG(IDX)-VELF(IDX),0.001)
          DDROP=3.*SIGMA(IDX)/(RHOG(IDX)*VELD**2)
          IF(DDROP.LT.1.5E-4) DDROP = 1.5E-4
          IF(DDROP.GT.3.E-3) DDROP = 3.E-3
          TERM5=1./(1.+0.35*CSUBPG(IDX)*AMAX1(TMPBDY-SATT(IDX),0.0001)
     1        /(SATHG(IDX)-SATHF(IDX)))**3.
          HCFD=0.4*3.14159/4.*(6.*(1.-VOIDG(IDX))/3.14159)**0.6666667
     1      *(9.81*RHOF(IDX)*RHOG(IDX)*(SATHG(IDX)-SATHF(IDX))
     2      *TERM5*CONVAP/(AMAX1(TMPBDY-TEMPF(IDX),0.0001)*VISCG(IDX)
     3      *(3.14159/6.)**0.3333333*DDROP))**0.25
          HCFB=HCFD
*I VEXPLT.9
          COMMON/IFLG2/IFLAG2(1000)
*I VEXPLT.322
          C0=1.0
          C1=1.0
          IIFL2=(I-IJ+IJSKP)/IJSKP
          IF(IFLAG2(IIFL2).EQ.1) THEN
            C0=1.2
            C1=(1.0-C0*VOIDGA)/AMAX1((1.-VOIDGA),1.0E-5)
            IF(C1.LT.0.7) C1=0.7
          ENDIF
*D VEXPLT.323
          FJFG=(FIJ(I)*DX*(ABS(C1*VELGJO(I)-C0*VELFJO(I))+0.01)
*D VEXPLT.507
            DIFF =  SCRACH+(FRICFJ+C0*FJFG+VPGNX+HLOSSF)*DT
*D VEXPLT.508
            DIFG = -SCRACH-(FRICGJ+C1*FJFG+VPGNX+HLOSSG)*DT
*I VIMPLT.8
          COMMON/IFLG2/IFLAG2(1000)
*I VIMPLT.435
          C0=1.0
          C1=1.0
          IIFL2=(I-IJ+IJSKP)/IJSKP
          IF(IFLAG2(IIFL2).EQ.1) THEN
            C0=1.2
            C1=(1.0-C0*VOIDGA)/AMAX1((1.-VOIDGA),1.0E-5)
            IF(C1.LT.0.7) C1=0.7
          ENDIF
*D VIMPLT.436
          FJFG=(FIJ(I)*DX*(ABS(C1*VELGJO(I)-C0*VELFJO(I))+0.01)
*D VIMPLT.591
            COEFV(IDG-1) = (FRICFJ+C0*FJFG+VPGNX+HLOSSF)*DT + SCRACH
*D VIMPLT.592
            COEFV(IDG)   =-(FRICGJ+C1*FJFG+VPGNX+HLOSSG)*DT - SCRACH
*C DEFINE,PHAINT,QFHTRC,VEXPLT,VIMPLT
```

APPENDIX C

Mathematical formulation of the implementation of the new bubbly/slug flow interphase friction correlation into RELAP5/MOD2

The near bubbly/slug flow interphase friction correlation from CATHARE is based on the following vapour drift velocity [4]:

$$V_d = K\{\frac{g\Delta\rho D_H}{\rho_g}\}^{1/2} \qquad (1)$$

where g is the gravity constant, $\Delta\rho = \rho_l - \rho_g$, D_H the hydraulic diameter of the channel and K = 0.186.
From eq. (1) it can be shown that the interfacial shear per unit volume f_i can be expressed [5]

$$f_i = F_i' \mid C_1 V_g - C_0 V_\ell \mid (C_1 V_g - C_0 V_\ell) \qquad (2)$$

where

$$F_i' = \frac{\alpha(1-\alpha)^3 \rho_g}{K^2 D_H} \qquad (3)$$

and

$$C_1 = \frac{1 - \alpha C_0}{1 - \alpha} \qquad (4)$$

and C_0 = 1.2.
In this form the correlation was implemented into TRAC-BD1/MOD1 with k = 0.124 which was found to give better agreement to the NEPTUN boiloff tests [5].
In RELAP5/MOD2 f_i is expressed as

$$f_i = F_i \mid V_g - V_\ell \mid (V_g - V_\ell) \qquad (5)$$

where F_i are coefficients depending on the flow-regime.
The momentum equations are those of the sum and the difference. They are of the form:

$$A^n V_{\ell,j}^{n+1} + B^n V_{g,j}^{n+1} = R^n V_{\ell,j}^n + S^n V_{g,j}^n + D^n - (P_L - P_K)^{n+1} \frac{\Delta t}{\Delta x_j} \qquad (6)$$

$$E^n V_{\ell,j}^{n+1} - G^n V_{g,j}^{n+1} = Q^n V_{\ell,j}^n - W^n V_{g,j}^n + (\frac{\Delta\rho}{\rho_\ell \rho_g})_j^n \frac{\Delta t}{\Delta x_j}(P_L - P_K)^{n+1} + \Delta t(\rho' F_i)^n \mid V_g - V_\ell \mid_j^n (V_g - V_\ell)_j^{n+1} \qquad (7)$$

where

$$\rho' = \frac{(1-\alpha)\rho_\ell + \alpha\rho_g}{\alpha(1-\alpha)\rho_\ell\rho_g} \tag{8}$$

n and $n+1$ refer to the old and new time levels, respectively, P is the pressure, $A^n, \ldots W^n$ are coefficients of variables evaluated at time n and also of mesh-size Δx_j and time-step Δt; j denotes the cell-boundary and K and L denote the cell-centres upstream and downstream of j, respectively.
After rearranging Eq. (7), Eqs. (6) and (7) form a system of two linear algebraic equations with $V_{g,j}^{n+1}$ and $V_{\ell,j}^{n+1}$ as unknowns and are solved for each n and j.

The bubbly/slug interphase friction correlation was implemented in RELAP5/MOD2 by modifying the difference phasic momentum equation both in the semi-implicit and the nearly-implicit solution schemes; for the former scheme, Eq. (7) now reads:

$$\begin{aligned} &\{E^n + (\rho' F_i')^n \Delta t C_0 \mid C_1 V_g - C_0 V_\ell \mid_j^n\} V_{\ell,j}^{n+1} \\ &-\{G^n + (\rho' F_i')^n \Delta t C_1 \mid C_1 V_g - C_0 V_\ell \mid_j^n\} V_{g,j}^{n+1} = \\ &= (\frac{\Delta\rho}{\rho_\ell \rho_g})_j^n (P_L - P_K)^{n+1} \frac{\Delta t}{\Delta x_j} + Q^n V_{\ell,j}^n - W^n V_{g,j}^n \end{aligned} \tag{9}$$

Hence, for bubbly or slug flow, Eqs. (6) and (7) are solved.

For the implementation of this new bubbly/slug flow interphase friction correlations the subroutines PHAINT, VEXPLT and VIMPLT had to be changed, as it can be seen in appendix B.

APPENDIX D

Summary description of the FLECHT-SEASET facility and tests

Summary description of the FLECHT-SEASET facility and tests will be presented in this appendix for reader convenience. Further detailed information about the facility and the tests can be obtained from the references given at the end of this appendix (references D.1 to D.3).

The USNRC/EPRI/Westinghouse jointly sponsored Full Length Emergency Core Heat Transfer Separate Effects And System Effects Test (FLECHT-SEASET) program was developed to obtain detailed two-phase flow and heat transfer information needed for developing or assessing best estimate computer models for the reflood phase of a postulated loss of Coolant Accident (LOCA).

The FLECHT-SEASET unblocked bundle test facility is a once-through forced or gravity flow reflood heat transfer system which includes:

1. A water injection system for either forced flooding or gravity reflooding. Initial flooding rates were varying between 1 cm/sec to 15 cm/sec inlet coolant velocities.
2. A full length heater rod bundle of 17 x 17 PWR fuel bundle assembly dimensions with 161 heater rods.
3. A lower plenum to straighten the inlet flow.
4. A upper plenum to act as a steam water separator.
5. Liquid collection tanks to collect the entrained liquid at the test section exit.
6. A steam water separator to permit the drying of the exit steam so that a single phase flow measurement can be made.
7. Various instrumentation to measure flows, heater rod, vapor, fluid, and piping temperatures, void fraction, and entrained liquid.

The facility was designed for 4.1 bar nominal pressure and is capable of repeated tests with heater rod temperatures not exceeding 1100°C. A schematic of the flow loop is shown in figure D.1.

A cross section of the test bundle is shown in figure D.2. The bundle is comprised of 161 heater rods (93 noninstrumented and 68 instrumented), 4 thimbles instrumented with wall thermocouples, 12 steam probes, 8 solid triangular fillers, and 8 grids. The triangular fillers reduced the amount of excess flow area from 9.3. to 4.7 percent and they were also welded to the grids to maintain the proper grid location. The axial power shape built in the heater rod was the modified cosine with a power peak-to-average ratio of 1.66 as shown in figure D-3. Peak power value of 2.3 kw/m could be achieved. Radial power distribution was uniform in the bundle. A low mass housing design was utilized in order to minimize the housing effects.

One of the key measurements made in the unblocked bundle tests was the non-equilibrium vapor temperature measurement. Aspirating steam probes were used to measure the vapor temperature and were located in the bundle and in the test section

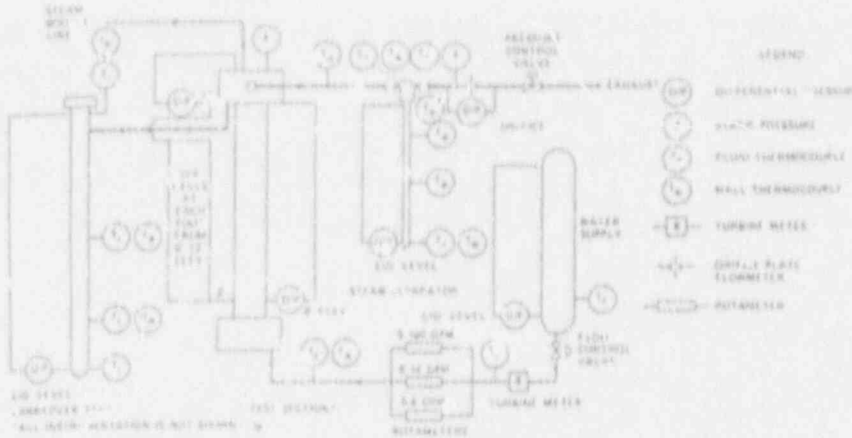

Figure D.1. Schematic of Test Loop

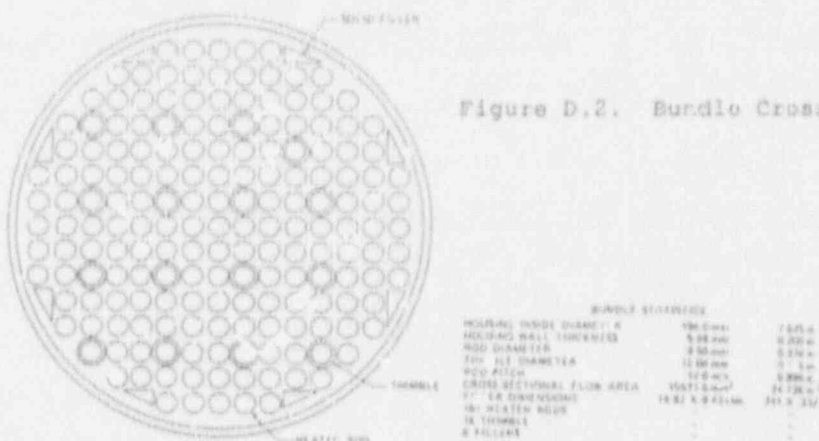

Figure D.2. Bundle Cross Section

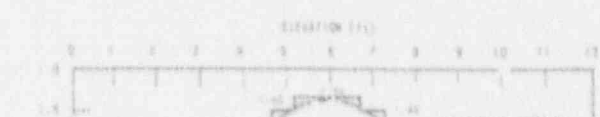

Figure D.3. Cosine Axial Power Profile for FLECHT-SEASET rods outlet. The test facility was designed for automatic operation whenever critical functions required a high degree of sophistication, safety or repeatability. The Computer Data Acquisition System (CDAS) was the heart of the operation by monitoring, protecting and controlling the facility operation besides collecting data.

The details on the design of the facility, the data obtained from FLECHT-SEASET tests, and the analysis of this data can be found in references D.1 - D.3.

References

D.1 M.J. Loftus, et.al. (1980)
"PWR FLECHT-SEASET Unblocked Bundle Forced and Gravity Reflood Data Report" NUREG/CR-1532, Vol.1.

D.2 M.J. Loftus, et.al. (1980)
"PWR FLECHT SEASET Unblocked Bundle Forced and Gravity Reflood Data Report" NUREG/CR-1532, Vol.2.

D.3 N. Lee, et.al (1982)
"PWR FLECHT-SEASET Unblocked Bundle, Forced and Gravity Reflood Task: Data Evaluation and Analysis" NUREG/CR-2256.

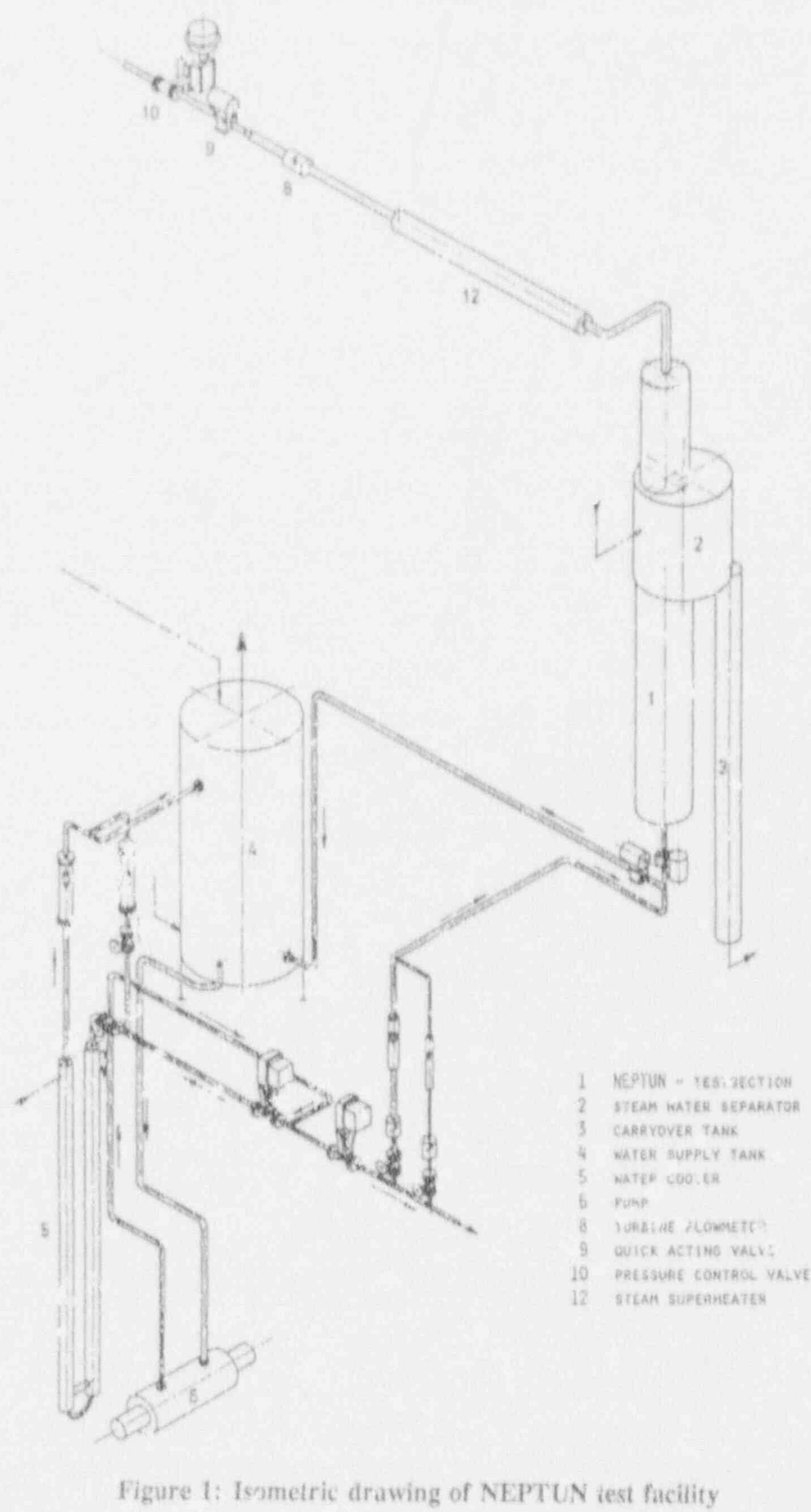

Figure 1: Isometric drawing of NEPTUN test facility

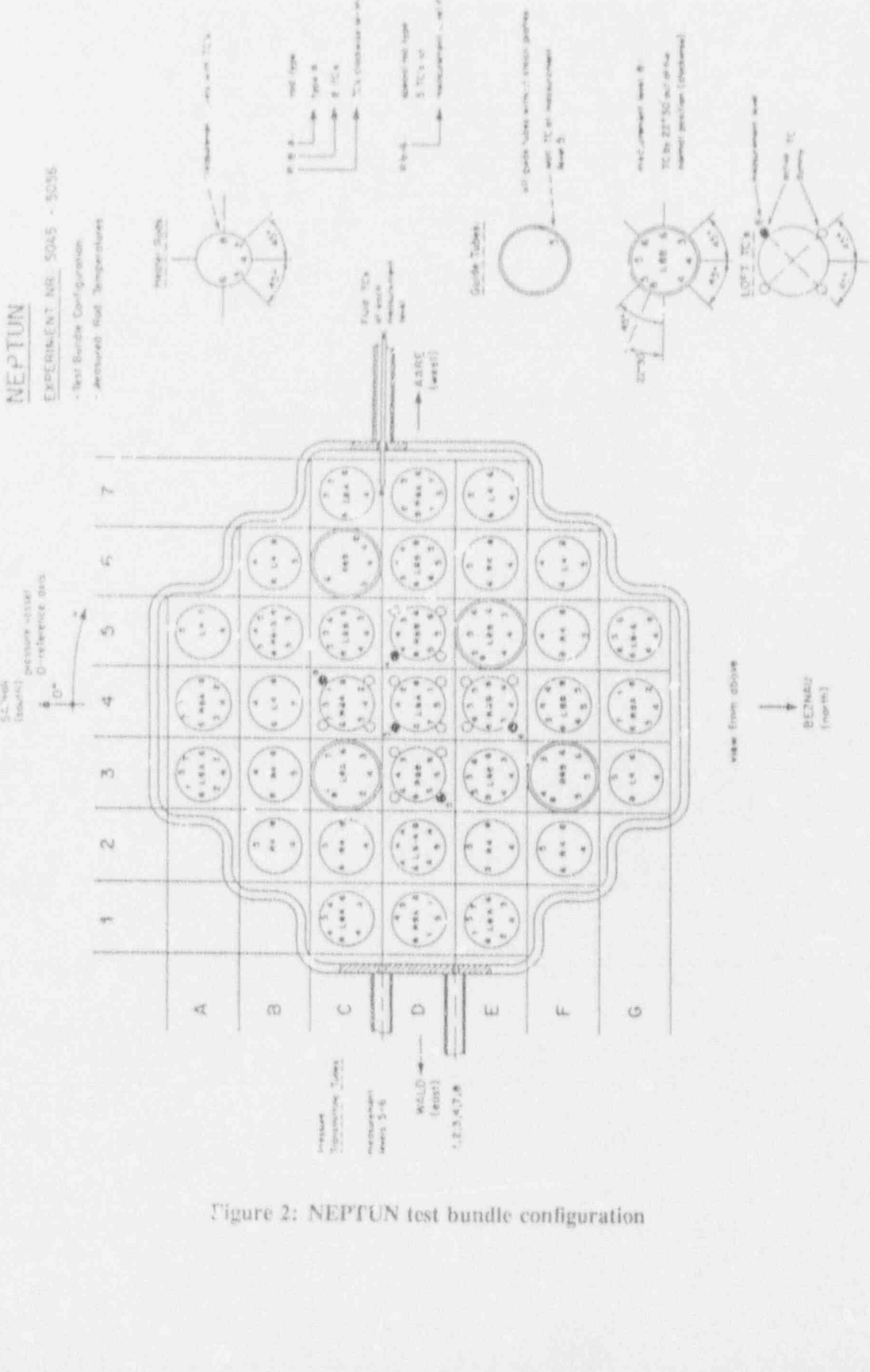

Figure 2: NEPTUN test bundle configuration

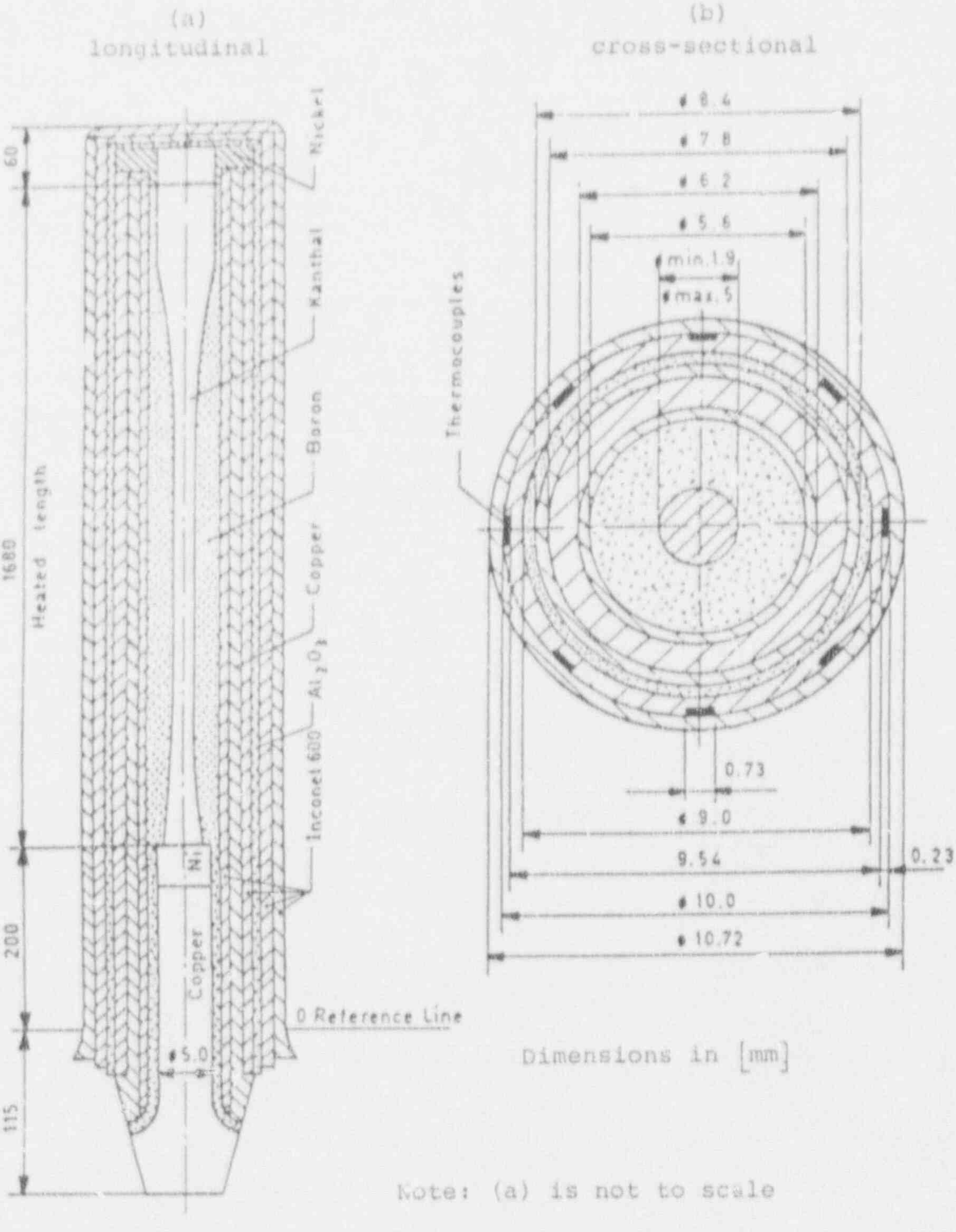

Figure 3: Geometry of NEPTUN heater element (schematic)

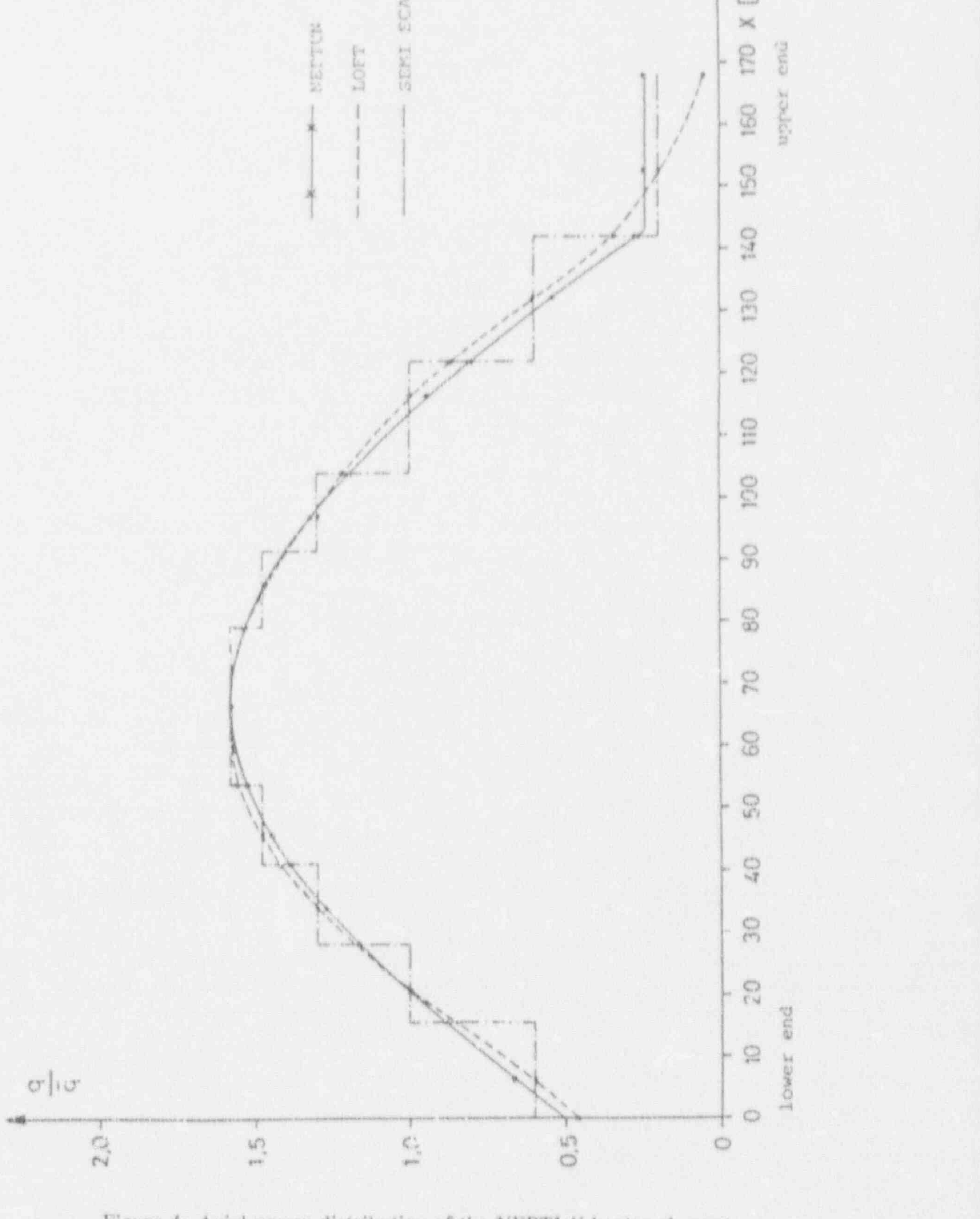

Figure 4: Axial power distribution of the NEPTUN heater element

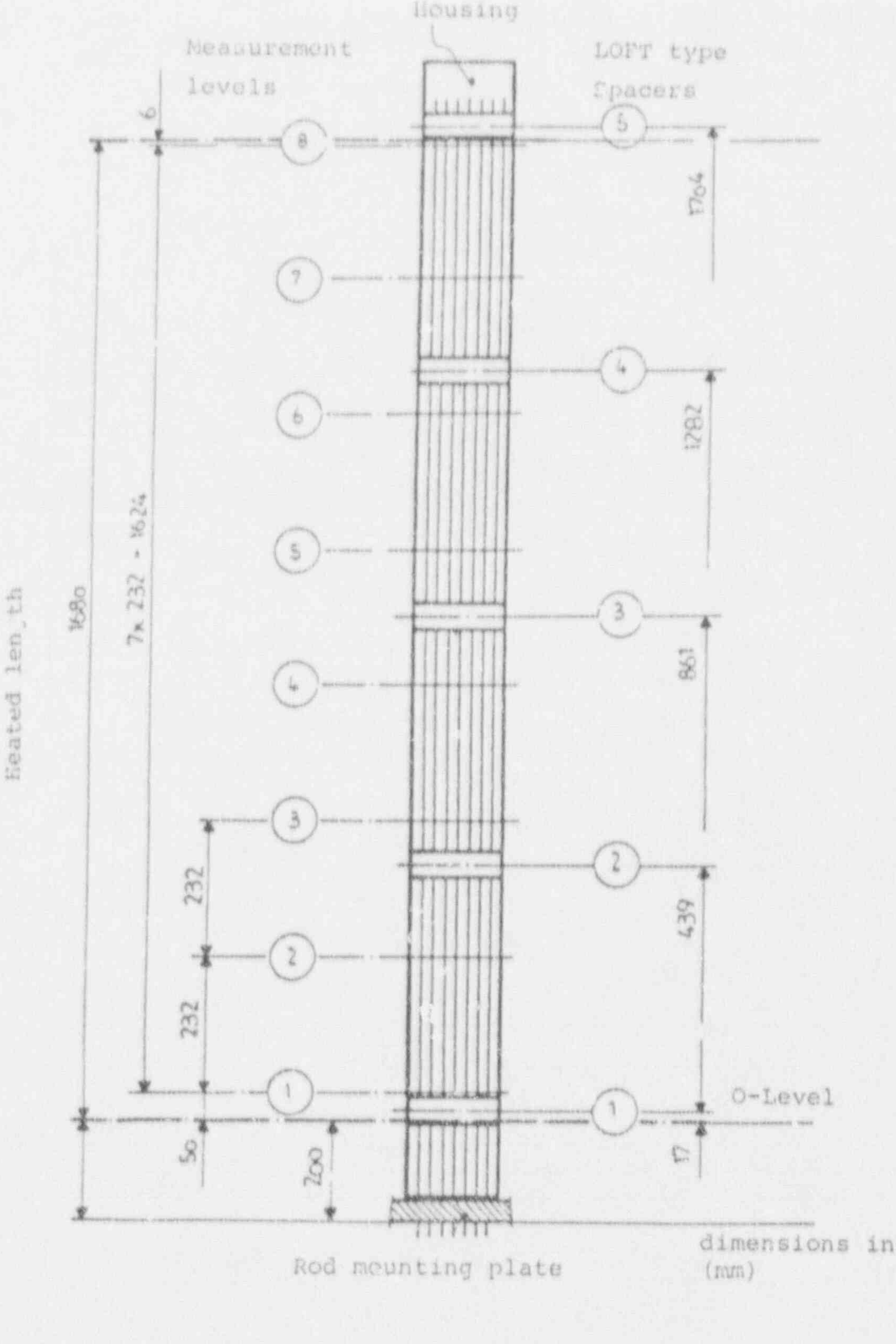

Figure 5: Axial distribution of the measurement levels in the NEPTUN facility

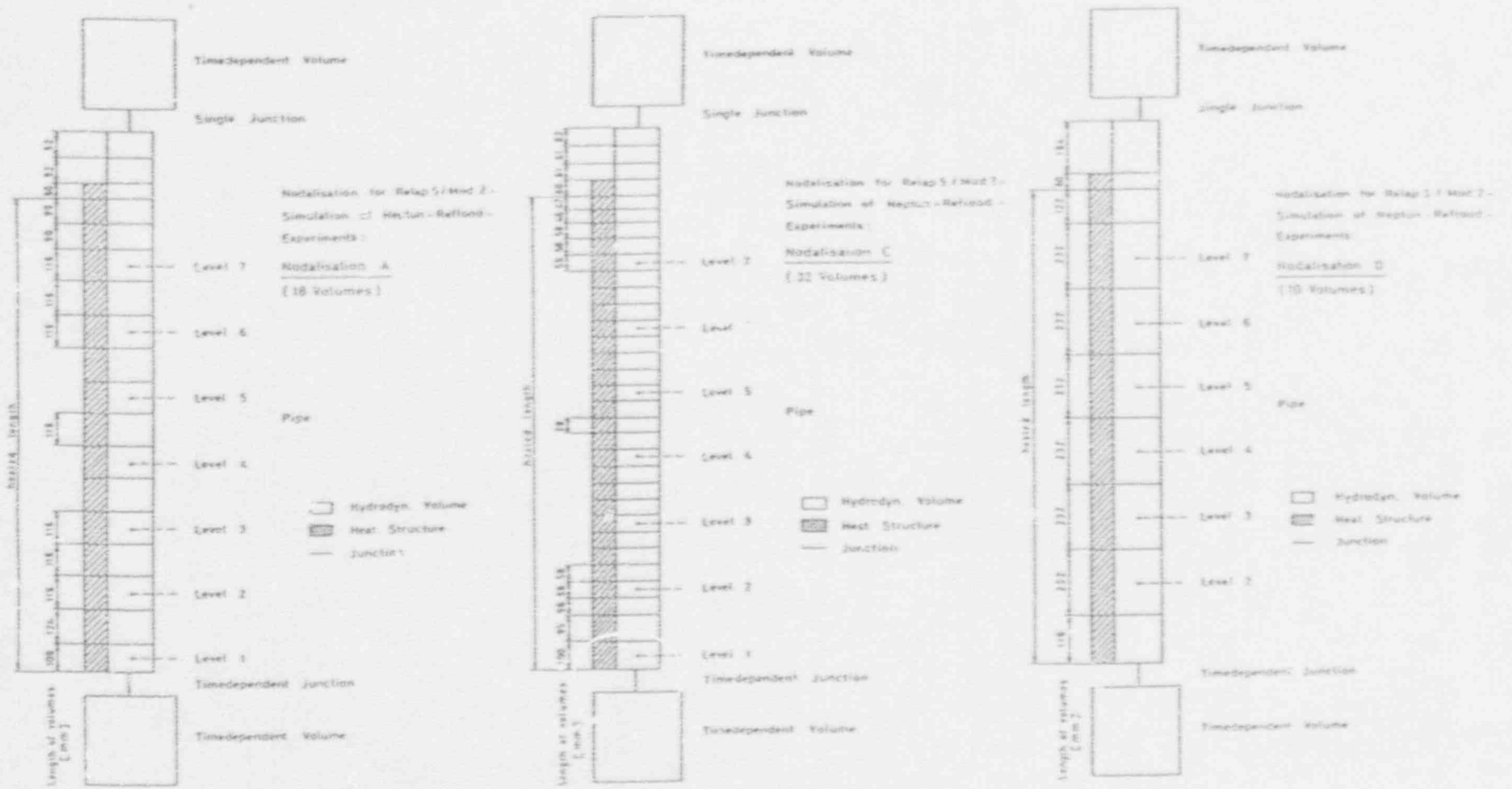

Figure 6: Tested nodalization for RELAP5/MOD2 simulations of NEPTUN reflooding experiments. The final model used was nodalization A with 18 volumes.

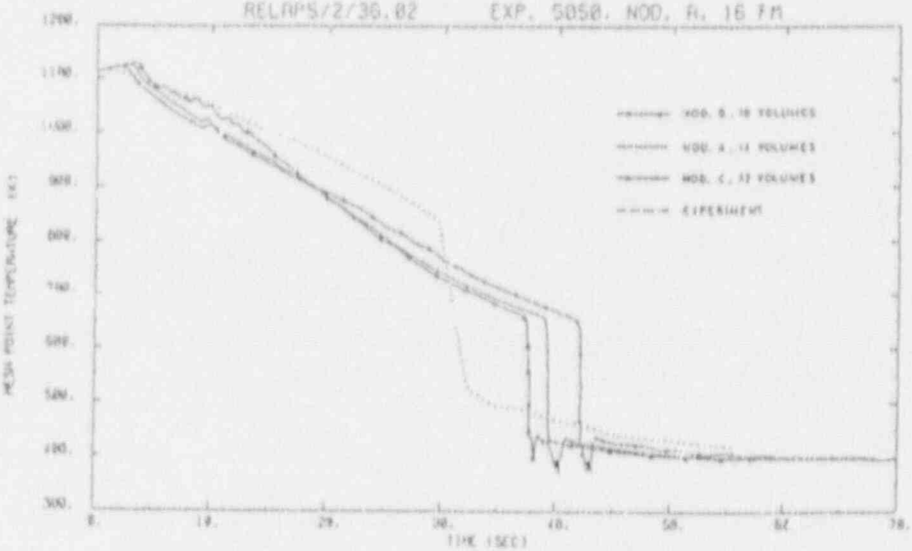

Figure 7: Rod cladding temperatures at measurement level 4 in NEPTUN high flooding rate experiment 5050, calculated by RELAP5: Effect of nodalization

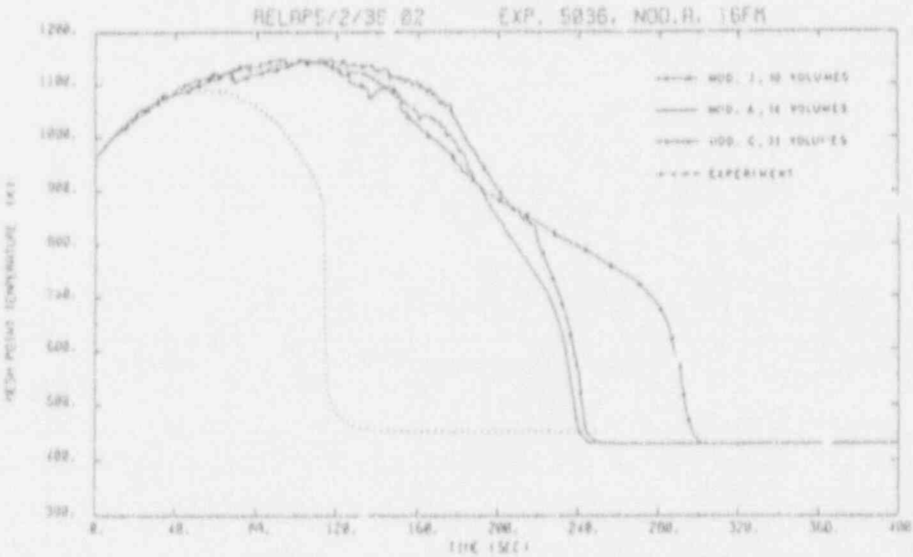

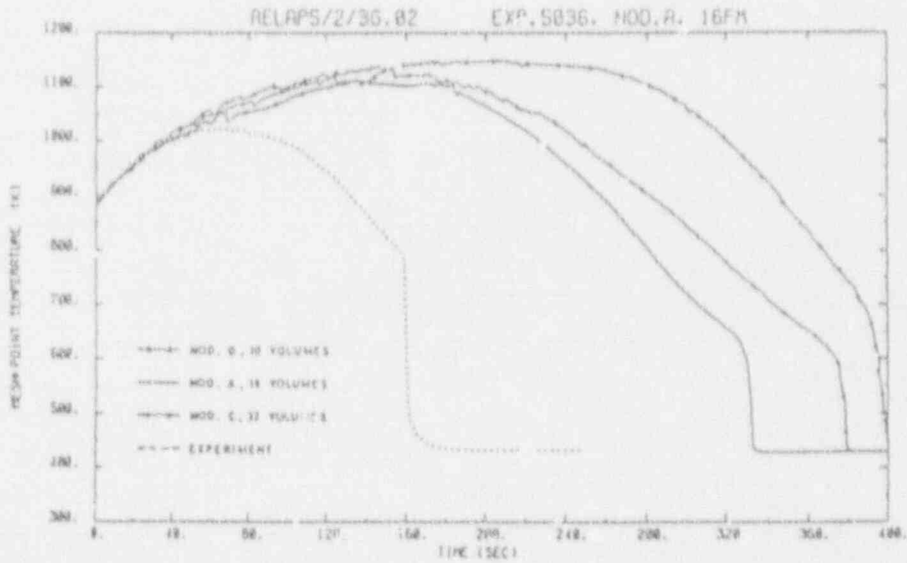

Figure 8: Rod cladding temperatures at measurement levels 4 and 5 in NEPTUN low flooding rate experiment 5036, calculated with the frozen version of RELAP5/MOD2: Effect of nodalization.

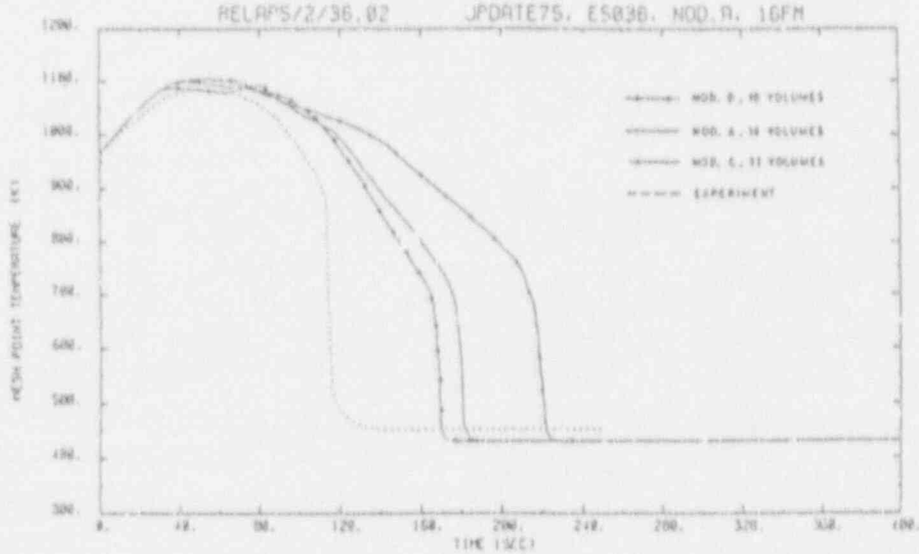

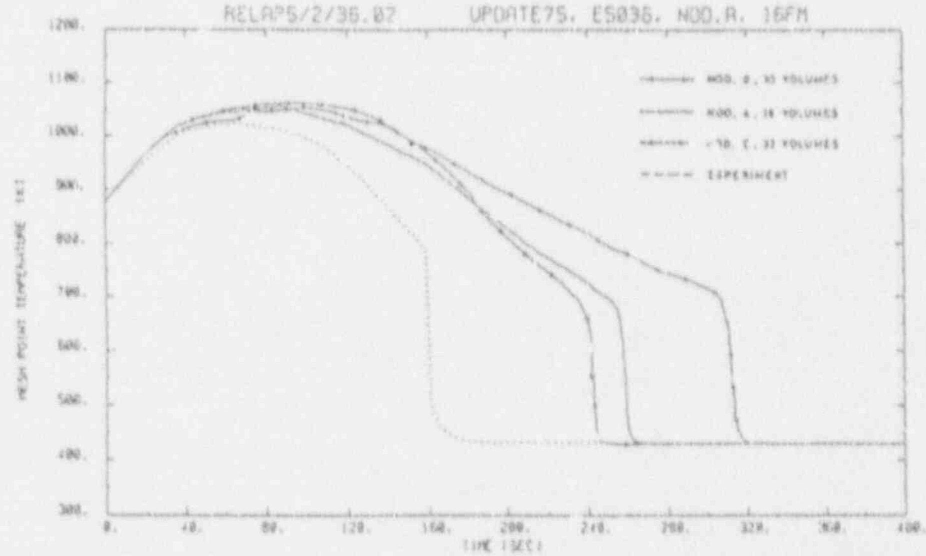

Figure 9: Rod cladding temperatures at measurements levels 4 and 5 in NEPTUN low flooding rate experiment 5036, calculated with the modified version EIR-update 75 of RELAP5/MOD2: Effect of nodalization.

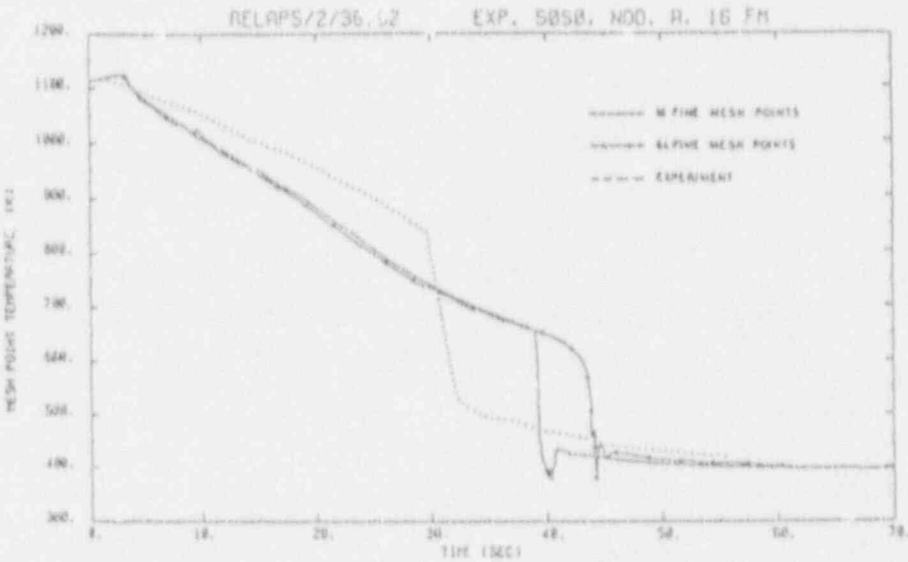

Figure 10: Rod cladding temperatures at measurement level 4 in NEPTUN high flooding rate experiment 5050, calculated by RELAP5/MOD2: Effect of the number of fine mesh nodes (per heat slab).

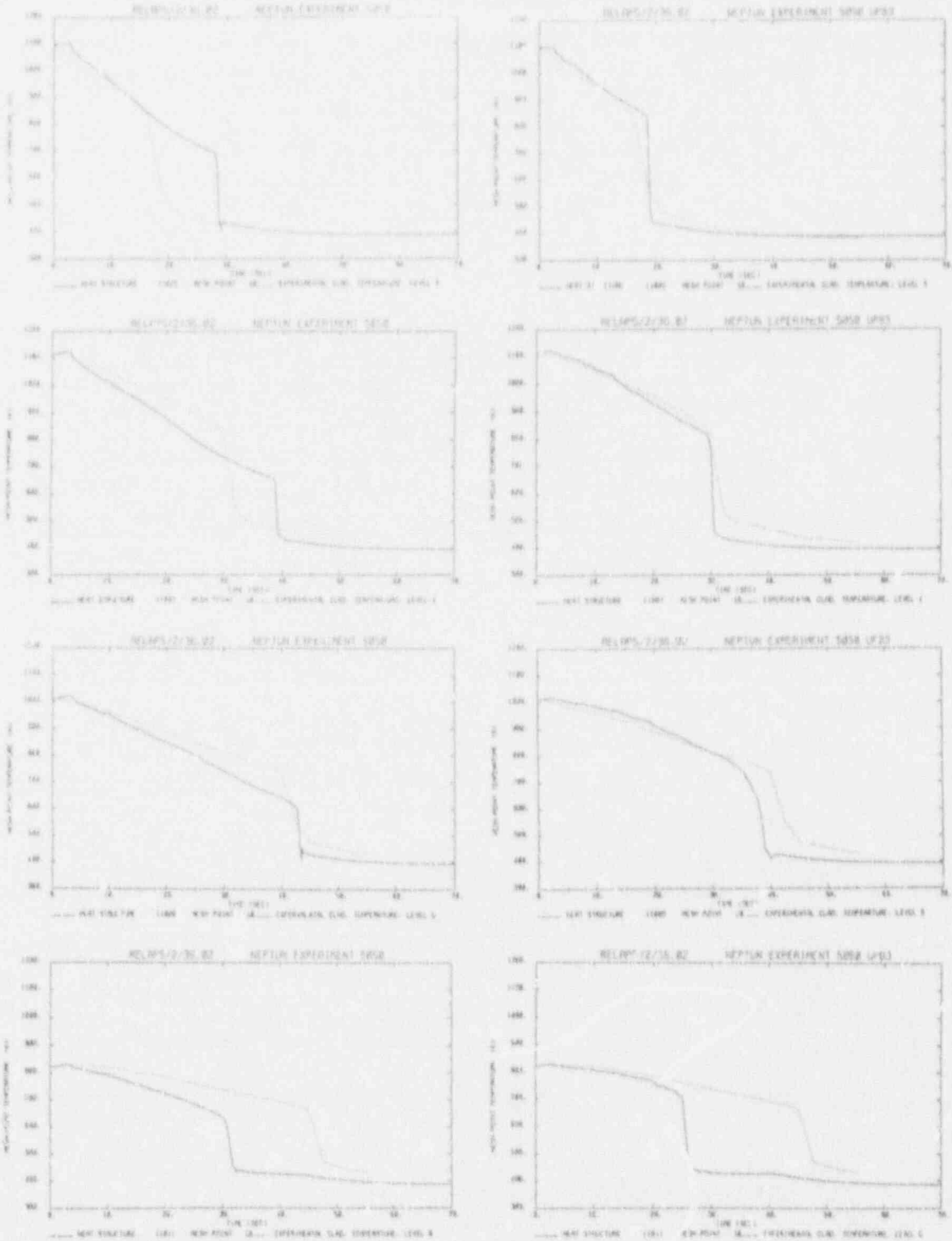

a b

Figure 11: Rod cladding temperatures at measurement levels 3-6 in NEPTUN high flooding rate experiment 5050, calculated by RELAP5/MOD2 with the frozen version (figure a)) and with version EIR-update 83 (figure b)).

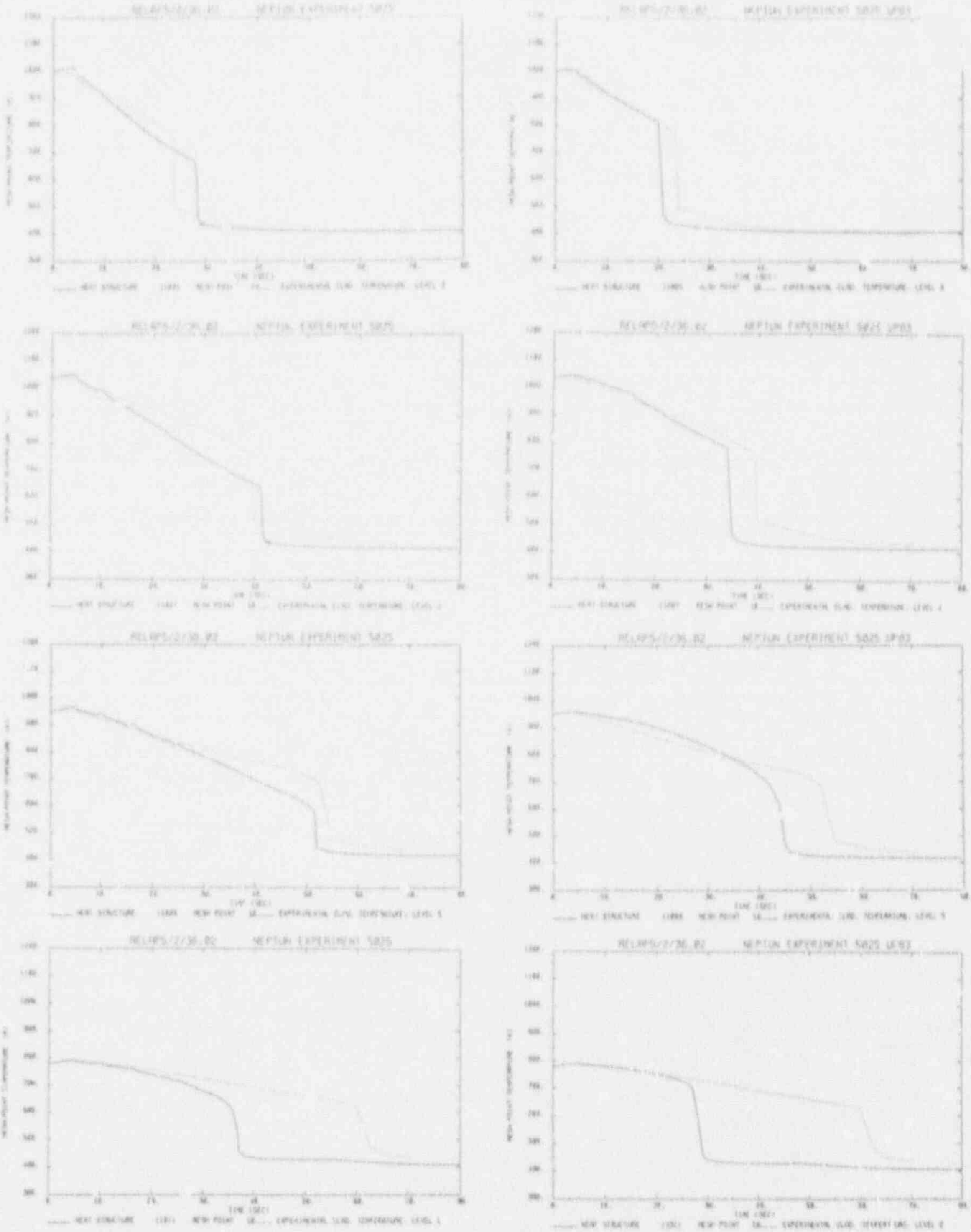

a b

Figure 12: Rod cladding temperatures at measurement levels 3-6 in NEPTUN high flooding rate experiment 5025, calculated by RELAP5/MOD2 with the frozen version (figure a)) and with version EIR-update 83 (figure b)).

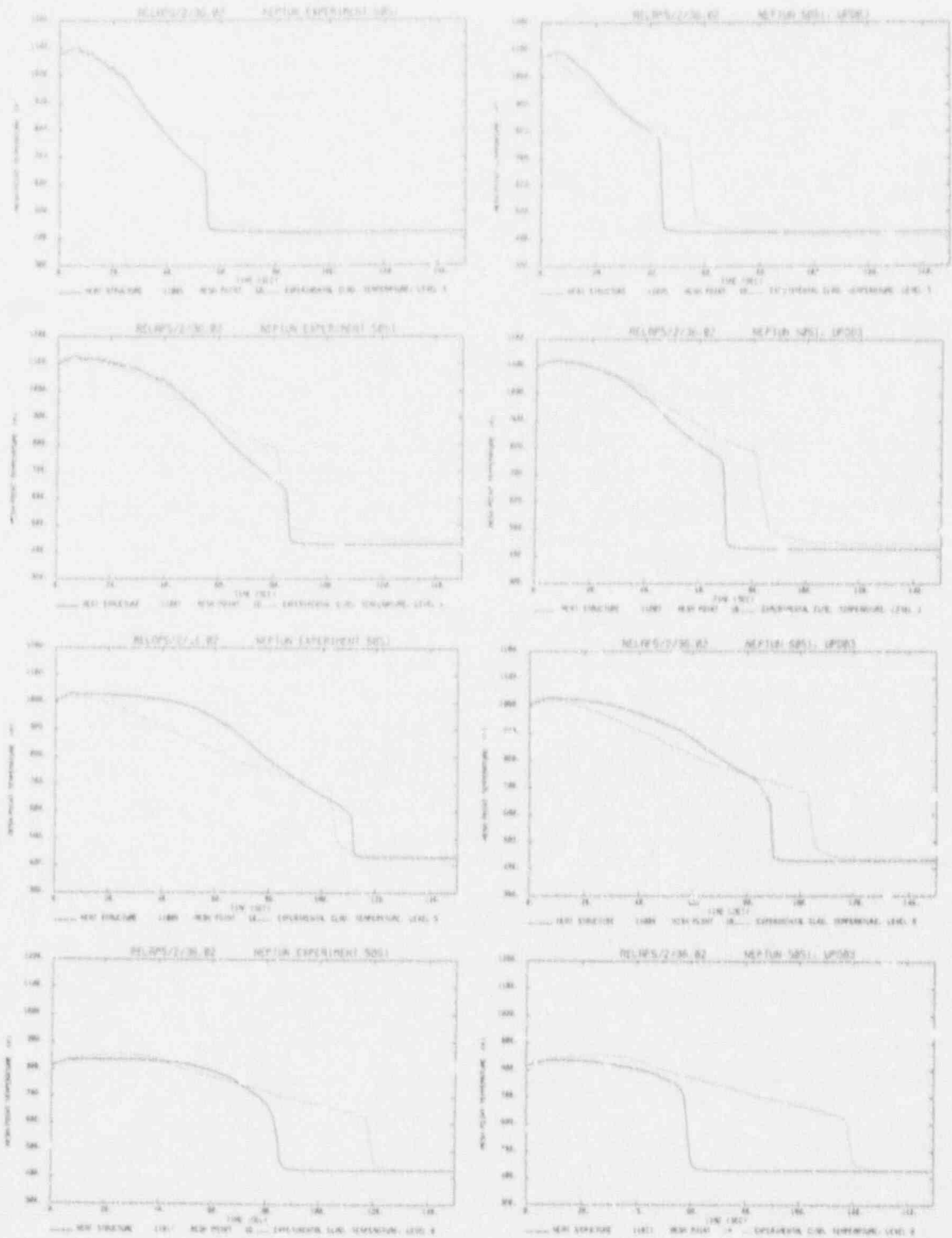

a b

Figure 13: Rod cladding temperatures at measurement levels 3-6 in NEPTUN medium flooding rate experiment 5051, calculated by RELAP5/MOD2 with the frozen version (figure a)) and with version EIR-update 83 (figure b)).

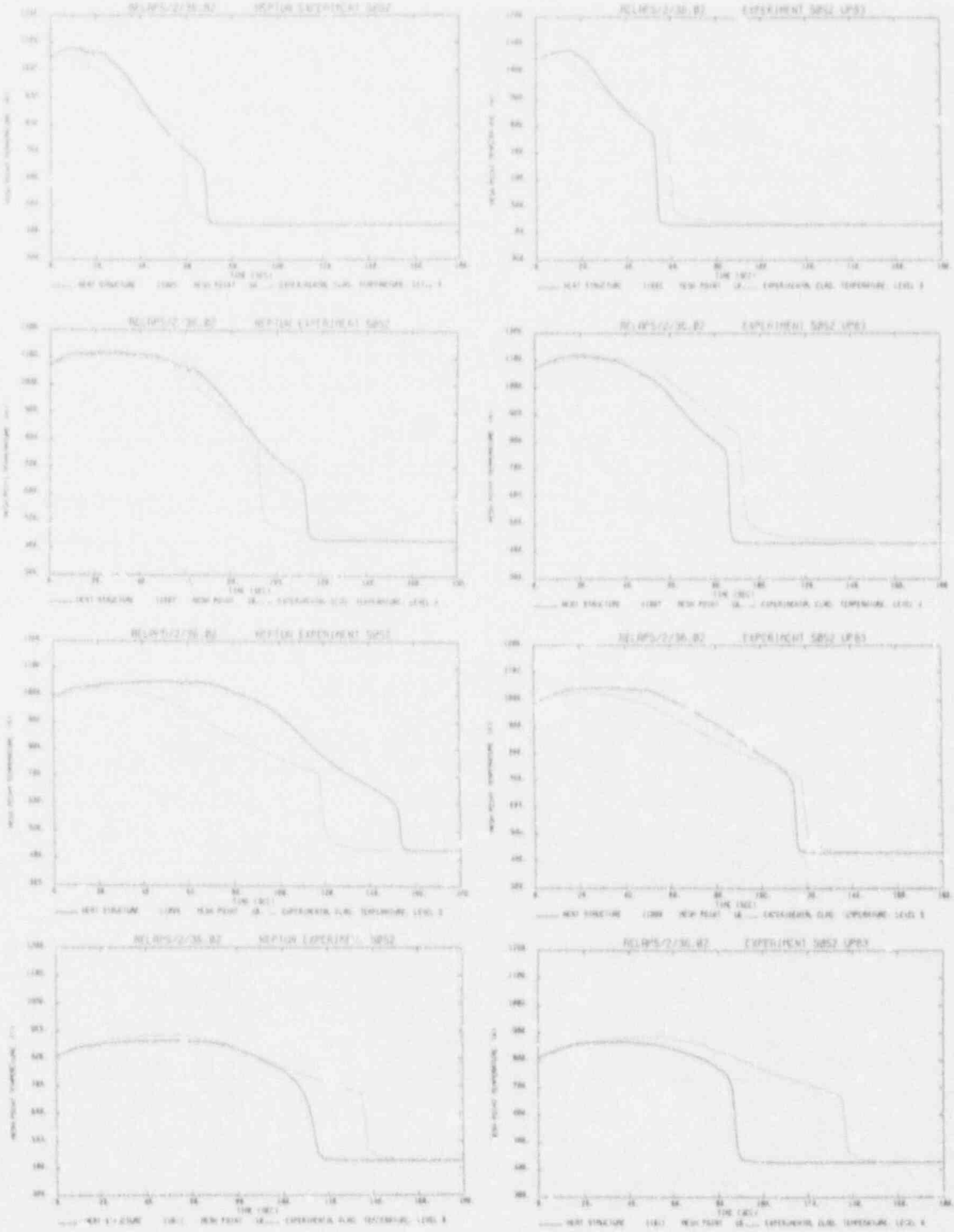

a

b

Figure 14: Rod cladding temperatures at measurement levels 3-6 in NEPTUN medium flooding rate experiment 5052, calculated by RELAP5/MOD2 with the frozen version (figure a)) and with version EIR-update 83 (figure b)).

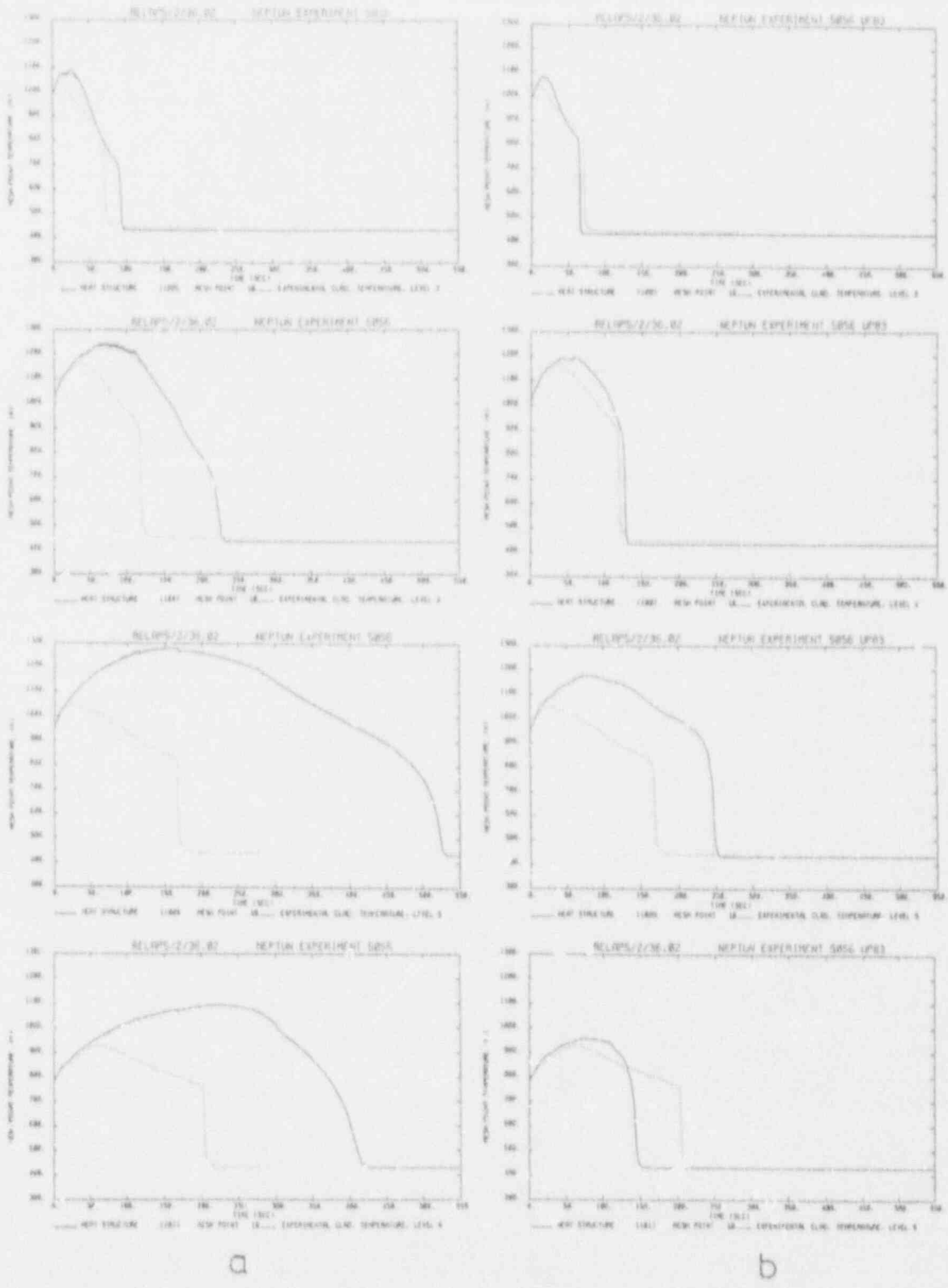

Figure 15: Rod cladding temperatures at measurement levels 3-6 in NEPTUN low flooding rate experiment 5056, calculated by RELAP5/MOD2 with the frozen version (figure a)) and with version EIR-update 83 (figure b)).

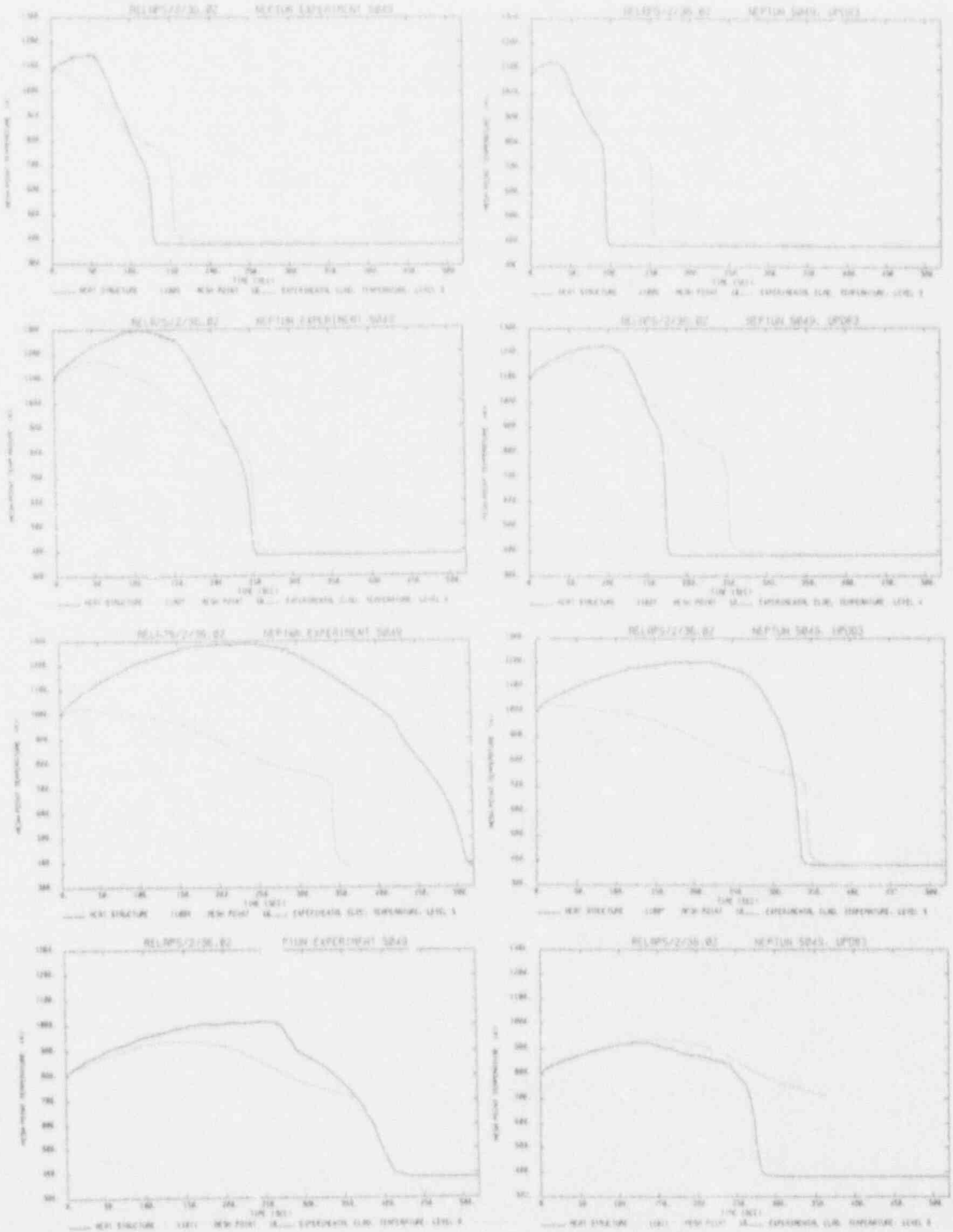

a b

Figure 16: Rod cladding temperatures at measurement levels 3-6 in NEPTUN low flooding rate experiment 5049, calculated by RELAP5/MOD2 v .h the frozen version (figure a)) and with version EIR-update 83 (figure b)).

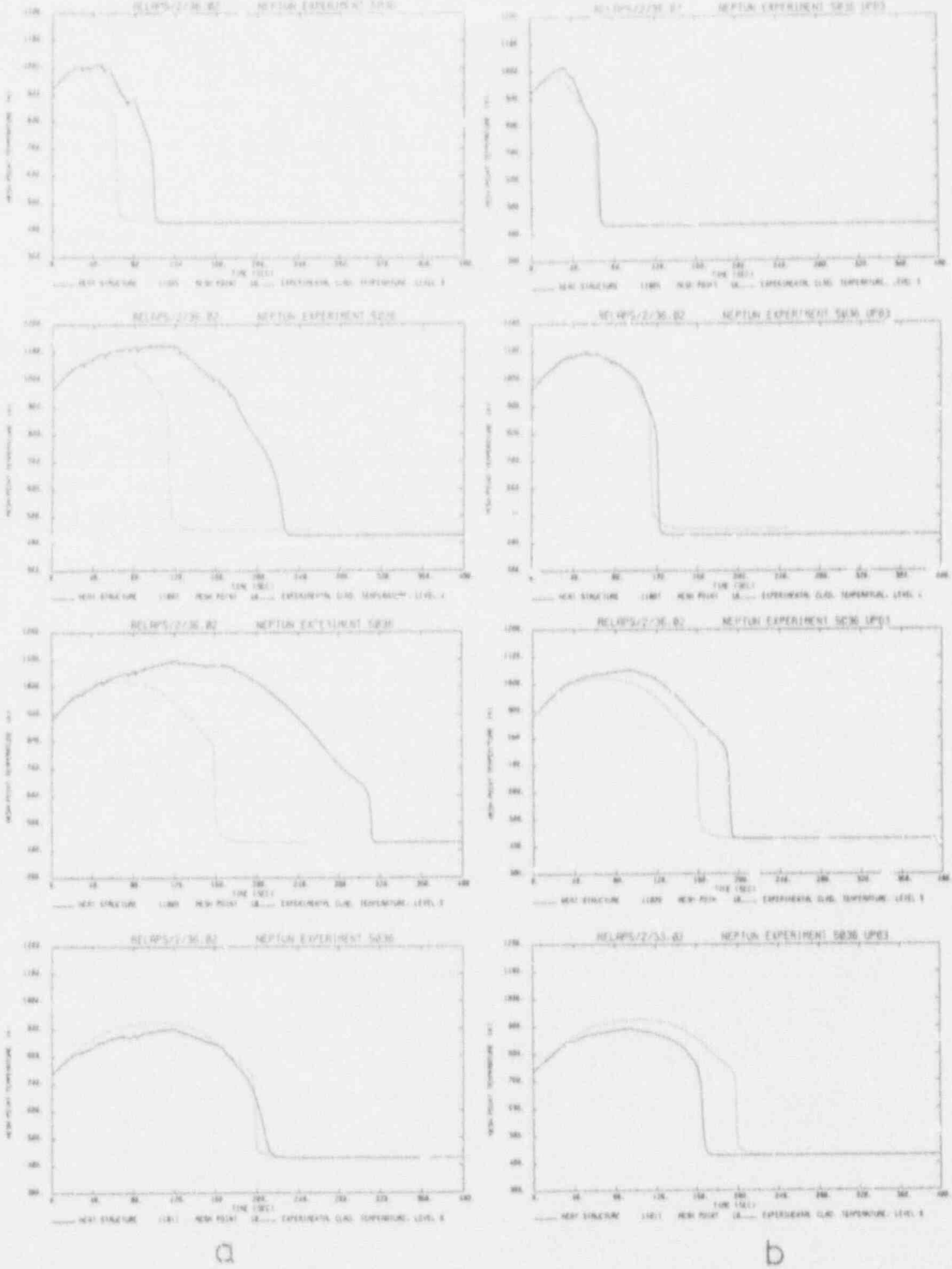

Figure 17: Rod cladding temperatures at measurement levels 3-6 in NEPTUN low flooding rate experiment 5036 calculated by RELAP5/MOD2 with the frozen version (figure a)) and with version EIR-update 83 (figure b)).

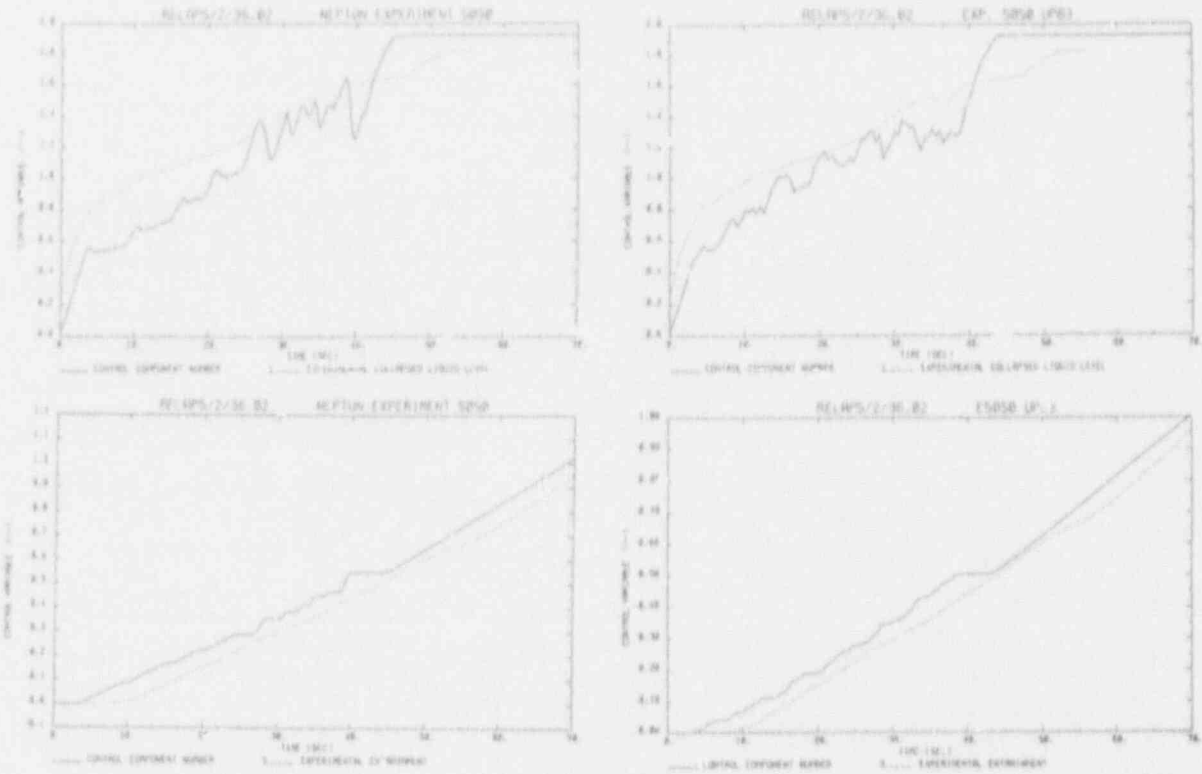

a b

Figure 18: Collapsed water level and water carry over in NEPTUN high flooding rate experiment 5050, calculated by RELAP5/MOD2 with the frozen version (figure a)), and with the modified version EIR-update 83 (figure b)).

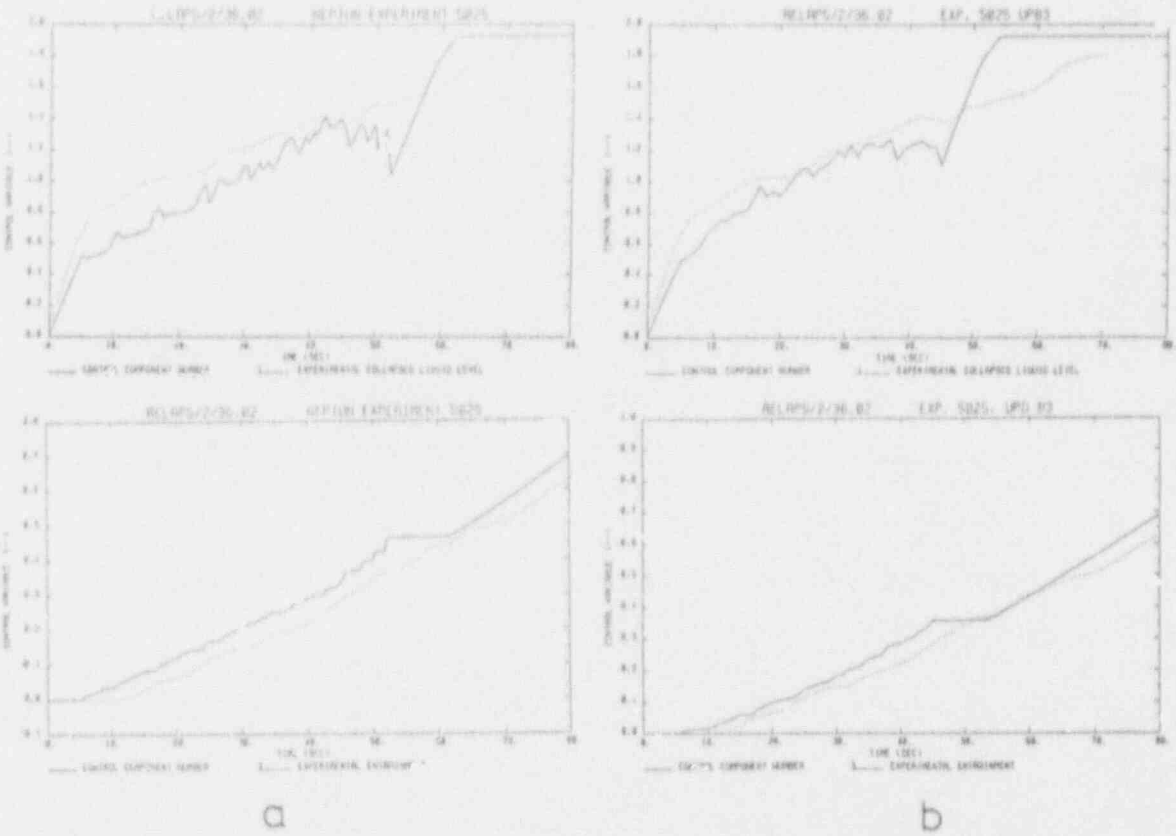

Figure 19: Collapsed water level and water carry over in NEPTUN high flooding rate experiment 5025, calculated by RELAP5/MOD2 with the frozen version (figure a)), and with the modified version EIR-update 83 (figure b)).

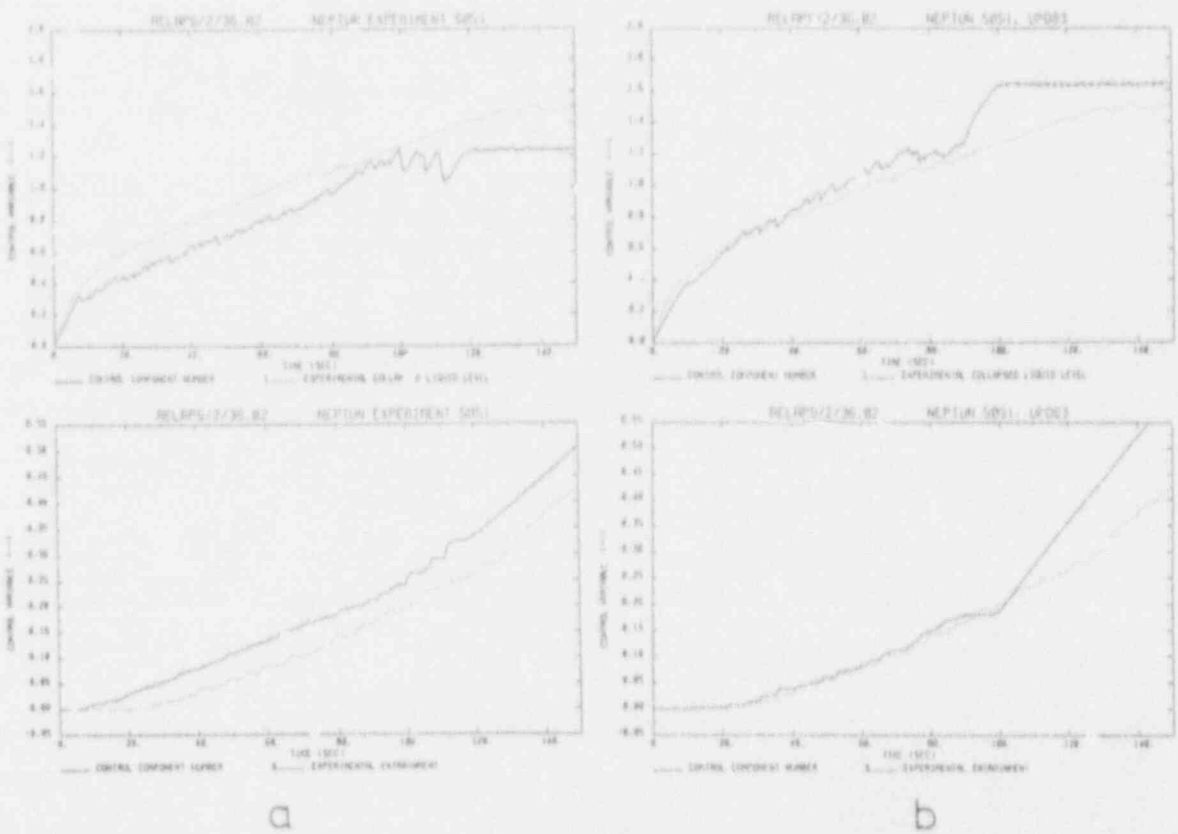

Figure 20: Collapsed water level and water carry over in NEPTUN medium flooding rate experiment 5051, calculated by RELAP5/MOD2 with the frozen version (figure a)), and with the modified version EIR-update 83 (figure b)).

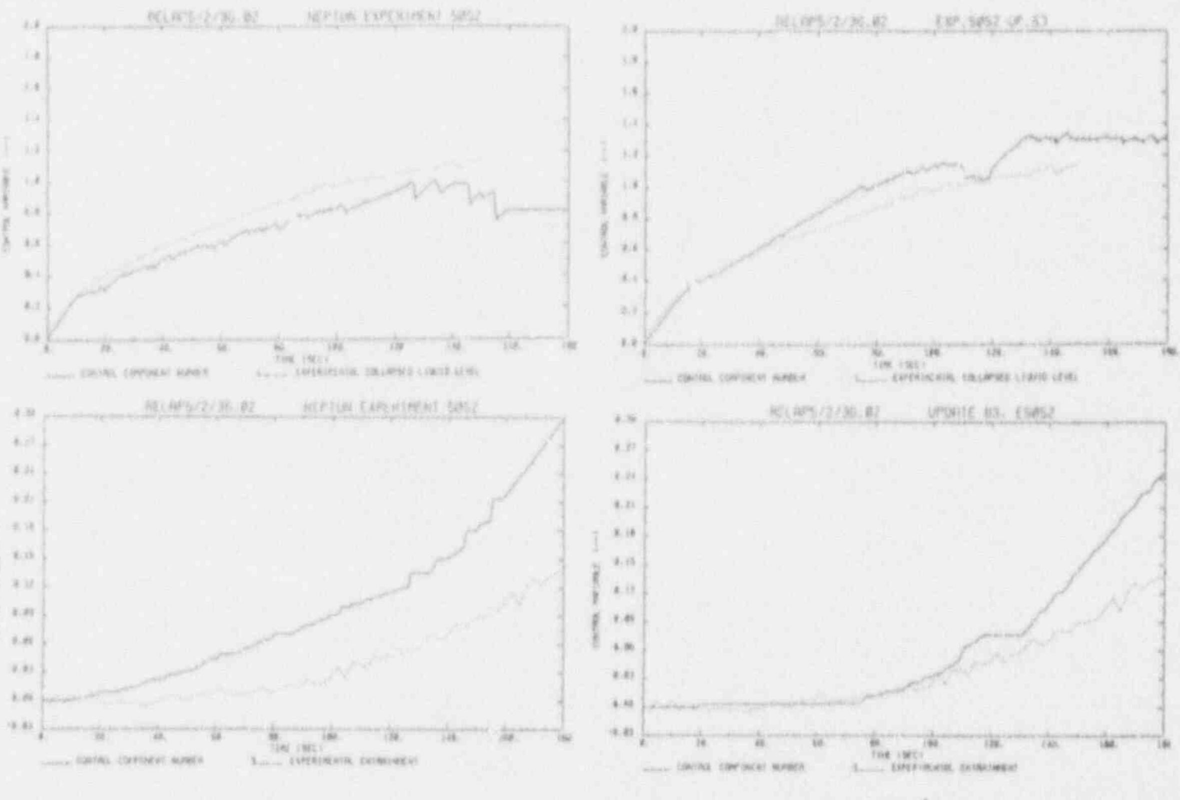

Figure 21: Collapsed water level and water carry over in NEPTUN low flooding rate experiment 5052, calculated by RELAP5/MOD2 with the frozen version (figure a)), and with the modified version EIR-update 83 (figure b)).

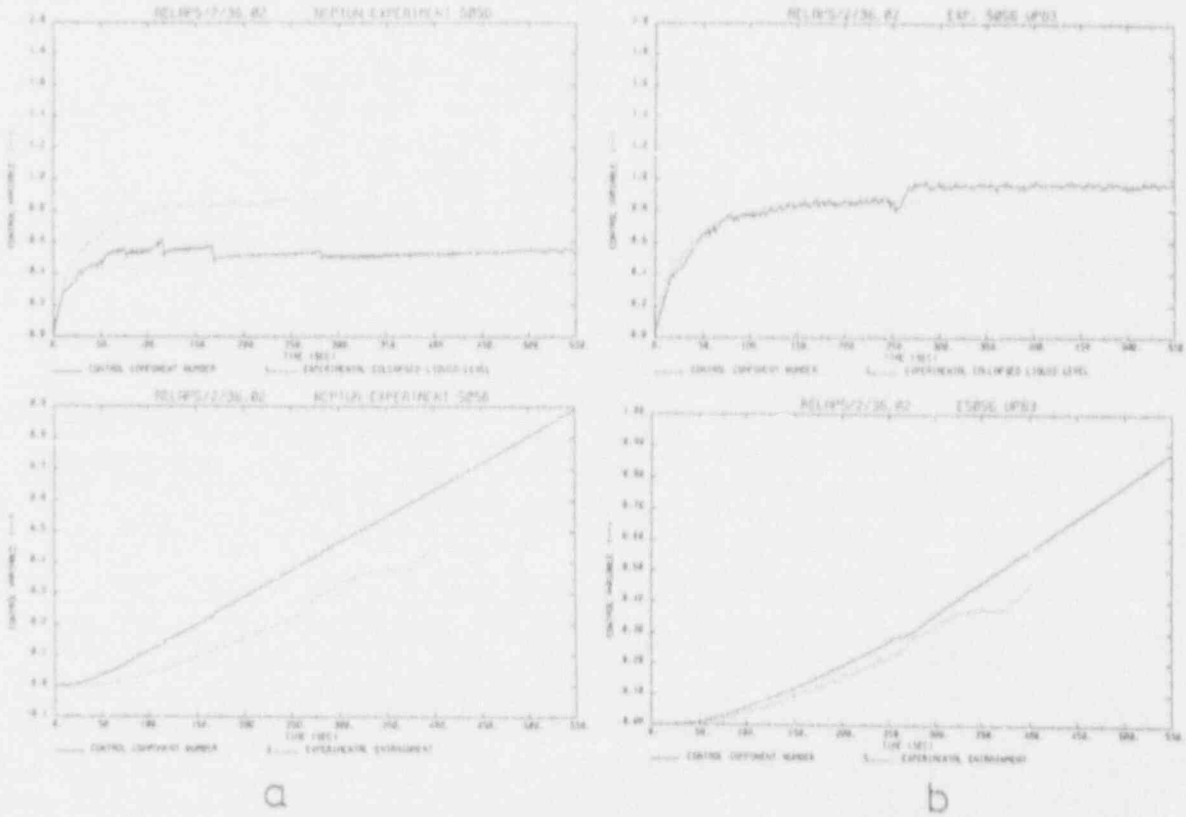

Figure 22: Collapsed water level and water carry over in NEPTUN low flooding rate experiment 5056, calculated by RELAP5/MOD2 with the frozen version (figure a)), and with the modified version EIR-update 83 (figure b)).

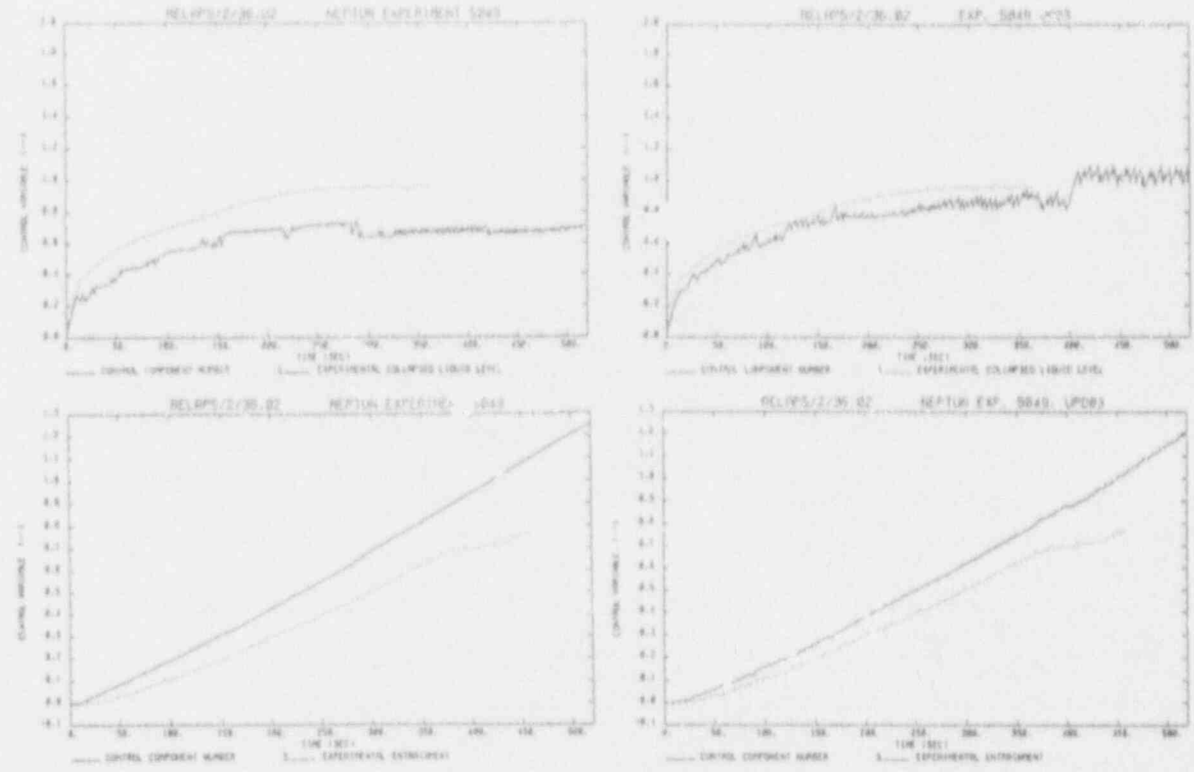

a

b

Figure 23: Collapsed water level and water carry over in NEPTUN low flooding rate experiment 5049, calculated by RELAP5/MOD2 with the frozen version (figure a)), and with the modified version EIR-update #3 (figure b)).

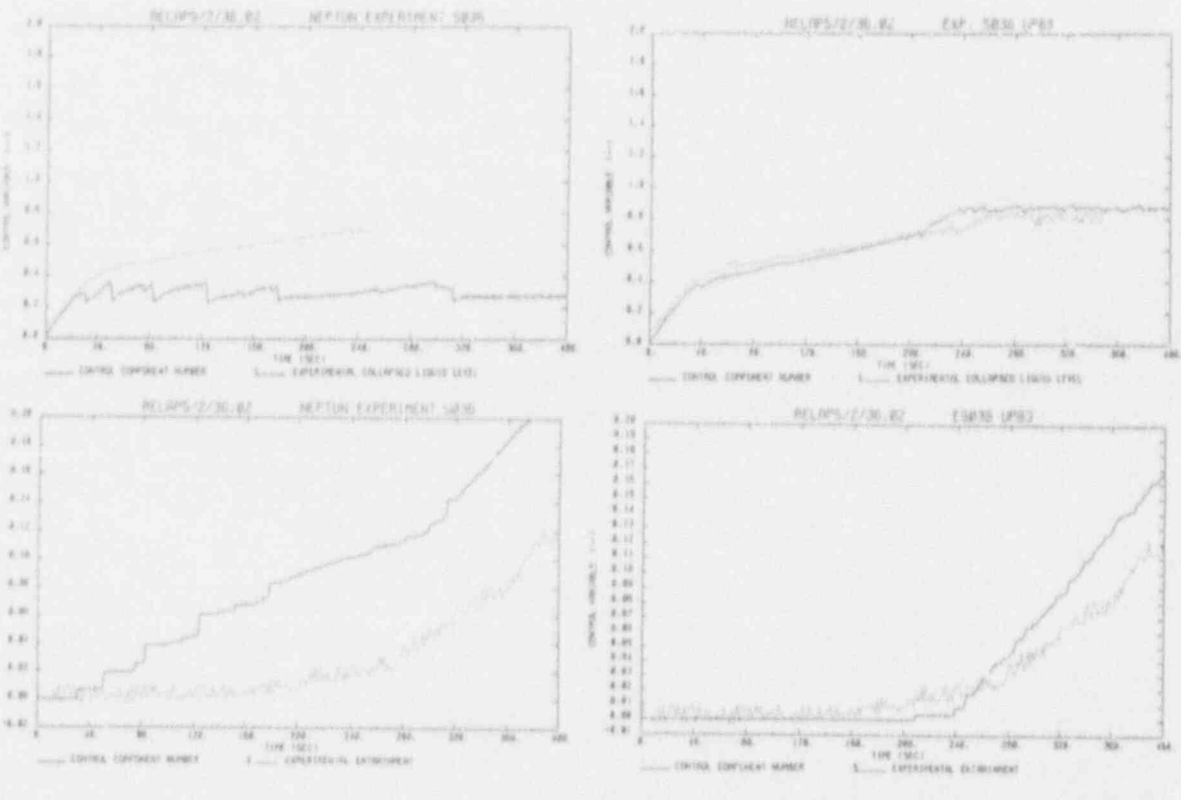

Figure 24: Collapsed water level and water carry over in NEPTUN low flooding rate experiment 5036, calculated by RELAP5/MOD2 with the frozen version (figure a)), and with the modified version EIR-update 83 (figure b)).

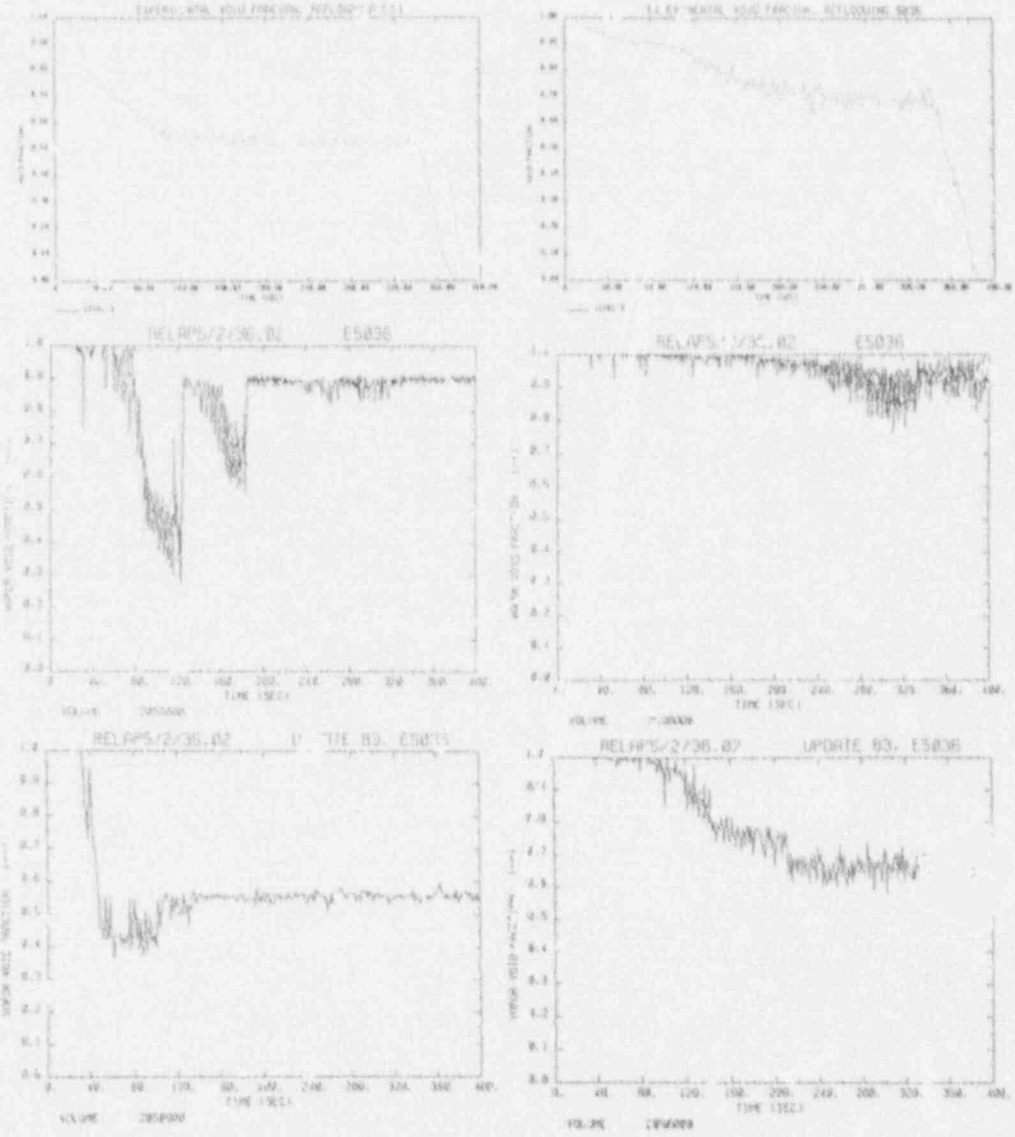

Figure 25: Void fractions at measurement levels 3 (left side) and 5 (right side) in NEPTUN low flooding rate experiment 5036, measured (top) and calculated by the frozen version of RELAP5/MOD2 (middle) and the modified version EIR-update 83 (bottom).

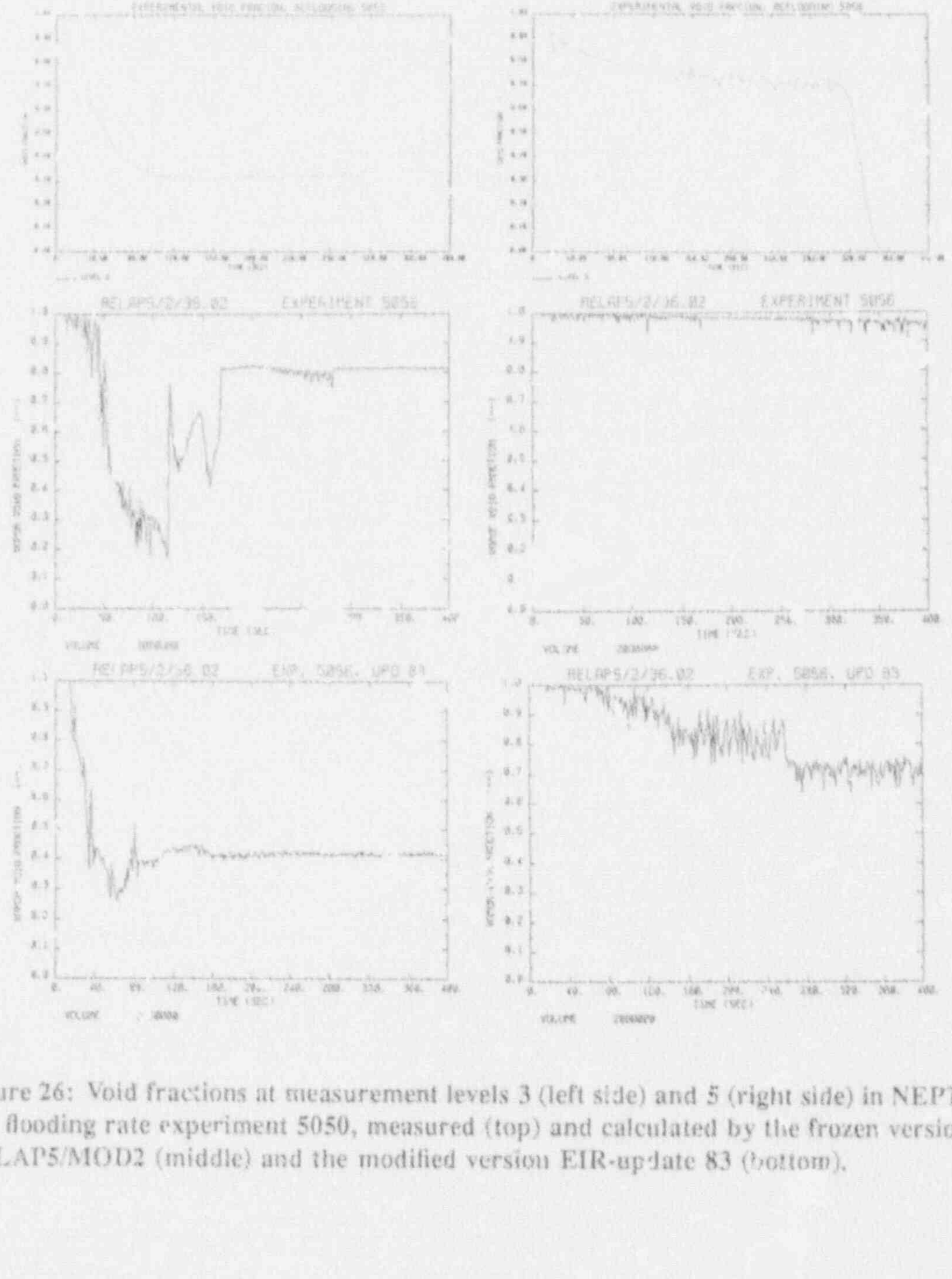

Figure 26: Void fractions at measurement levels 3 (left side) and 5 (right side) in NEPTUN low flooding rate experiment 5050, measured (top) and calculated by the frozen version of RELAP5/MOD2 (middle) and the modified version EIR-update 83 (bottom).

Correction of the Modified Bromley Correlation

Frozen version of RELAP5/MOD2:

$$h_{Br} = \left[k_g^3(\rho_f - \rho_g)\rho_g\left[\frac{h_{fg}}{T_w - T_{sat}} + 0.68C_{pv}\right]\sqrt{\frac{\rho_f - \rho_g}{\sigma}}\frac{1}{\eta_g}\right]^{0.25} \cdot \left[1 + 0.4(1-\alpha)^2\right]^2$$

Correction, same formula as in the manual (EIR-update 53 ff.):

$$h_{Br} = 0.62\left[k_g^3(\rho_f - \rho_g)\rho_g\left[\frac{h_{fg}}{T_w - T_{sat}} + 0.68C_{pv}\right]\frac{g}{2\pi}\sqrt{\frac{g(\rho_f - \rho_g)}{\sigma}}\frac{1}{\eta_g}\right]^{0.25} \cdot$$

~~$\cdot\left[1 + 0.4(1-\alpha)^2\right]^2$~~

Effect of this correction:

$$0.62\left[\frac{g}{2\pi}\sqrt{g}\right]^{0.25} = 0.922$$

~~$\left[1 + 0.4(1-\alpha)^2\right]^2 = 1 \ldots 1.96$~~

Figure 27: Corrections performed in the Modified Bromley Correlation.

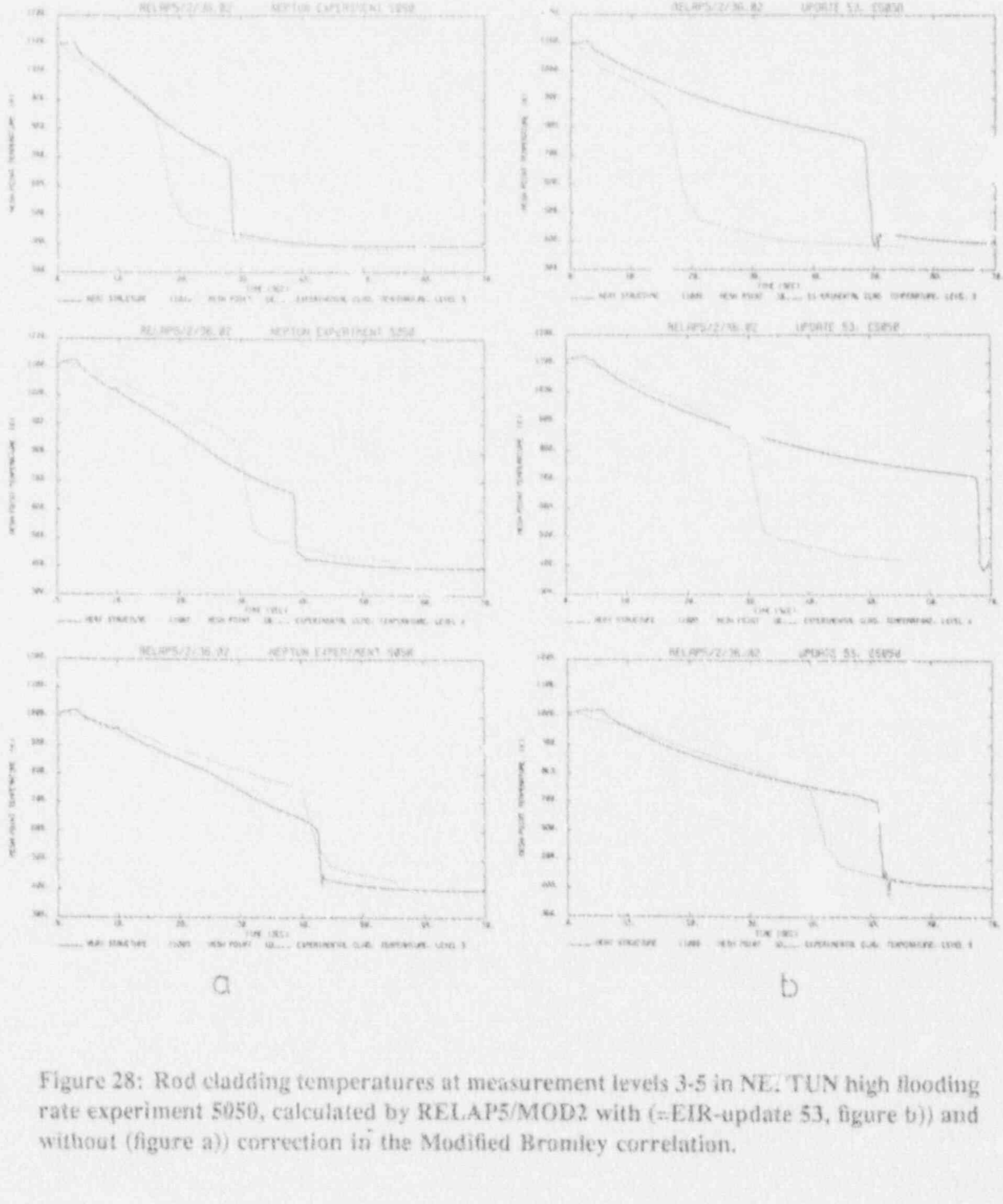

Figure 28: Rod cladding temperatures at measurement levels 3-5 in NE. TUN high flooding rate experiment 5050, calculated by RELAP5/MOD2 with (=EIR-update 53, figure b)) and without (figure a)) correction in the Modified Bromley correlation.

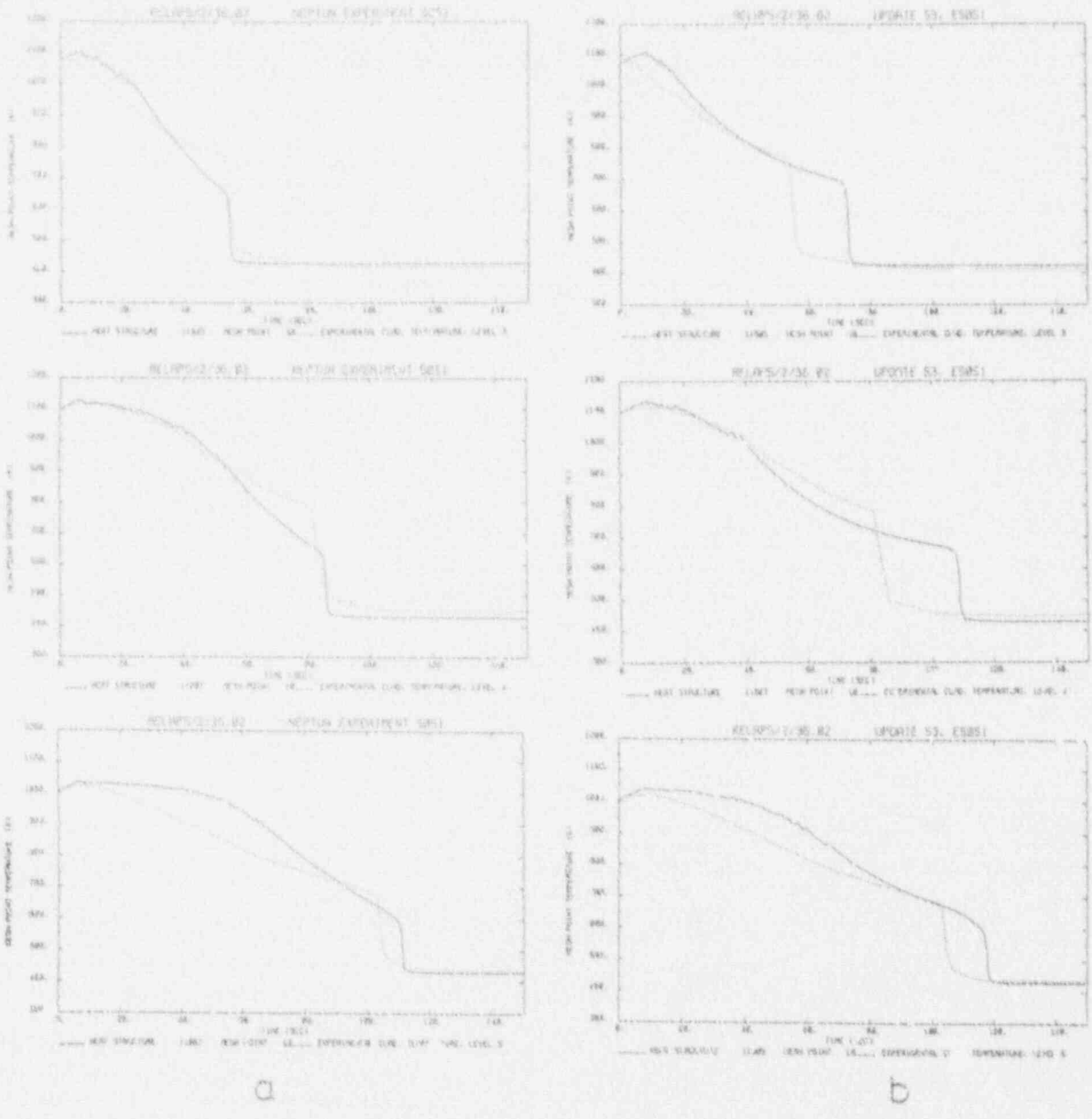

Figure 29: Rod cladding temperatures at measurement levels 3-5 in NEPTUN medium flooding rate experiment 5051, calculated by RELAP5/MOD2 with (=EIR-update 53, figure b)) and without (figure a)) correction in the Modified Bromley correlation.

Implementation of a new interphase friction correlation for bubbly and slug flow in rod bundles in RELAP5/MOD2

Original correlation:

$$\tau_i = 28.2\frac{\alpha(1-\alpha)^3\rho_g}{d_h}(c_1 v_g - c_0 v_f)^2$$

$$\text{with } c_0 = 1.2, c_1 = \frac{1 - c_0\alpha}{1-\alpha}$$

TRAC-BD1/MOD1 assessment with NEPTUN boil-off experiments:

$$\tau_i = 65\frac{\alpha(1-\alpha)^3\rho_g}{d_h}\,|c_1 v_g - c_0 v_f|\cdot(c_1 v_g - c_0 v_f) \quad c_0, c_1 \text{ same}$$

In RELAP5/MOD2 (EIR-update 68 ff.):

same formula as in TRAC, c_0 and c_1 same, but with

$$0.7 \leq c_1 \leq 1$$

(to eliminate some problems in the upper parts of the test section)

Figure 30: Implementation of a new interphase friction correlation for bubbly and slug flow in rod bundle geometry into RELAP5/MOD2.

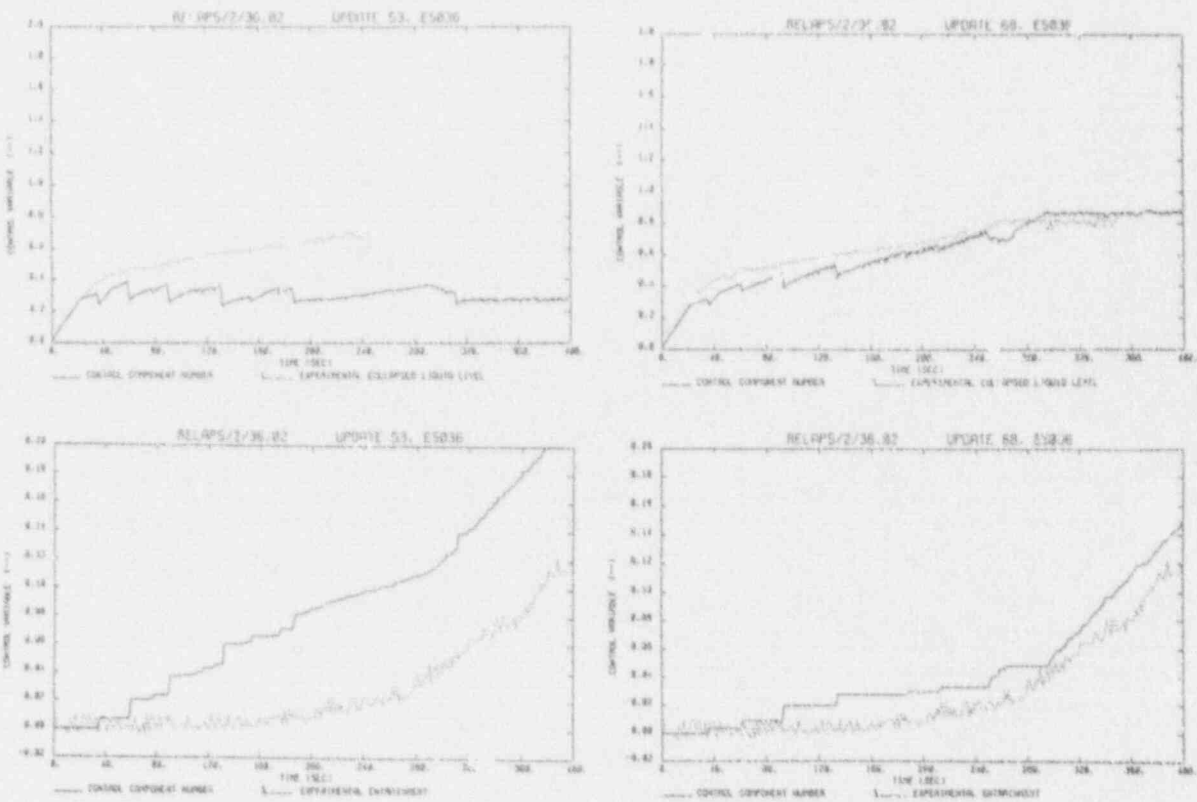

a b

Figure 31: Collapsed liquid level and water entrainment in NEPTUN low flooding rate experiment 5036, calculated with (=EIR-update 68, figure b)) and without (=EIR-update 53, figure a)) new formula for the interphase friction in bubbly and slug flow, and with previous update.

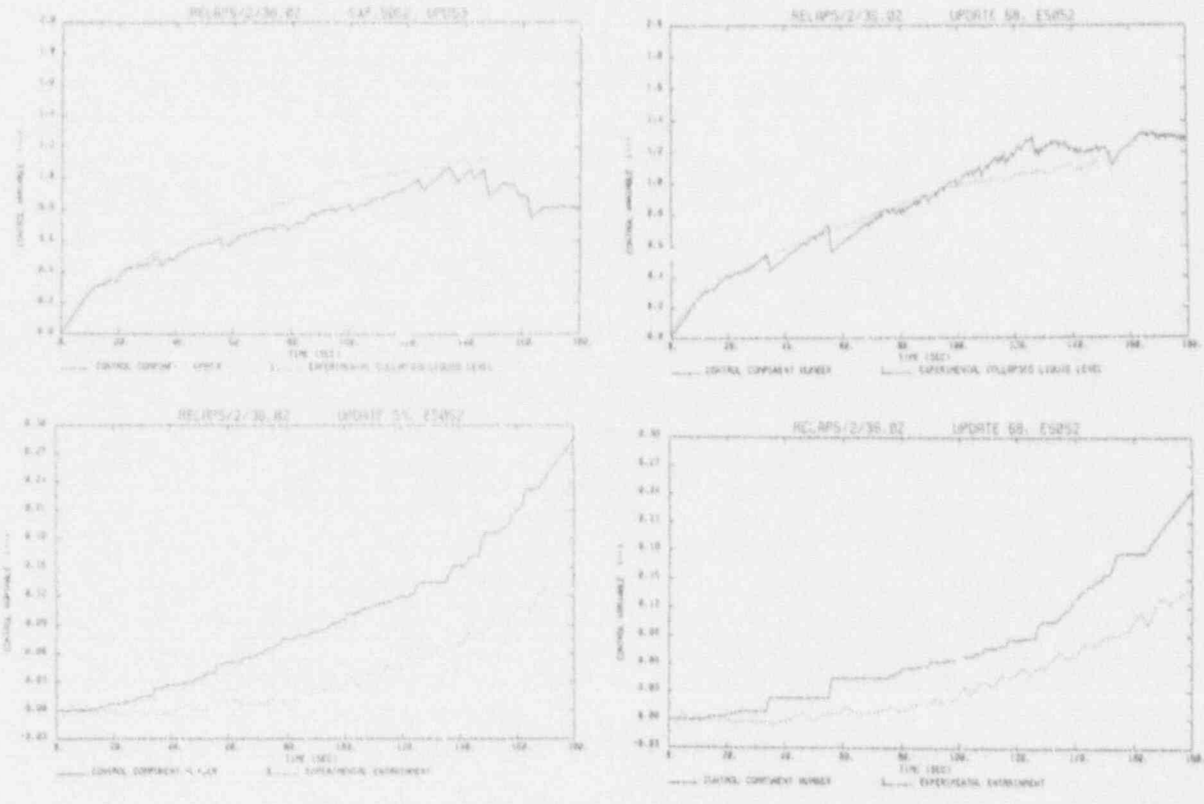

Figure 32: Collapsed liquid level and water entrainment in NEPTUN low flooding rate experiment 5052, calculated with (=EIR-update 68, figure b)) and without (=EIR-update 53, figure a)) new formula for the interphase friction in bubbly and slug flow, and with previous update.

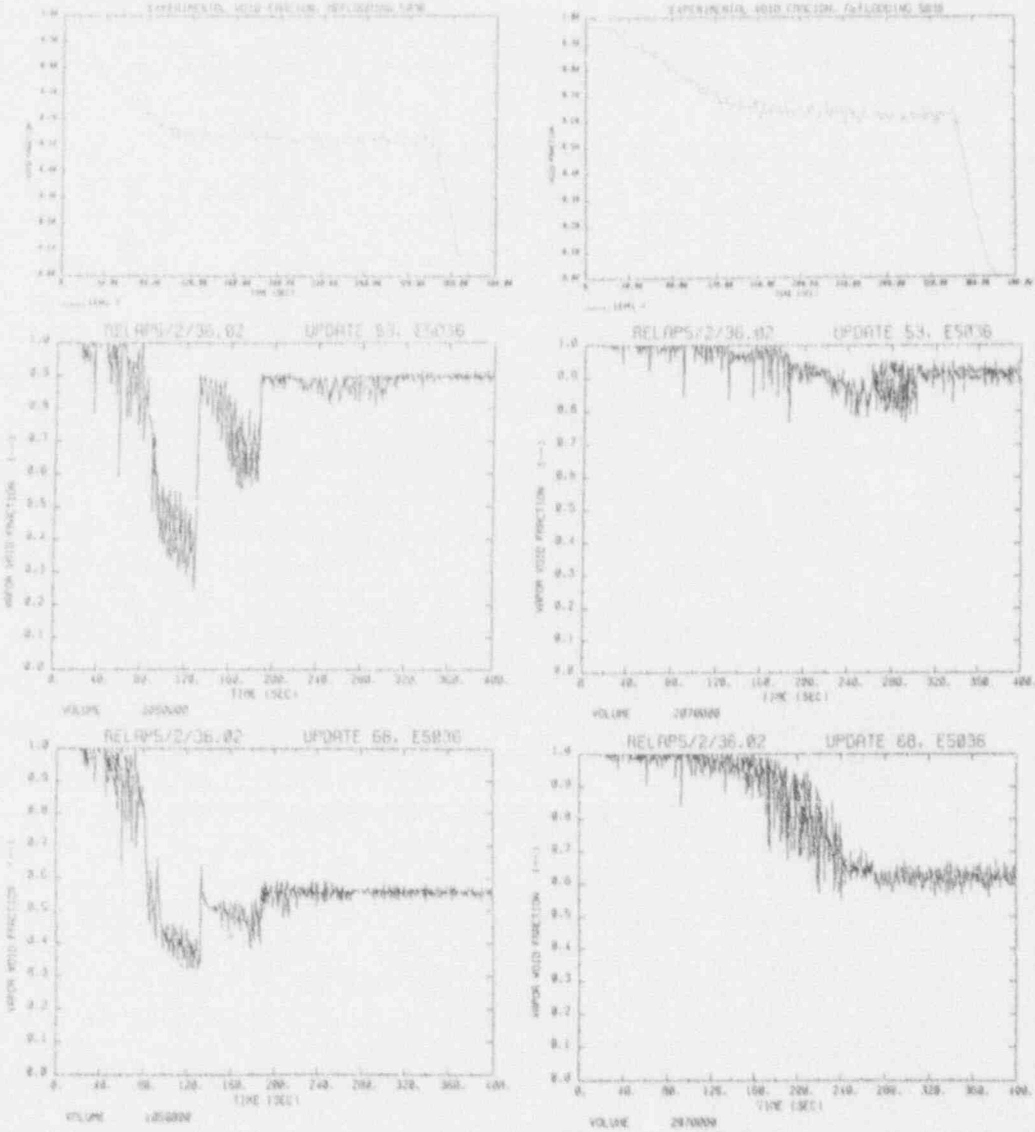

Figure 33: Void fractions at measurement levels 3 (left side) and 4 (right side) in NEPTUN low flooding rate experiment 5036, measurement (top) and calculated by RELAP5/MOD2, without (=EIR-update 53, middle) and with (=EIR-update 68, bottom) new formula for the interphase friction in bubbly and slug flow, and with previous update.

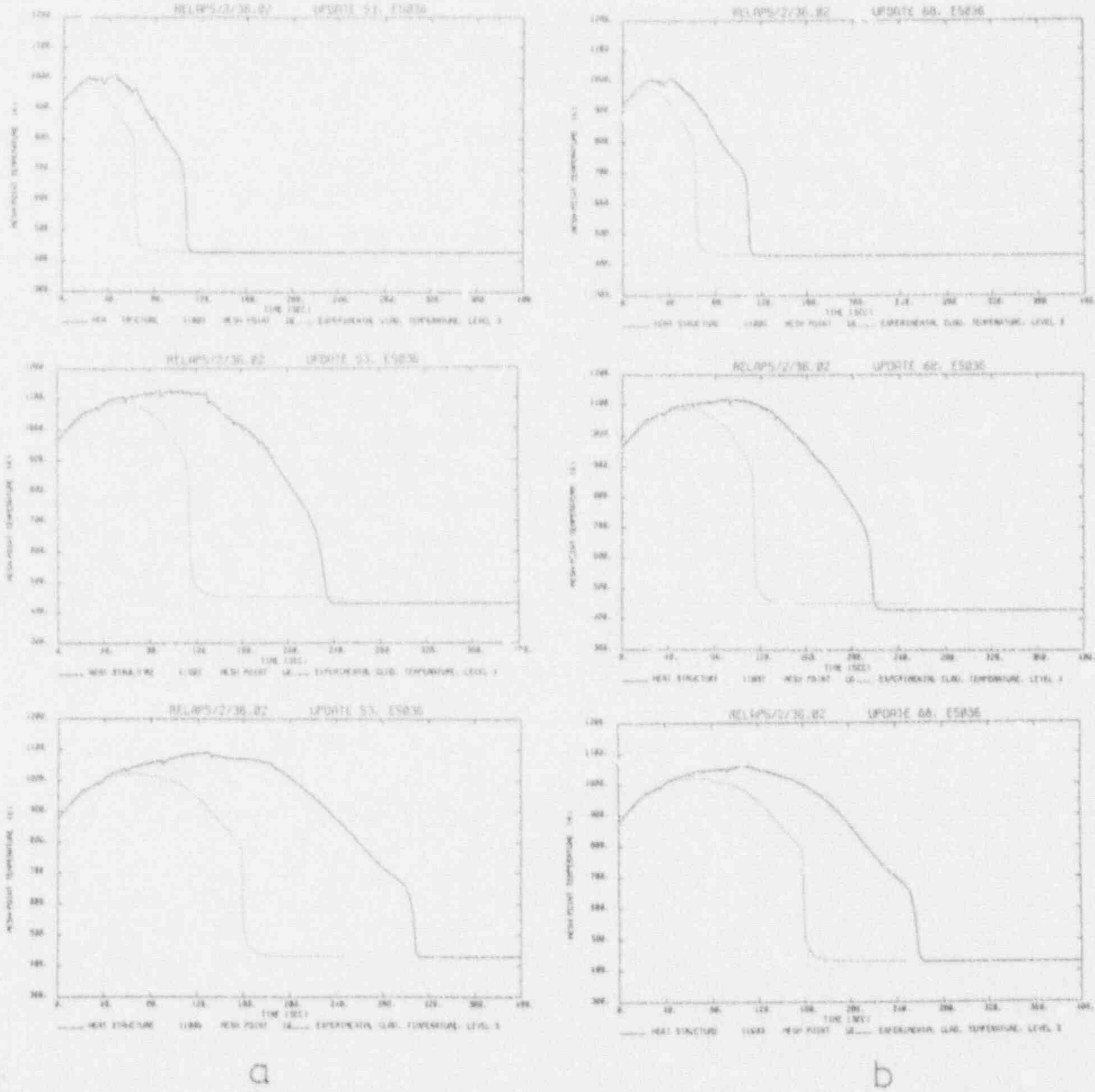

Figure 34: Rod cladding temperatures at measurement levels 3-5 in NEPTUN low flooding rate experiment 5036, calculated by RELAP5/MOD2 with (=EIR-update 68, figure b)) and without (=EIR-update 53, figure a)) new correlation for the interphase friction in bubbly and slug flow, and with previous update.

Implementation of the formula of Forslund-Rohsenow for the reflood heat transfer coefficient at high void fractions in RELAP5/MOD2

RELAP5/MOD2 (frozen version):

$\alpha \leq 0.91$: $h_{tot} = h_{FB} + h_{DR} + \ldots$

$0.91 < \alpha < 0.99$: Interpolation

$\alpha \geq 0.99$: $h_{tot} = (1-\alpha)h_{FB} + \alpha h_{DR} + \ldots$

with

h_{FB} : Maximum of modified Bromley film boiling and Weismann transition boiling heat transfer coefficient;

h_{DR} : Dougall-Rohsenow heat transfer coefficient

$\ldots$: Radiation terms

Formula of Forslund-Rohsenow for dispersed film boiling:

$$h_{FR} = 0.2\frac{\pi}{4}\left(\frac{6}{\pi}\right)^{2/3}(1-\alpha)^{2/3}\left[\frac{g\rho_f\rho_g h_{fg}k_g^3}{(T_w - T_f)\mu_g(\pi/6)^{1/3}d_d}\right]^{0.25}$$

implemented in RELAP5 with:

prefactor 0.4 instead of 0.2

$d_d = \frac{3.0\sigma}{\rho_g(v_g - v_f)^2}$ droplet diameter with restriction $1.5 \cdot 10^{-4}m \leq d_d \leq 3 \cdot 10^{-3}m$

New in RELAP5/MOD2 (EIR-update 71 ff.):

$\alpha \leq 0.6$: $h_{tot} = h_{FB} + h_{DR} + \ldots$ as before

$0.6 \leq \alpha \leq 0.8$: Interpolation

$\alpha \geq 0.8$: $h_{tot} = h_{FR} + h_{DR} + \ldots$

Figure 35: Implementation of the formula of Forslund-Rohsenow for the reflood dispersed film boiling wall heat transfer coefficient in RELAP5/MOD2.

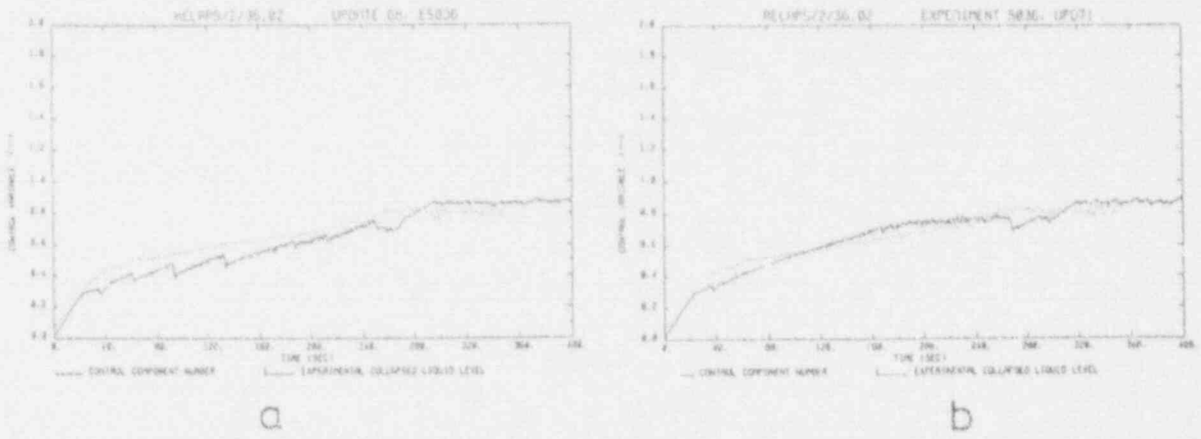

Figure 36: Collapsed liquid level in NEPTUN low flooding rate experiment 5036, calculated with (=EIR-update 71, figure b)) and without (=EIR-update 68, figure a)) new formula of Forslund-Rohsenow for the reflood dispersed film boiling wall heat transfer coefficient, and with previous updates.

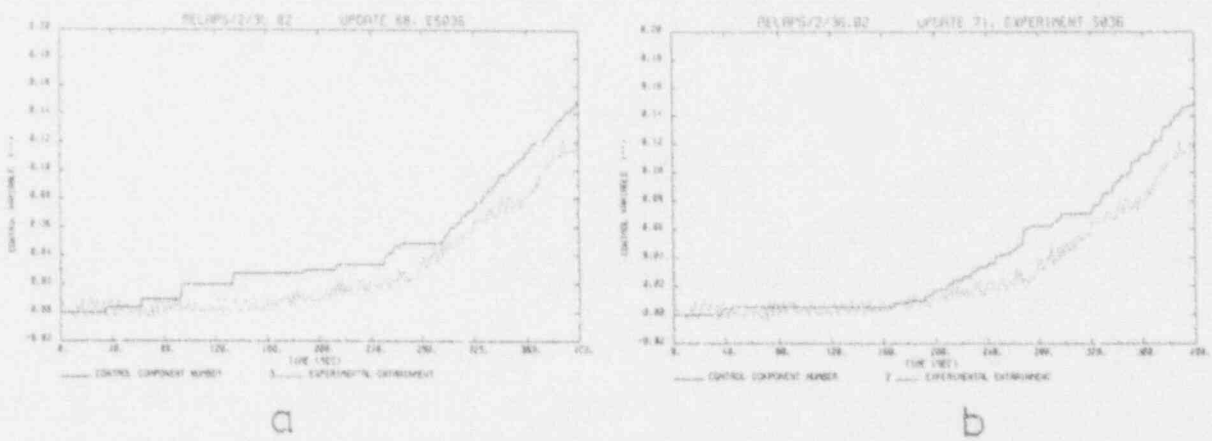

Figure 37: Water entrainment in NEPTUN low flooding rate experiment 5036, calculated with (=EIR-update 71, figure b)) and without (=EIR-update 68, figure a)) new formula of Forslund-Rohsenow for the reflood dispersed film boiling wall heat transfer coefficient, and with previous updates.

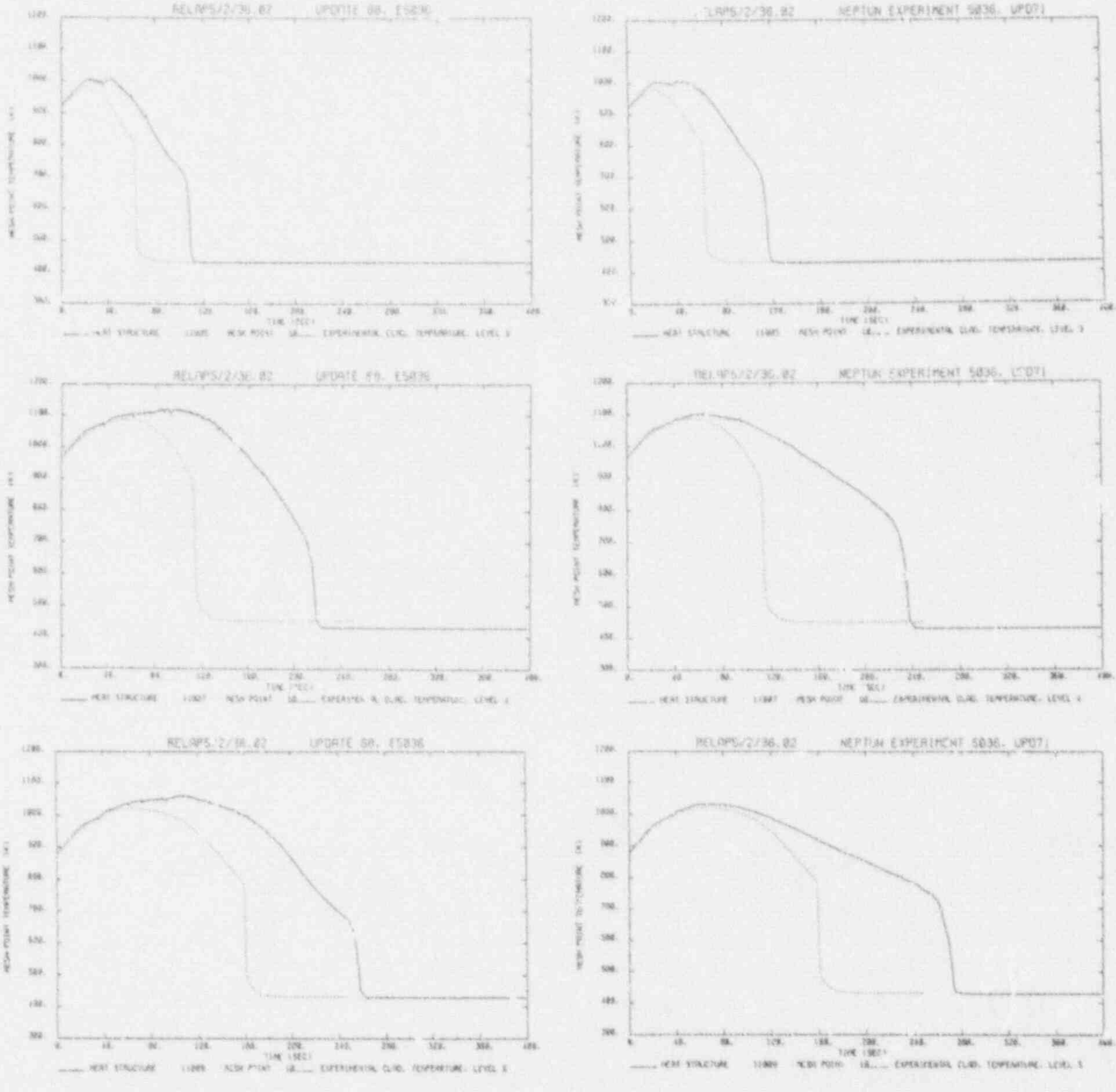

a b

Figure 38: Rod cladding temperatures at measurement levels 3-5 in NEPTUN low flooding rate experiment 5036, calculated with (=EIR-update 71, figure b)) and without (=EIR-update 68), figure a)) new formula of Forslund-Rohsenow for the reflood dispersed film boiling wall heat transfer coefficient, and with previous updates.

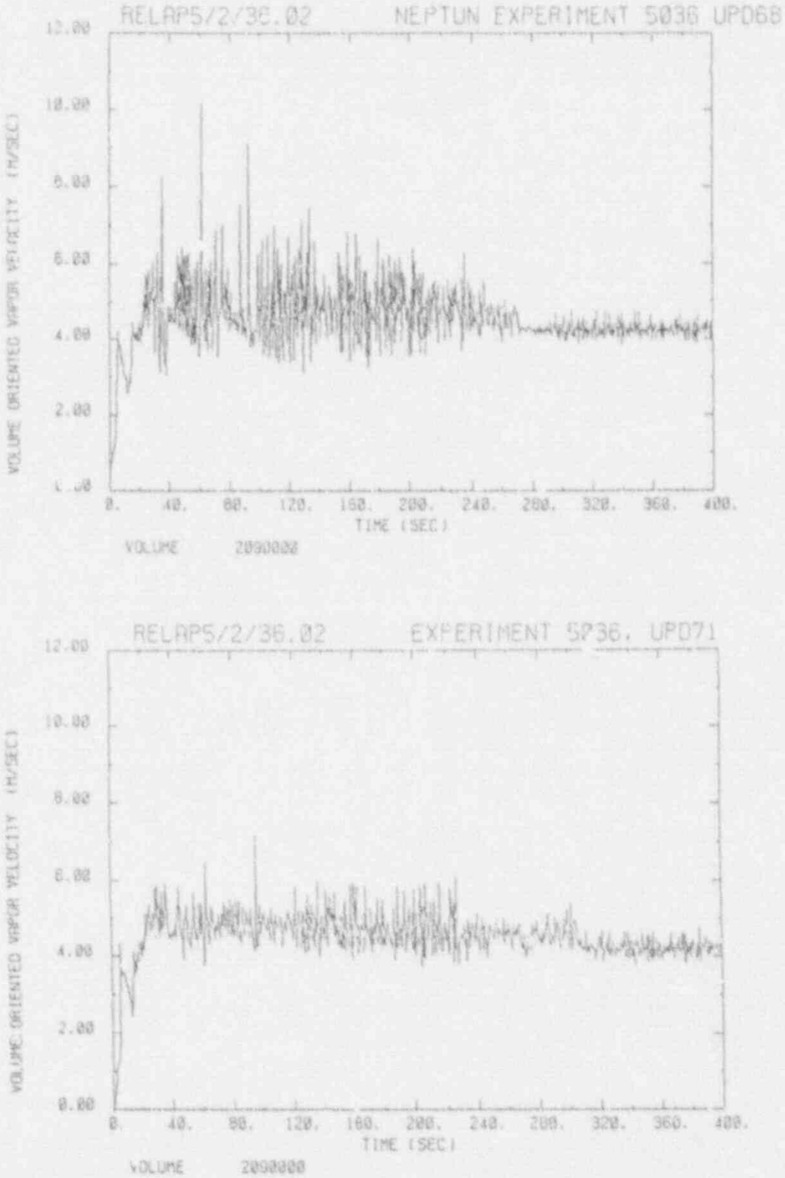

Figure 39: Steam velocities at measurement level 5 in NEPTUN low flooding rate experiment 5036, calculated with (=EIR-update 71, figure b)) and without (=EIR-update 68, figure a)) new formula of Forslund-Rohsenow for the reflood dispersed film boiling wall heat transfer coefficient, and with previous updates.

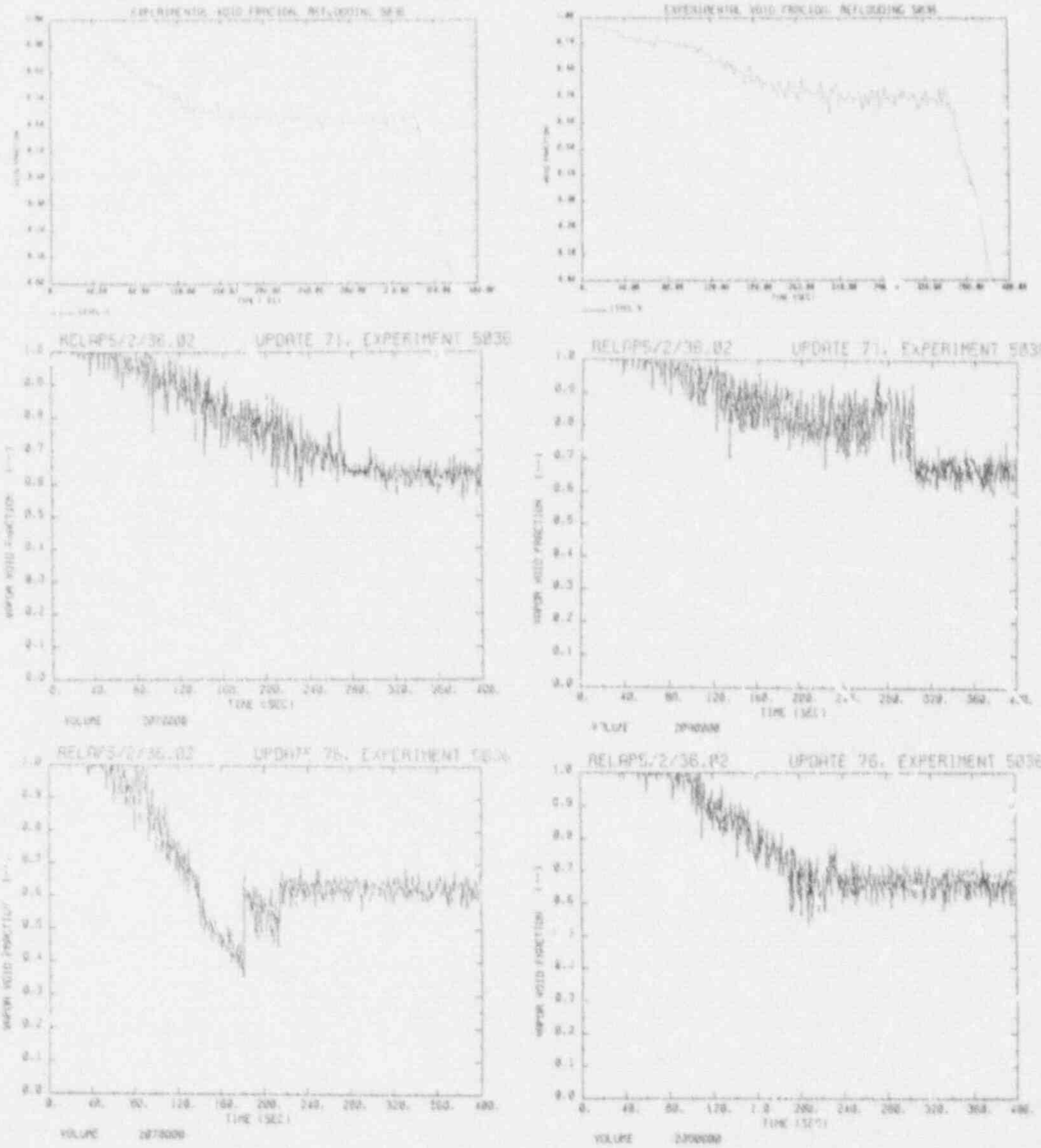

Figure 40: Void fractions at measurement levels 4 (left side) and 5 (right side) in NEPTUN low flooding rate experiment 5036, measured (top) and calculated without (=EIR-update 71, middle) and with (=EIR-update 76, bottom) reduction of interphase friction in inverted slug flow by 0.4 and in dispersed flow and in annular mist flow by 0.5, and with previous updates.

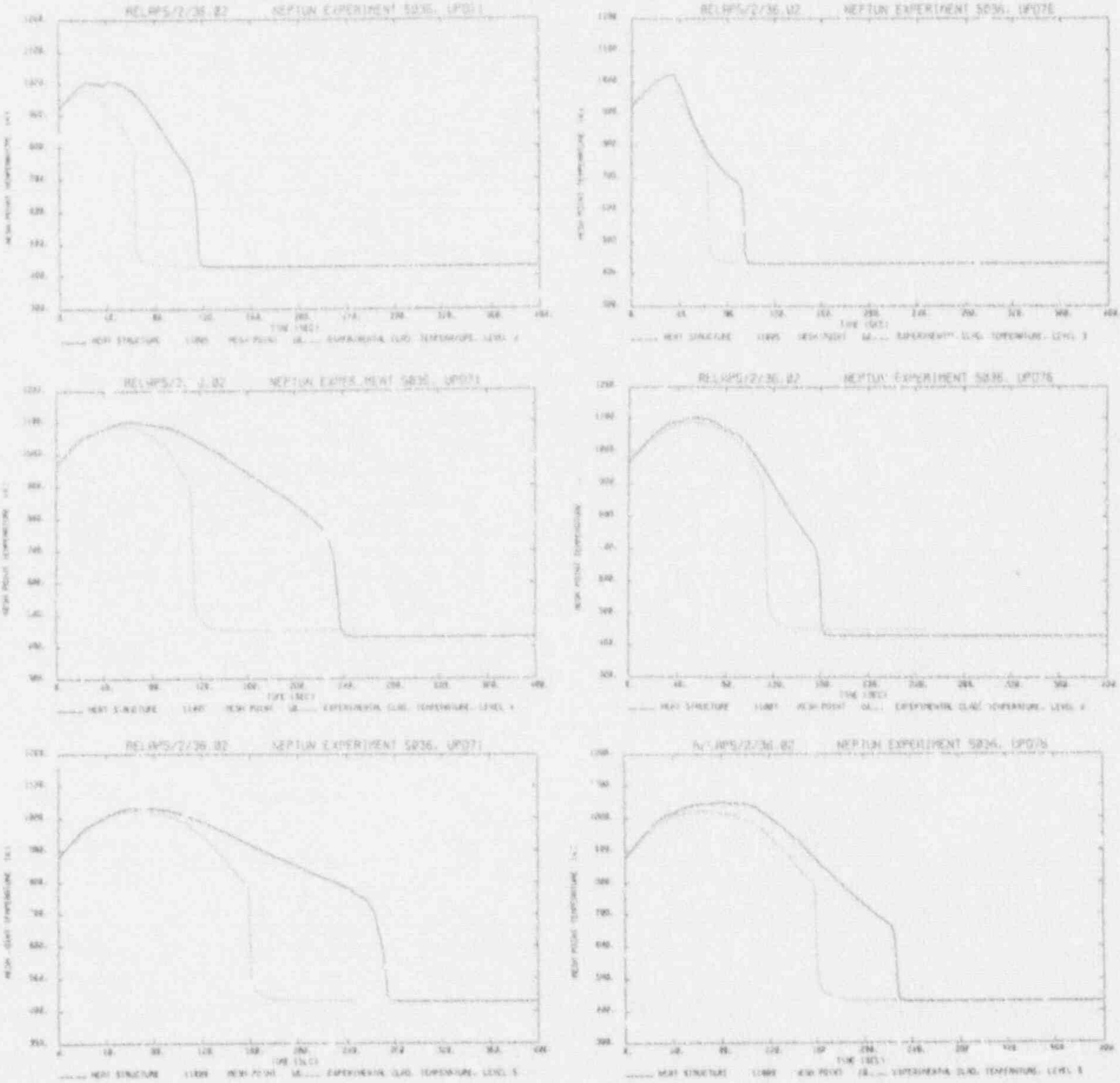

a b

Figure 41: Rod cladding temperatures at measurement levels 3-5 in NEPTUN low flooding rate experiment 5036, calculated with (=EIR-update 76, figure b)) and without (=EIR-update 71, figure a)) reduction of the interphase friction in inverted slug flow by 0.4 and in dispersed flow and in annular mist flow by 0.5, and with previous updates.

Modification to criterion for selecting the pre-dry out interphase friction correlations near the quench front in RELAP5/MOD2

Criterion for selecting the pre-dry out interphase friction correlations in RELAP5/MOD2:

$$P \geq 1$$

where

$$\begin{aligned} P &= max\{0, \min \{1, P'(0.4 - \alpha_B) \cdot 10\}\} \\ P' &= (1 - e^{-0.8 T_{gs}}) 1.0009454 \\ T_{gs} &= T_g - T_{sat} - 1 \end{aligned}$$

and α_B is the void fraction for the transition from bubbly to slug or inverted slug flow.

<u>Correction performed</u> (EIR-update 77 ff.):

$$T_{gs} = T_g - T_{sat} - 40(1 - \alpha)$$

instead of

$$T_{gs} = T_g - T_{sat} - 1$$

Figure 42: Criterion for selection of the pre-dry out interphase friction correlations near the quench front in RELAP5/MOD2, and correction performed in EIR-update 77.

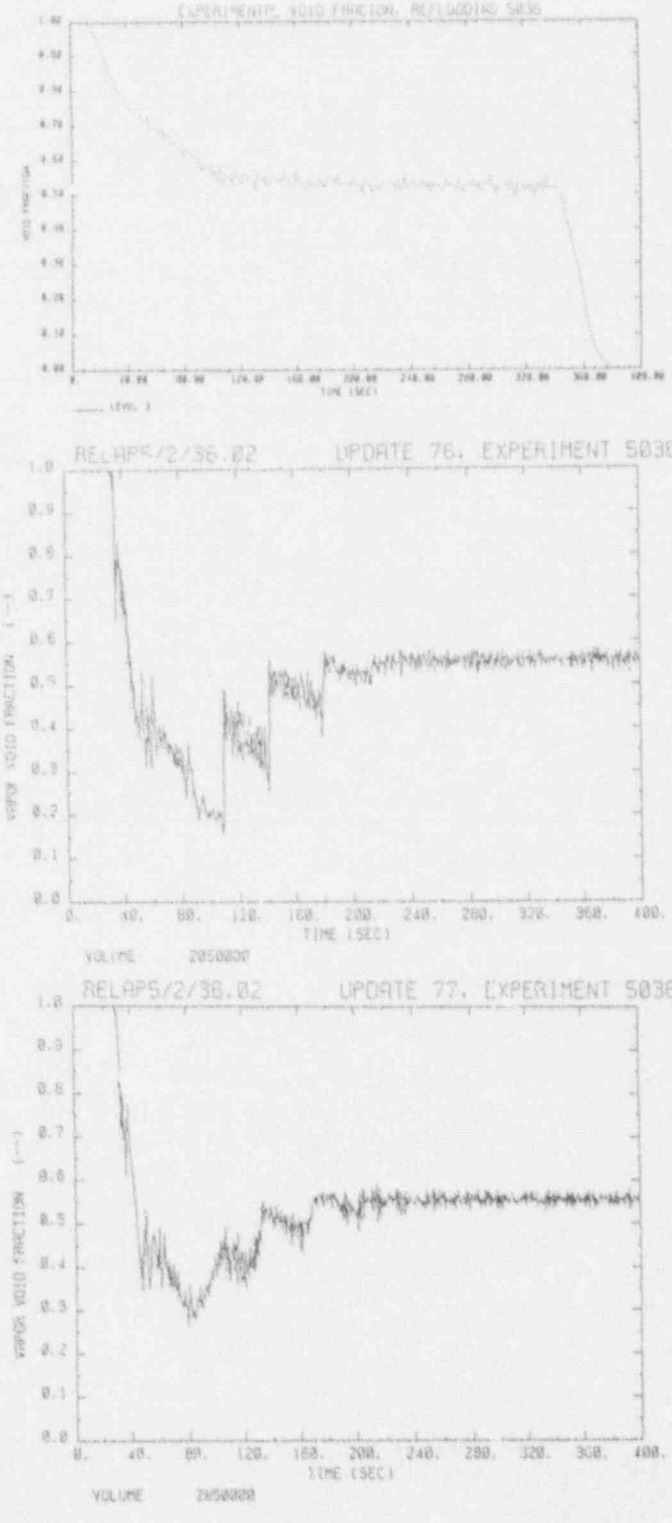

Figure 43: Void fraction at measurement level 3 in NEPTUN low flooding rate experiment 5036, measured (top) and calculated without (=EIR-update 76, middle) and with (=EIR-update 77, bottom) performed void fraction correction, and with previous updates.

Modification of the Weismann reflood transition boiling heat transfer coefficient in RELAP5/MOD2

Frozen version of RELAP5/MOD2:

Transition boiling heat transfer coefficient (Weismann):

$$h_{TB} = h_m e^{-0.040\Delta T} + 4500\left(\frac{G}{G_R}\right)^{0.2} e^{0.012\Delta T}$$

where

$$h_m = \frac{q_{cr}}{\Delta T_m}$$

$$\Delta T = T_w - T_{sat} - \Delta T_m$$

$$\Delta T_m = S\left(\frac{q_{cr}}{2.253}\right)^{0.259}$$

and S is the Chen's boiling suppersion factor, q_{cr} the critical heat flux, G the mass flux and G_R = 67.8 kg/m^{2}s

Modification (EIR-update 83):

Decreasing exponent 0.040 in first term of h_{TB} to value of 0.0175

Modification also included in EIR-update 83:

Multiplying modified Bromley heat transfer coefficient correlation with factor

$$1 + 0.025(T_{sat} - T_f)$$

to consider to the effect of the subcooling

Figure 44: Modification in the Weismann reflood transition film boiling heat transfer correlation performed in RELAP5/MOD2 to increase the quench temperature of the code and implementation of a correction factor to consider the effect of subcooling.

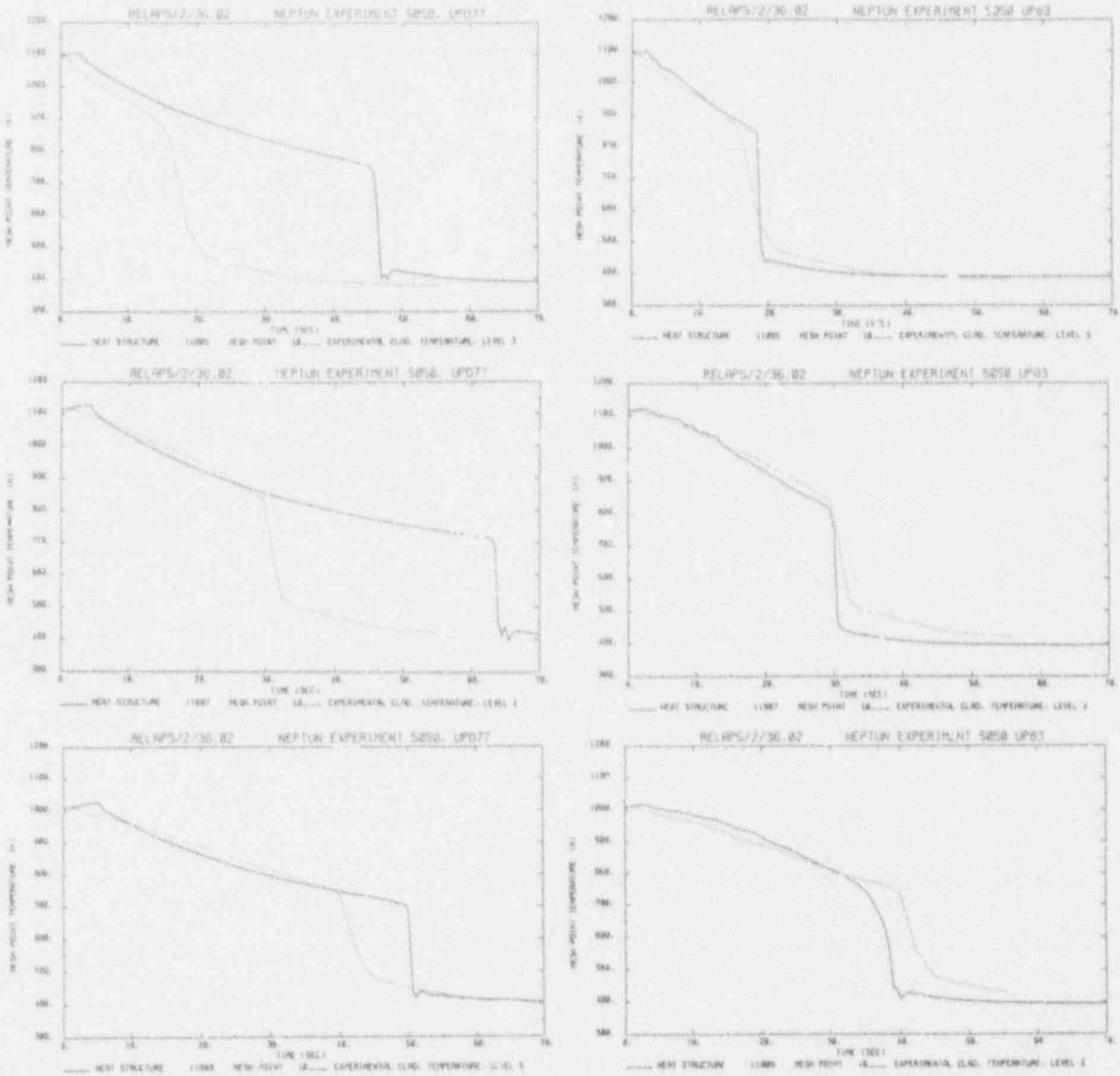

a b

Figure 45: Rod cladding temperatures at measurement levels 3-5 in NEPTUN high flooding rate experiment 5050, calculated with (=EIR-update 83, figure b)) and without (=EIR-update 77, figure a)) the modification of the Weismann correlation and the correction factor to consider subcooling, and with previous updates.

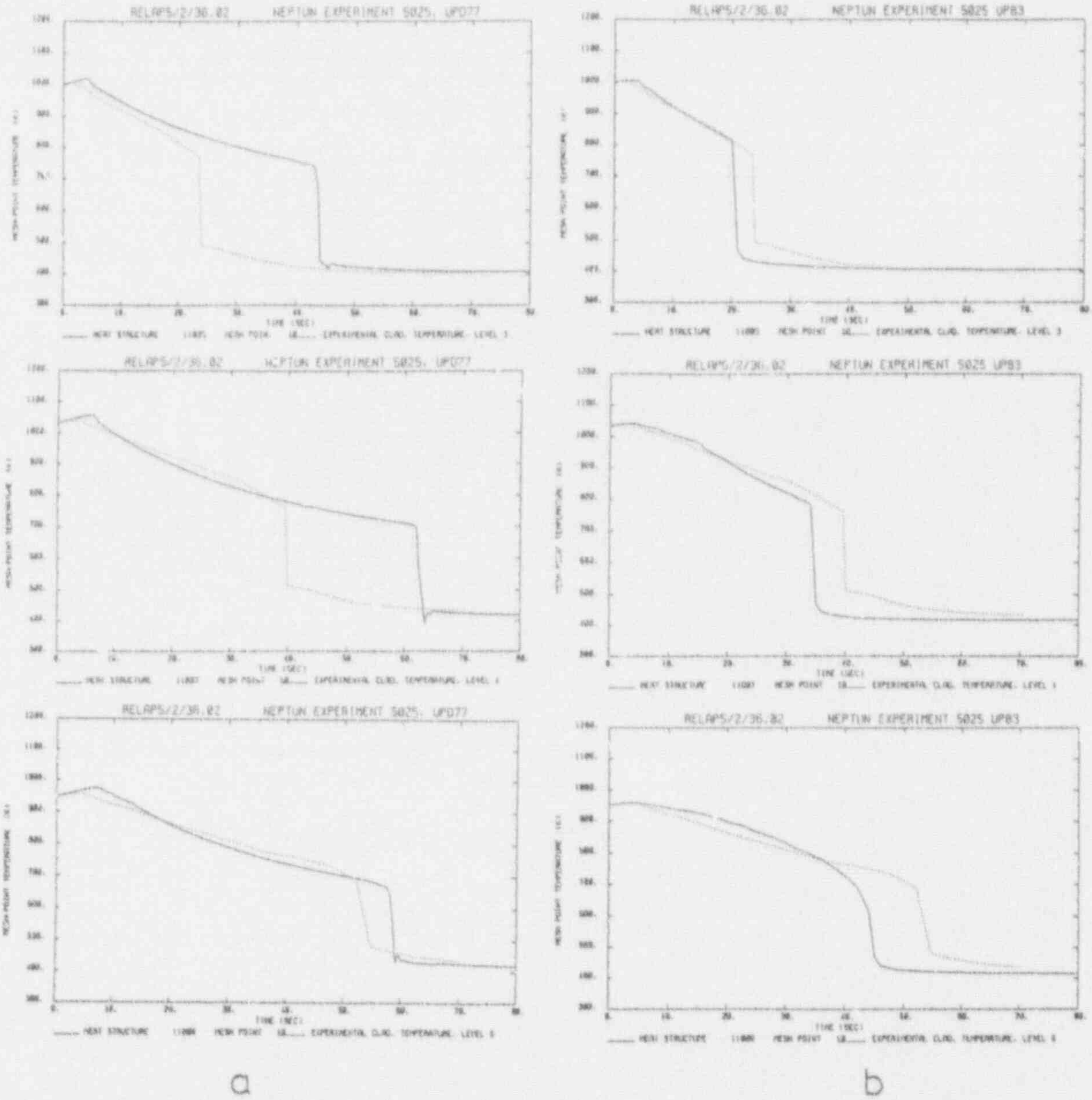

Figure 46: Rod cladding temperatures at measurement levels 3-5 in NEPTUN high flooding rate experiment 5025, calculated with (=EIR-update 83, figure b)) and without (=EIR-update 77, figure a)) the modification of the Weismann correlation and the correction factor to consider subcooling, and with previous updates.

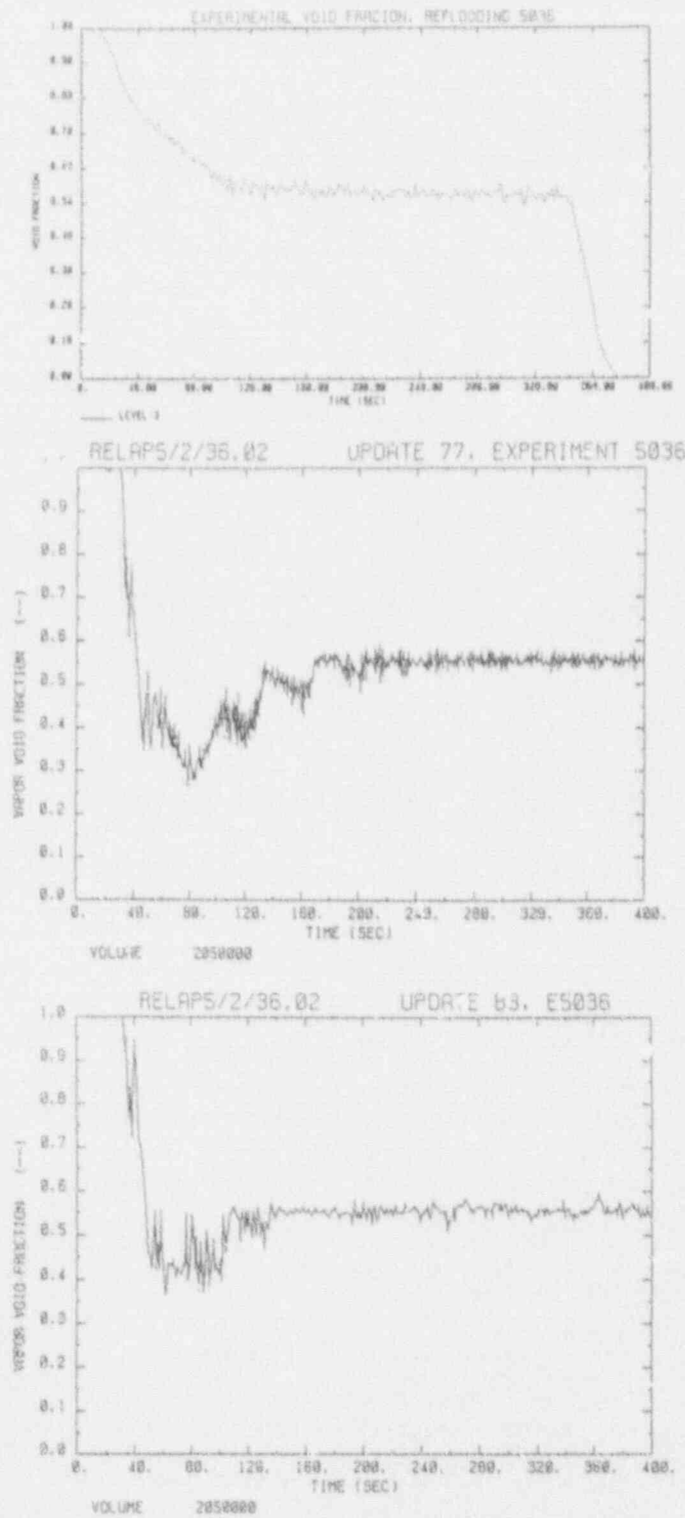

Figure 47: Void fraction at measurement level 3 in NEPTUN low flooding rate experiment 5036, measured (top) and calculated without (=EIR-update 77, middle) and with (=EIR-update 83, bottom) the modification of the Weismann reflood transition film boiling heat transfer coefficient, and with previous updates.

Updates in RELAP5/MOD2/36.02 performed at EIR

In a higher EIR-update number the modifications of the lower update numbers are included.

EIR-update 53:	Correction of the Modified Bromley correlation.
EIR-update 68:	Implementation of a new correlation for the interphase friction in bubbly and slug flow in rod bundle geometry.
EIR-update 71:	Implementation of the formula of Forslund-Rohsenow for the reflood dispersed film boiling heat transfer coefficient.
EIR-update 76:	Reduction of the interphase friction in rod bundle geometry in inverted slug flow by a factor of 0.4 and in dispersed flow and annular mist flow by a factor of 0.5.
EIR-update 77:	Changing the criterion for selecting the pre-dry out interphase friction correlation near the quench front to reduce unphysical void fraction oscillations.
EIR-update 83:	Changing an exponent in the Weismann reflood transition boiling correlation to increase the quench temperature of the code and adding a factor to the Modified Bromley heat transfer coefficient to consider the effect of subcooling.

Figure 48: Summary of all updates in RELAP5/MOD2 performed at EIR.

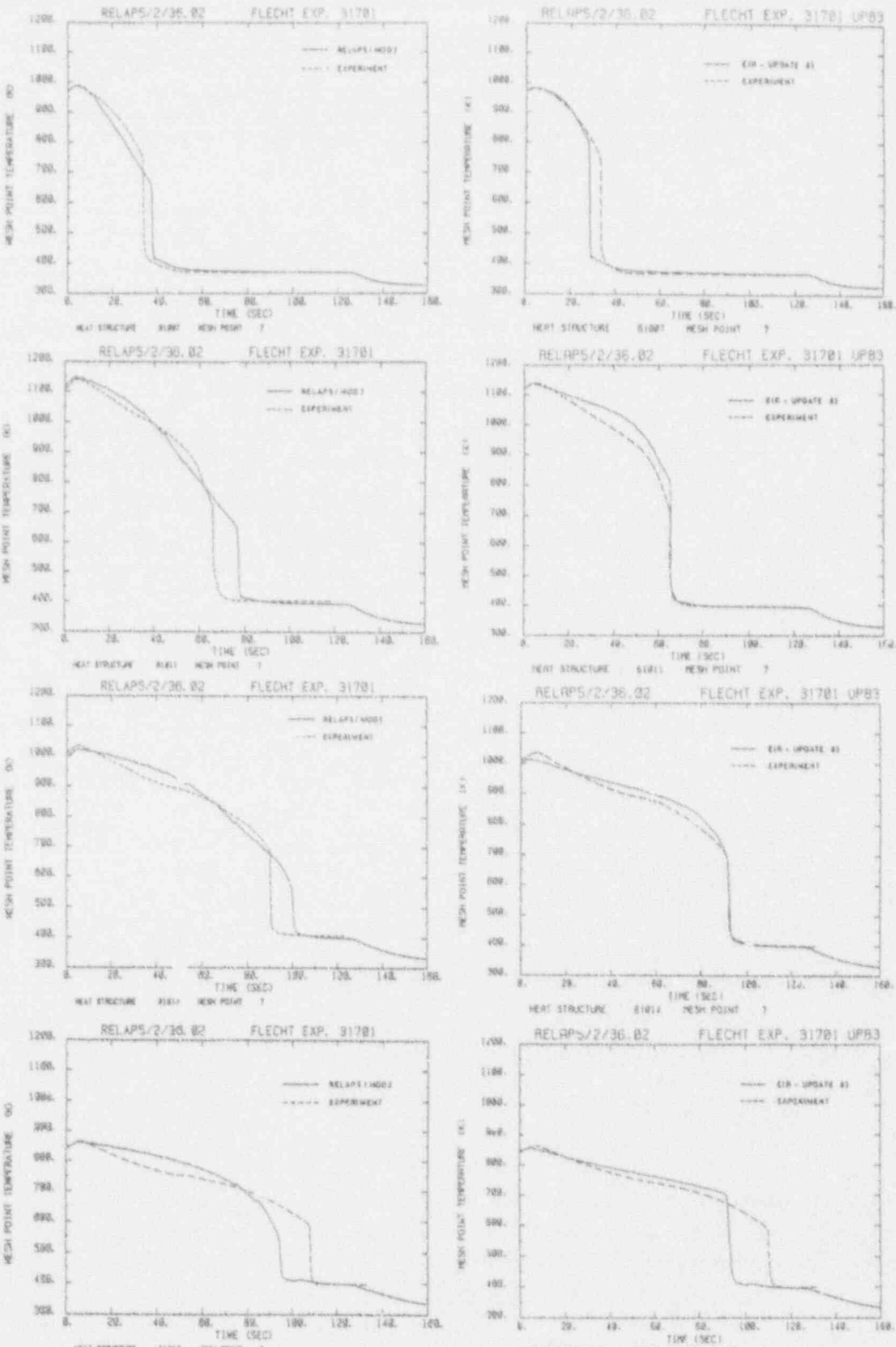

Figure 49: Rod cladding temperatures at elevations 1.19 m, 1.92 m, 2.47 m and 2.84 m in FLECHT-SEASET high flooding rate experiment 31701, calculated by RELAP5/MOD2 with the frozen version (left side) and with the modified version EIR-update 83 (right side).

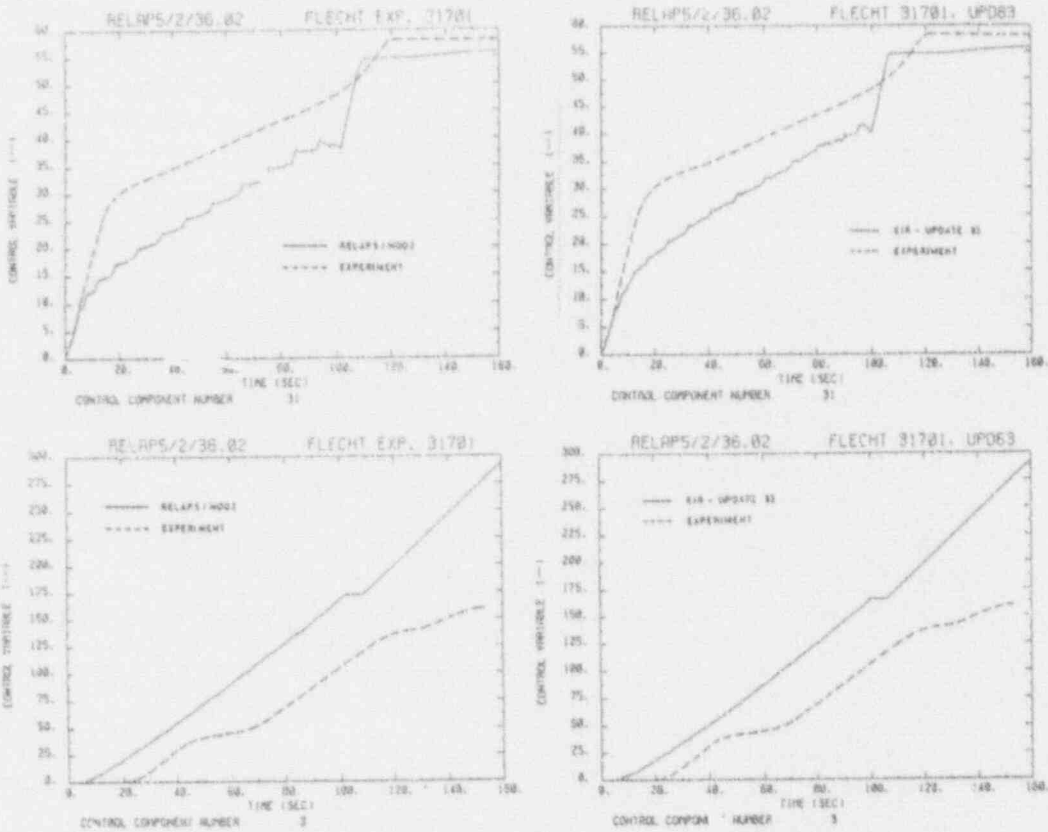

Figure 50: Mass in the bundle and water e‹ rainment in FLECHT-SEASET high flooding rate experiment 31701, calculated by RELAP5/MOD2 with the frozen version (figure a)) and the modified version EIR-update 83 (figure b)).

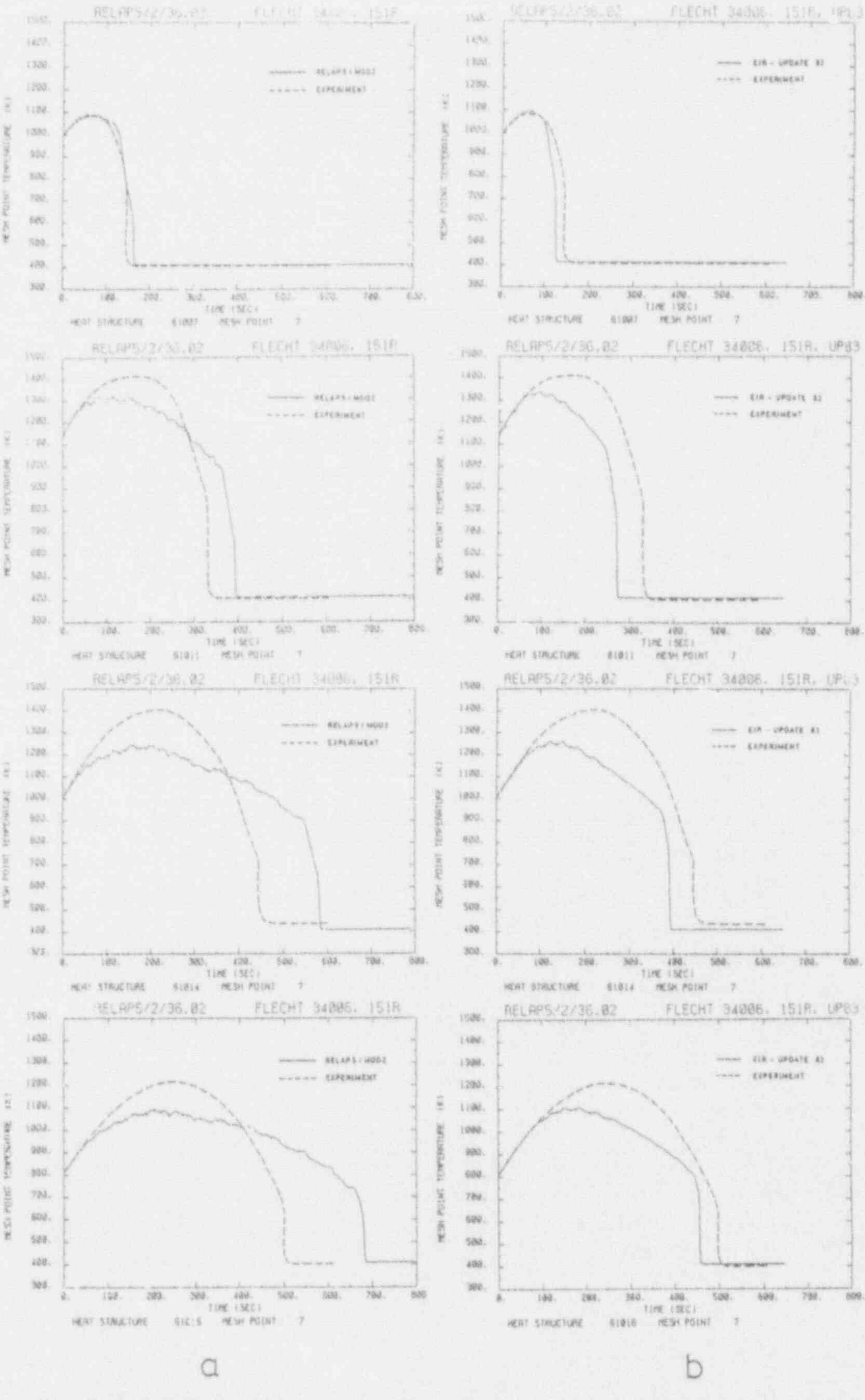

Figure 51: Rod cladding temperatures at elevations 1.19 m, 1.92 m, 2.47 m and 2.84 m in FLECHT-SEASET low flooding rate experiment 34006, calculated by RELAP5/MOD2 with the frozen version (figure a)) and with the modified version EIR-update 83 (figure b)).

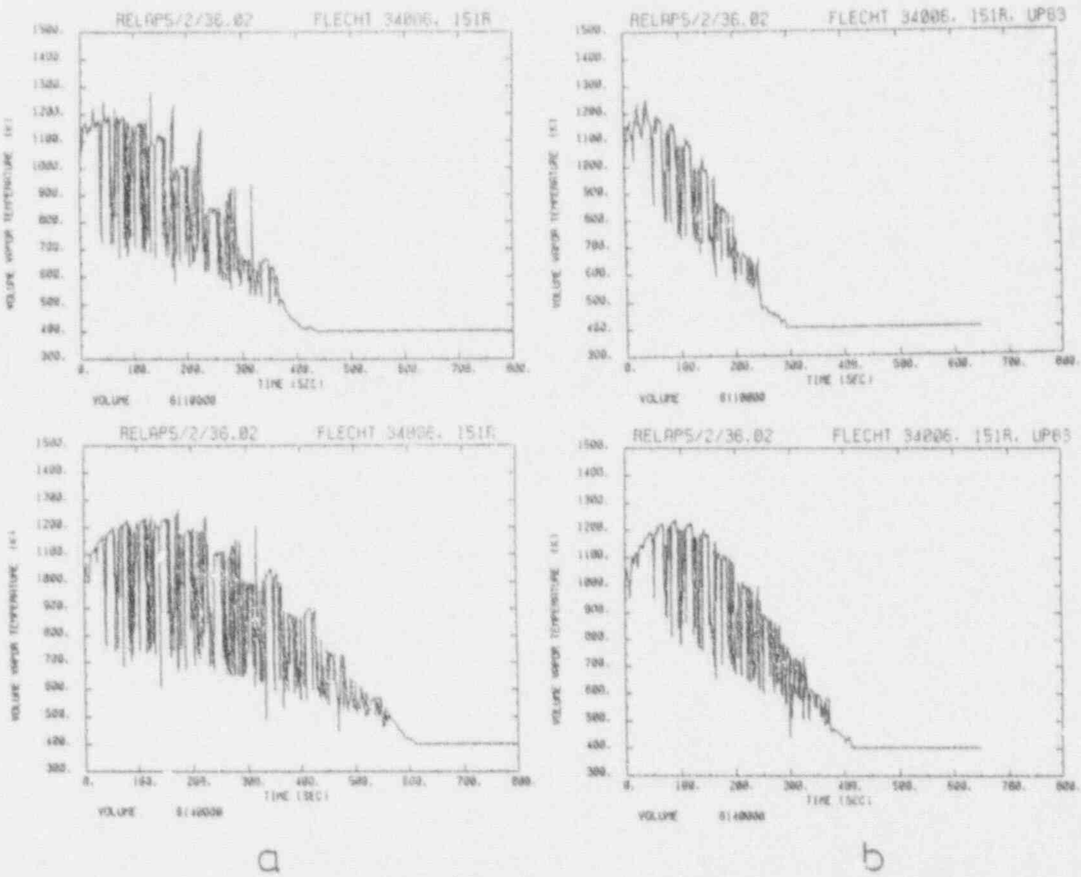

Figure 52: Steam temperatures at elevations 1.92 m and 2.47 m in FLECHT-SEASET low flooding rate experiment 34006, calculated by RELAP5/MOD2 with the frozen version (figure a)) and with the modified version EIR-update 83 (figure b)).

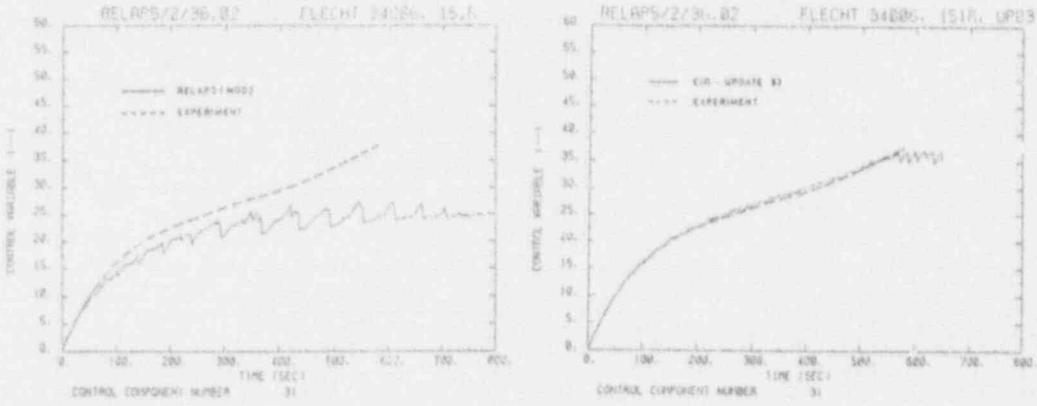

Figure 53: Mass in the bundle in FLECHT-SEASET low flooding rate experiment 34006, calculated by RELAP5/MOD2 with the frozen version (figure a)) and with the modified version EIR-update 83 (figure b)).

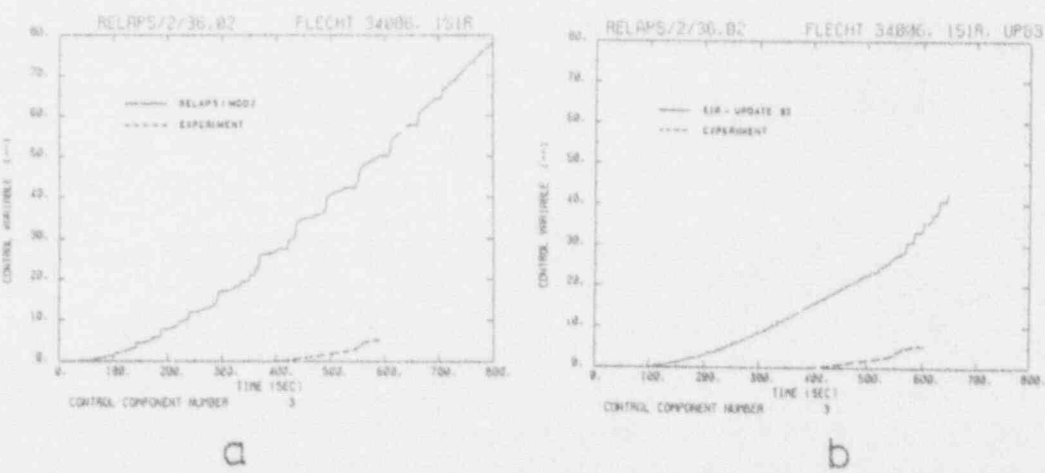

Figure 54: Water entrainment in FLECHT-SEASET low flooding rate experiment 34006, calculated by RELAP5/MOD2 with the frozen version (figure a)) and with the modified version EIR-update 83 (figure b)).

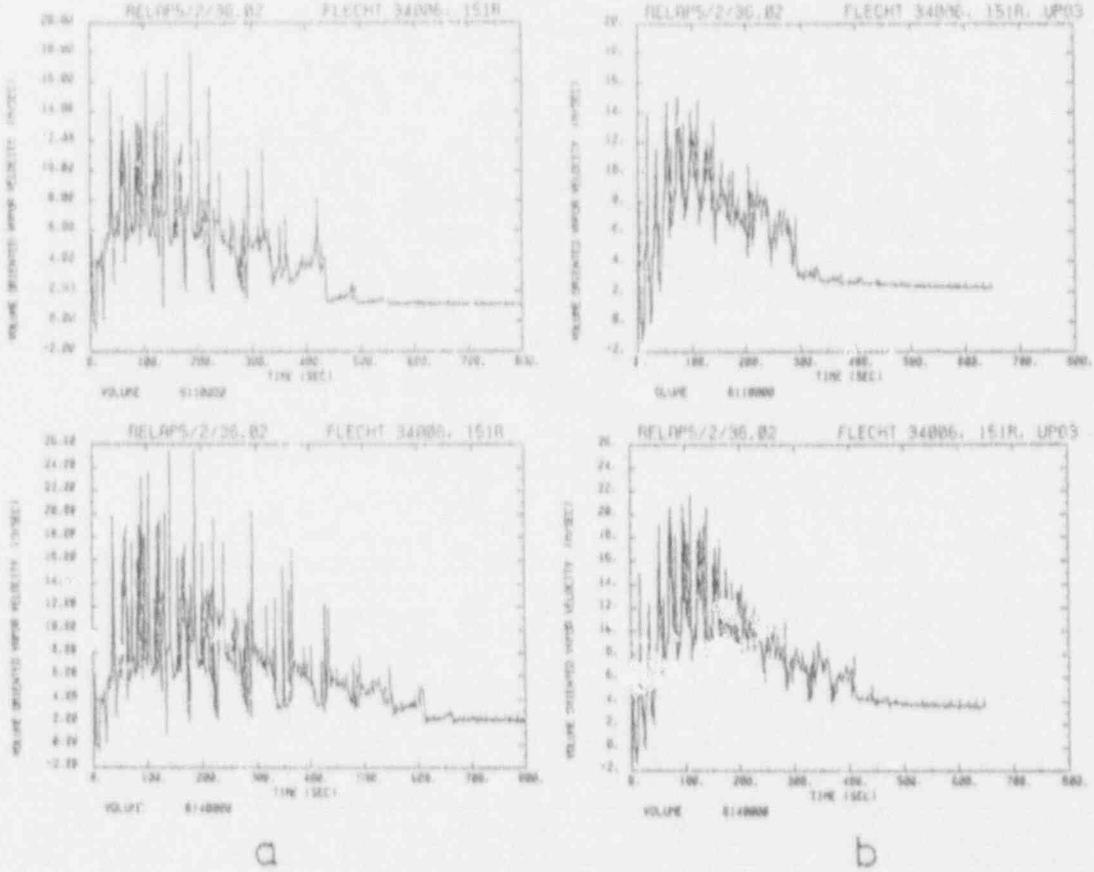

Figure 55: Steam velocities at elevations 1.92 m and 2.47 m in FLECHT-SEASET low flooding rate experiment 34006, calculated by RELAP5/MOD2 with the frozen version (figure a)) and with the modified version EIR-update 83 (figure b)).

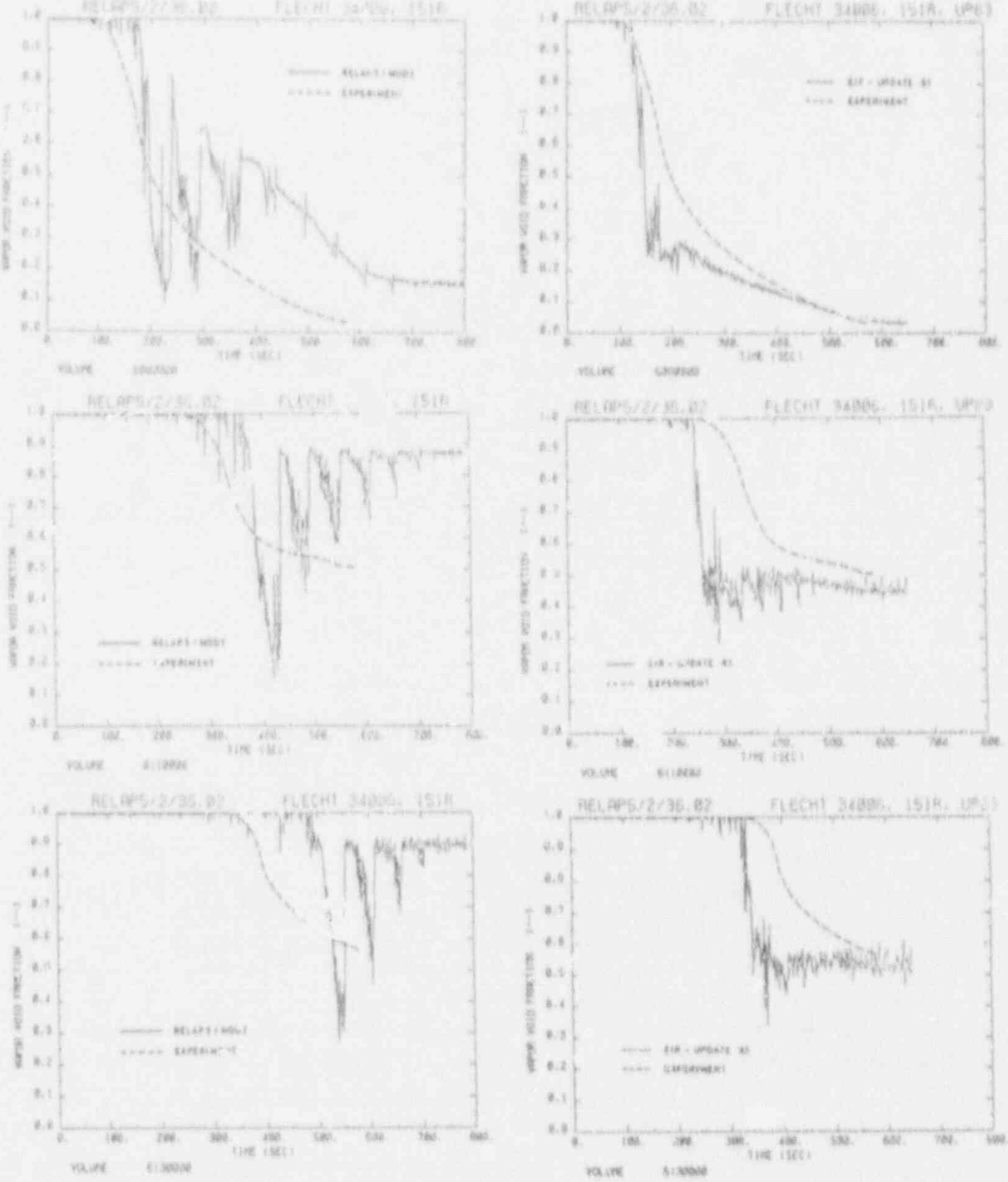

a b

Figure 56: Void fractions at elevations 1.37 m, 1.92 m and 2.29 m in FLECHT-SEASET low flooding rate experiment 34006, calculated by RELAP5/MOD2 with the frozen version (figure a)) and with the modified version EIR-update 83 (figure b)).

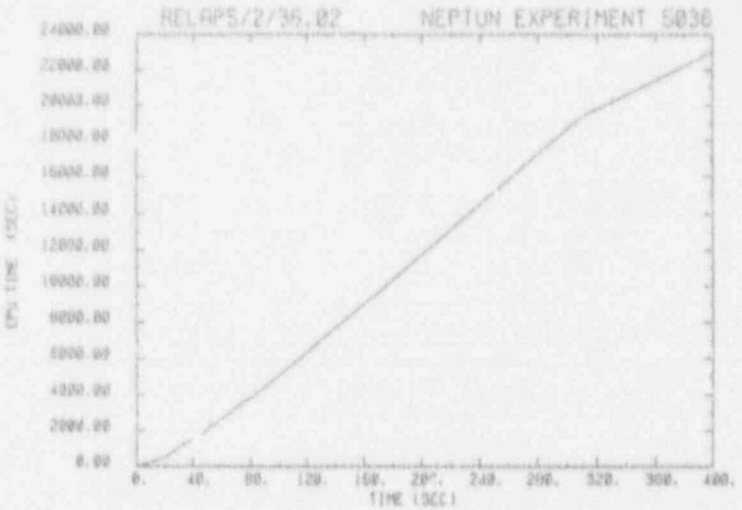

Figure 57: CPU-time of RELAP5/MOD2 base case calculation of NEPTUN low flooding rate experiment 5036.

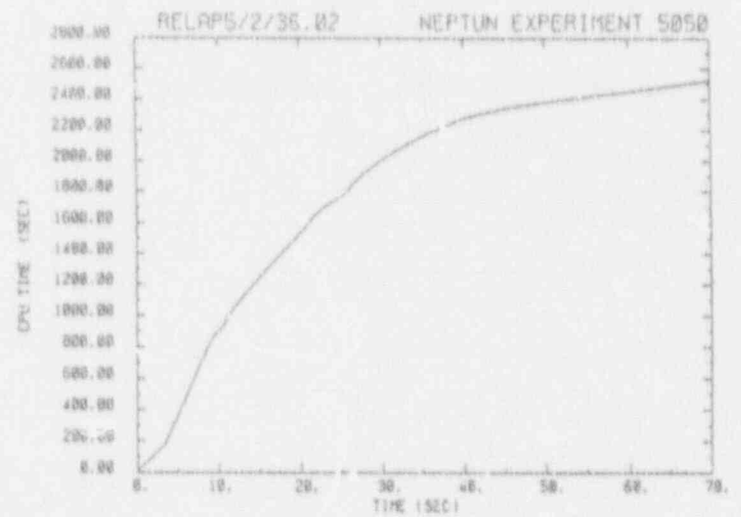

Figure 58: CPU-time of RELAP5/MOD2 base case calculation of NEPTUN high flooding rate experiment 5050.

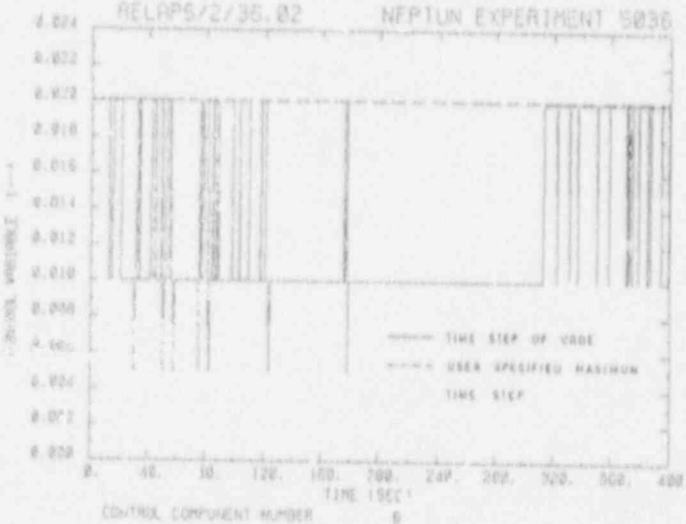

Figure 59: Time step size of RELAP5/MOD2 base case calculation of NEPTUN low flooding rate experiment 5036.

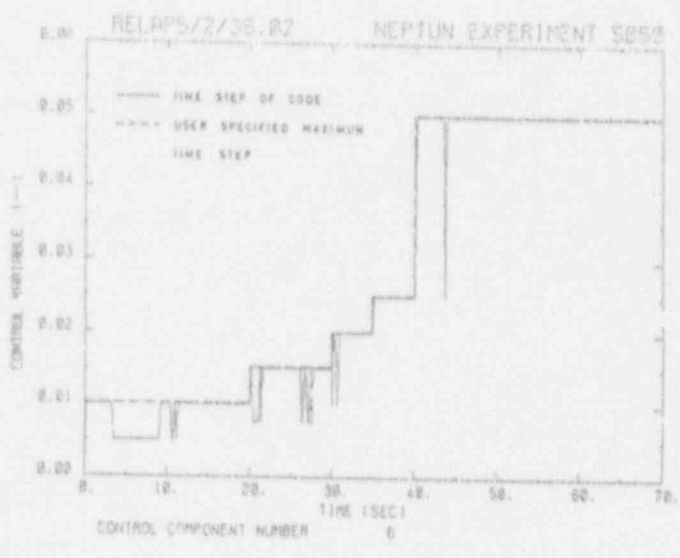

Figure 60: Time step size of RELAP5/MOD2 base case calculation of NEPTUN high flooding rate experiment 5050.

NRC FORM 335 (2-89) NRCM 1102, 3201, 3202

U.S. NUCLEAR REGULATORY COMMISSION

BIBLIOGRAPHIC DATA SHEET

(See instructions on the reverse)

1. REPORT NUMBER (Assigned by NRC, Add Vol., Supp., Rev., and Addendum Numbers, if any.)

NUREG/IA-0054

2. TITLE AND SUBTITLE

Assessment of RELAP5/MOD2, Cycle 36.02, Using NEPTUN Reflooding Experimental Data

3. DATE REPORT PUBLISHED

MONTH	YEAR
August	1992

4. FIN OR GRANT NUMBER

A4682

5. AUTHOR(S)

M. Richner, G. Th. Analytis, S. N. Aksan

6. TYPE OF REPORT

Technical

7. PERIOD COVERED (Inclusive Dates)

8. PERFORMING ORGANIZATION – NAME AND ADDRESS (If NRC, provide Division, Office or Region, U.S. Nuclear Regulatory Commission, and mailing address; if contractor, provide name and mailing address.)

Paul Scherrer Institute (PSI)
Wurenlingen and Villigen
CH-5232 Villigen PSI
Switzerland

9. SPONSORING ORGANIZATION – NAME AND ADDRESS (If NRC, type "Same as above"; if contractor, provide NRC Division, Office or Region, U.S. Nuclear Regulatory Commission, and mailing address.)

Office of Nuclear Regulatory Research
U.S. Nuclear Regulatory Commission
Washington, D.C. 20555

10. SUPPLEMENTARY NOTES

11. ABSTRACT (200 words or less)

Seven NEPTUN reflooding experiments with varying parameters flooding rate, single rod power, pressure and initial rod temperatures were simulated with the code RELAP5/MOD2, version 36.02, to assess the code, especially its reflood model. These calculations were performed with the specific objectives of evaluating the general prediction capability as well as specific problem areas of the RELAP5/MOD2 code in modelling boil-off and reflood behavior. The differences between code predictions and experiments are described and analyzed. Implementing new correlations into the code and modifying or correcting existing correlations, for example for wall heat transfer or interphase friction, some of the weak points of the code during reflooding could be identified.

12. KEY WORDS/DESCRIPTORS (List words or phrases that will assist researchers in locating the report.)

RELAP5/MOD2, NEPTUN, reflooding tests

13. AVAILABILITY STATEMENT

Unlimited

14. SECURITY CLASSIFICATION

(This Page)
Unclassified

(This Report)
Unclassified

15. NUMBER OF PAGES

16. PRICE

NRC FORM 335 (2-89)

UNITED STATES
NUCLEAR REGULATORY COMMISSION
WASHINGTON, D.C. 20555-0001

OFFICIAL BUSINESS
PENALTY FOR PRIVATE USE, $300

SPECIAL FOURTH-CLASS RATE
POSTAGE AND FEES PAID
USNRC
PERMIT NO. G-67

120555139531 1 1AN1CI
US NRC-OADM
DIV FOIA & PUBLICATIONS SVCS
TPS-PDR-NUREG
P-211
WASHINGTON DC 20555